

This work is protected by copyright and other intellectual property rights and duplication or sale of all or part is not permitted, except that material may be duplicated by you for research, private study, criticism/review or educational purposes. Electronic or print copies are for your own personal, non-commercial use and shall not be passed to any other individual. No quotation may be published without proper acknowledgement. For any other use, or to quote extensively from the work, permission must be obtained from the copyright holder/s.

Study to determine the rate of kill of anti-
leishmanial drugs using a novel bioluminescence-
based assay

Abigail Leah Freakley



Thesis submitted to Keele University for the degree of Master of
Philosophy in Parasitology

June 2023

Abstract

Leishmaniasis is a neglected tropical disease associated with poverty, deprived socio-economic settings and population displacement, primarily due to conflict. The causative agent are species of *Leishmania* parasites that are transmitted by sand flies. It is a disease that affects millions every year and manifests into three primary forms; cutaneous, mucocutaneous and visceral leishmaniasis. Each of these forms are extremely debilitating to the everyday life of those living with leishmaniasis. The current drugs used are re-purposed treatments that are far from ideal. Emerging reports of resistance, poor patient cooperation as a result of long treatment regimens and highly toxic side effects are indicative of essential improvements needed.

This thesis focuses on using a transgenic *Leishmania* cell line in a novel bioluminescence-based assay to determine the rate of kill of four current anti-leishmanial drugs: amphotericin B, miltefosine, pentamidine and potassium antimonyl tartrate. This axenic *in vitro* assay is studied to address the pharmacodynamic gap in the early drug discovery process and to evaluate the use of a novel technique and its potential in the development of more dynamic and predictive assays. At 3-fold the EC₅₀ concentration, amphotericin B had completely eliminated all viable parasites within 4 hours, demonstrating that it is a fast-acting drug. Miltefosine on the other hand, failed to reduce total parasite viability after 72-hour exposure and we therefore characterised miltefosine as slow-acting. Pentamidine and potassium antimonyl tartrate exhibited an intermediate rate of kill, reaching maximal effect on parasite growth within 72 hours at 9 x the EC₅₀. The bioluminescence-based assay provides a dynamic reporter for parasite viability and exciting potential for fast, sensitive results in early drug screening as shown by the ability to quickly discriminate between fast- and slow- acting compounds. Addressing and identifying this research gap can aid with treatment regimens and dosage improvements of current and novel drug treatments for leishmaniasis.

Table of Contents

List of Figures.....	viii
List of Tables.....	x
Abbreviations	xii
Acknowledgements.....	xiv
Chapter 1 – Introduction	1
1.1 The <i>Leishmania</i> parasite	2
1.1.1 Life cycle.....	2
1.1.2 Structure and gene expression.....	8
1.1.2.1 Structure	8
1.1.2.2 Gene expression in kinetoplastids.....	10
1.2 Leishmaniases	13
1.2.1 Leishmaniasis forms and pathology.....	13
1.2.2 Epidemiology and Risk Factors	17
1.2.3 Immune response to <i>Leishmania</i>	21
1.2.3.1 Innate immune response.....	21
1.2.3.2 Adaptive immune response.....	25
1.2.4 Diagnosis of leishmaniasis.....	29
1.2.4.1 Microscopy	29
1.2.4.2 Culturing	31

1.2.4.3 Immunological tools for diagnosis.....	32
1.2.4.4 Molecular tools for diagnosis	33
1.2.5 Treatments	36
1.2.5.1 Pentavalent antimonials.....	38
1.2.5.2 Amphotericin B and AmBisome.....	40
1.2.5.3 Miltefosine	43
1.2.5.4 Paromomycin.....	45
1.2.5.5 Pentamidine.....	46
1.2.6 Drug discovery for leishmaniasis	48
1.2.6.1 Current anti-leishmanial screening assays	53
1.2.6.2 Absorbance and Fluorescence-based assays.....	53
1.2.6.3 Bioluminescent transgenic parasites.....	55
1.2.7 Rate of Kill of the anti-leishmanial drugs pentamidine, miltefosine, amphotericin B and potassium antimonial tartrate	57
1.2.8 Aims	61
Chapter 2 – Materials.....	62
2.1 Materials	63
2.1.1 Plasticware, glassware and equipment.....	63
2.1.2 Chemicals and Reagents.....	64
2.1.3 Drug Stocks Preparation.....	64

Chapter 3 – Methods	65
3.2.1 Cell culture of <i>L. mexicana</i>	66
3.2.2 Nano-Glo Luciferase Expression and stability	66
3.2.3 PrestoBlue® Assay: Determining the EC ₅₀ of amphotericin B, miltefosine, pentamidine and potassium pentavalent antimonial in <i>L. mexicana</i> cell lines	67
3.2.4 Statistical analysis used	69
3.2.5 Determining the Rate of Kill in <i>L. mexicana</i> cell lines	70
Chapter 4 - Results	74
4.1 Analysing the use of bioluminescence- and fluorescence-based assays for drug screening	75
4.2 Determining the EC₅₀ of Amphotericin B, Miltefosine, Pentamidine and Potassium Antimony Tartrate	79
4.3 Determining the Rate of Kill of Amphotericin B, Miltefosine, Pentamidine and Potassium Antimony Tartrate	84
Chapter 5 - Discussion	88
5.1 Rate of kill: Fast- or slow-acting compounds	89
5.2 Evaluation of experimental approaches	94
5.2.1 Bioluminescence vs fluorescence	94
5.2.2 Evaluating experimental test models for rate of kill research	97
5.3 The relevance of rate of kill	99
5.3.1 Possible use for improving treatment duration regimens	99

5.4 Future work.....	102
<i>Conclusion</i>	103
<i>References.....</i>	104

List of Figures

Figure 1 The digenetic life cycle of <i>Leishmania</i> spp (Sourced from (CDC, 2019).	3
Figure 2a-b <i>Leishmania</i> spp lifecycle within the sandfly vector. The <i>Leishmania</i> parasites undergo multiple transformations, from procyclic promastigotes to the infective metacyclic promastigotes (A). These various morphological changes occur within different areas of the sandfly (Figures sourced from Bates, 2007; Kamhawi, 2006).	7
Figure 3 Organelles and structure of <i>Leishmania</i> promastigote (A) and amastigote (B) forms.	8
Figure 4a-b Distribution maps of reported cases of cutaneous (A) and visceral (B) leishmaniasis in 2018 (WHO, 2018).	20
Figure 5 Trojan horse model of innate immune response to <i>Leishmania</i> infection. The phagocytosis of infective promastigotes by neutrophils, either results in apoptosis of the cell or phagocytosis by macrophages (John and Hunter, 2008).	22
Figure 6 Light microscopic image of a Giemsa-stained infected macrophage (CDC, 2018).	29
Figure 7 The general pathway of drug discovery (Alcântara, Ferreira, Gadelha and Miguel, 2018).	49
Figure 8 The mechanism of resazurin reduction into resorufin of resazurin-based assays, such as alamarBlue and Presto Blue (ABP Biosciences, 2020).	54

Figure 9 The mechanism of NanoLuc luciferase activity to produce bioluminescence (Modified from England, Ehlerding and Cai, 2016).	56
Figure 10 Schematic diagram of the fluorescence and bioluminescence-based assays used to measure the rate of kill of drug compounds.	73
Figure 11 Growth curve of <i>L. mexicana</i> NanoLuc-PEST promastigotes. Cells were diluted to a starting concentration of 1×10^5 and monitored every 24 hours over five days. The growth curve was generated in GraphPad Prism and the Y-axis was transformed by \log_{10} . All mean values are shown as $n=3 \pm \text{SEM}$	76
Figure 12 Initial analysis of luciferase-expressing <i>L. mexicana</i> transgenic cell line compared to fluorescence-based method. Cell density dilution series are plotted for the transgenic promastigote and amastigote form (B) and on parental <i>L. mexicana</i> M379 promastigotes (C). Both X- and Y-axis were transformed by \log_{10} . All mean values are shown as $n=3 \pm \text{SEM}$	77
Figure 13 EC50 curves of amphotericin B, miltefosine, pentamidine and potassium antimonyl tartrate against (blue) wild type and (red) NanoLuc-PEST expressing <i>L. mexicana</i> axenic amastigotes (A,C,E,G) and promastigotes (B,D,F,H). Data represents $n=3$ with SEM error bar.....	80
Figure 14 Rate of kill curves of amphotericin B, miltefosine, pentamidine and potassium antimonyl tartrate against the NanoLuc-PEST <i>L. mexicana</i> amastigotes. The normalised bioluminescence signal (a,c,e,g) and fluorescence signal (b,d,e,f) after 4, 24, 48 and 72 hours and 24, 48 and 72 hours of exposure respectively, is plotted as $n=3 \pm \text{SEM}$ error bars.	86

List of Tables

Table 1 The human pathogenic Leishmania species for the three main forms of leishmaniasis.....	15
Table 2 Structures of sodium stibogluconate, amphotericin B, AmBisome, miltefosine, pentamidine and paromomycin, drawn in ChemDraw JS.	37
Table 3 Target product profiles for cutaneous leishmaniasis.....	51
Table 4 The treatment regimen target product profile for visceral leishmaniasis and visceral leishmaniasis combination therapies.	52
Table 5 The preparation and storage conditions of Amphotericin B, Miltefosine, Pentamidine and Potassium Antimonial Tartrate.	64
Table 6 Table showing the preparation of amphotericin B, miltefosine, pentamidine and potassium antimonyl tartrate concentrations used for determining the EC50 values. All stock concentrations were diluted to a top concentration at 1mL and diluted using Schneider's media pH5.5.....	68
Table 1 Table collating the EC50 values in literature for Amphotericin B, Miltefosine, Pentamidine and Potassium Antimonyl Tartrate. All studies show EC50 values against <i>L. mexicana</i> strain M379 unless stated otherwise in the table.....	82
Table 2 EC ₅₀ values of amphotericin B, miltefosine, pentamidine and potassium antimonyl tartrate. These values were determined for wild type and NanoLuc-expressing <i>L. mexicana</i> axenic amastigotes and promastigotes using a fluorescence-	

based assay. Treated cells were incubated in triplicate for 72 hours in the dark with positive (5 μ M amphotericin B) and negative (Schneider's medium) controls. Calculated Z' score and 95% CI for each assay is presented. All data represents n=6 as assay was performed in biological triplicate and technical duplicate.....83.

Table 9 Assay parameter, Z' factor values calculated for the rate of kill of amphotericin B, miltefosine, pentamidine and potassium antimonyl tartrate, for the PrestoBlue and the luciferase assays.....87

Abbreviations

AMB	Amphotericin B
CL	Cutaneous leishmaniasis
DMSO	Dimethyl sulfoxide
DNA	Deoxyribonucleic acid
DNDI	Drugs for Neglected Diseases initiative
EC50	Half maximal effective concentration
FBS	Foetal bovine serum
HIV	Human Immunodeficiency Virus
kDNA	Kinetoplast DNA
LPG	Lipophosphoglycan
MCL	Mucocutaneous leishmaniasis
mRNA	Messenger RNA
NLucP	NanoLuc-PEST
NTDs	Neglected Tropical diseases
PAT	Potassium Antimony Tartrate
Pen-strep	Penicilin-Streptomycin
PK/PD	Pharmacokinetic/Pharmacodynamic
ROK	Rate of kill
S:B	Signal: Background

SB ^v	Pentavalent Antimony
SL	Spliced leader
VL	Visceral leishmaniasis
WHO	World Health Organisation
WT	Wild Type

Acknowledgements

I would first like to express my deepest gratitude to my supervisor, Professor Helen Price, for the opportunity to progress my studies into an MPhil. I am unbelievably grateful for your unfaltering support and patience with me – particularly when writing my thesis; and providing me with guidance and advice that will live with me. You have been a supervisor that I am so incredibly thankful to have started my scientific journey with.

I would also like to thank Dr Liz King for your stories and endless wisdom - I appreciate all of your advice and support. Thank you also to everyone in the Haldane laboratory, Huxley, for your entertainment and help. I wish you all the best of luck in your endeavours.

To Mike and Hasana, I cannot describe how grateful I am, to and for, you both. We started together as early as college and your support and company have been unmatched throughout. I look forward to celebrating your inevitable successes and continuing to trip through life together.

Finally, I would like to thank my family. Thank you to my mum and my sister for your continuous support. You always make time to talk to me when I'm struggling and know how to give me a not-so gentle push to not give up. Lastly, thank you to Larry and George for the comic relief and emotional support throughout.

Chapter 1 – Introduction

1.1 The *Leishmania* parasite

Leishmaniasis is one of 21 neglected tropical diseases that manifest in a spectrum of pathologies within a range of vertebrate hosts. The clinical forms of leishmaniasis are collectively known as the leishmaniases and range from disfiguring cutaneous lesions to fatal systemic disease. Despite the severity and debilitation caused by this disease to millions of people, leishmaniasis has been greatly neglected due to its association with extreme poverty and poor socio-economic settings.

The protozoan parasite *Leishmania*, of the family Trypanosomatidae and order Kinetoplastida is primarily transmitted by a phlebotomine sandfly bite and is the causative agent of Leishmaniasis. The genus *Leishmania* is further categorised into the two subgenera, *Leishmania* and *Viannia*, with differences between them including vector species and geographic distribution. The classification of the two subgenera was originally determined by the location within the sandfly gut that the parasites developed, which has been further supported by phylogenetic analysis (Lainson, Ward and Shaw, 1977). Collectively, there are over thirty known species and subspecies of *Leishmania* but only twenty of these are pathogenic for humans.

1.1.1 Life cycle

The life cycle of human infective *Leishmania* parasites involves two different host species; the sandfly vector and the human host, as shown in Figure 1. Due to the need for *Leishmania* parasites to survive and grow within two hosts, these parasites are known to have a digenetic life cycle. The two main lifecycle stages of *Leishmania* have different distinct morphological

forms and the parasite can therefore also be described as dimorphic. These lifecycle stages are the flagellated promastigote and the non-motile amastigote form; that reside in the sandfly vector and the macrophages of a mammalian host, respectively.

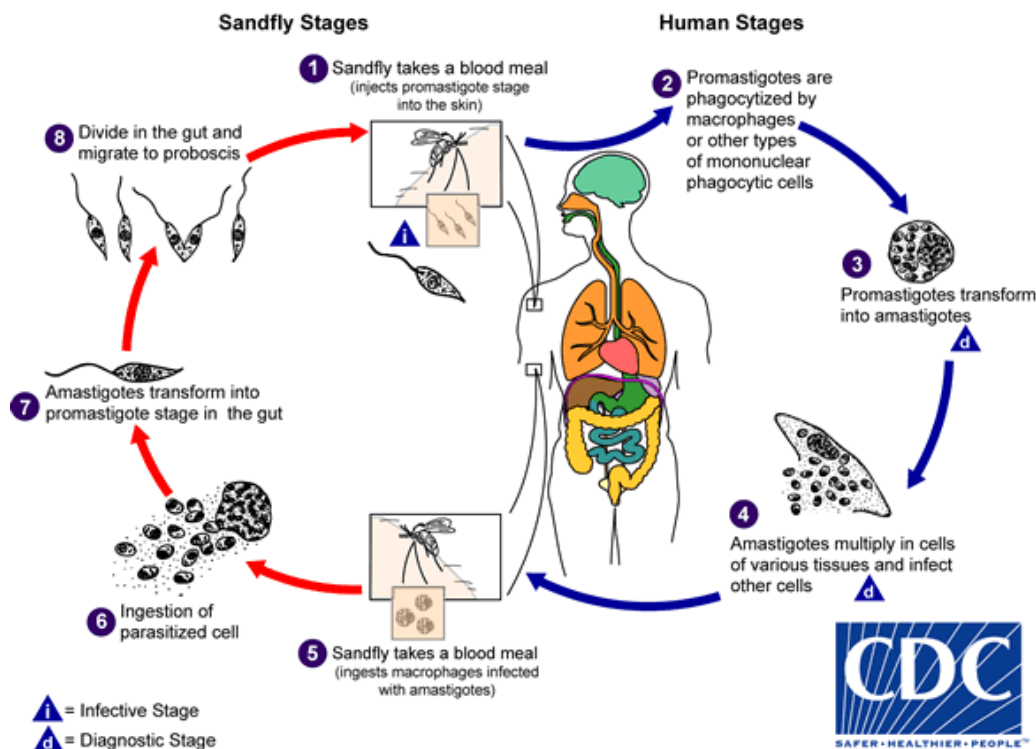


Figure 1 The digenetic life cycle of *Leishmania* spp. 1. When an infected female sand fly takes a blood meal, metacyclic promastigotes are released into the wound; infecting the host. 2. The host's immune cells (macrophages) phagocytose the metacyclic promastigotes in the blood stream. 3. Within the macrophages and acidic conditions, the promastigotes transform into amastigotes. 4. Amastigotes rapidly proliferate, resulting in cell death and go on to infect other cells. 5, 6. When a sand fly takes a blood meal from an infected host, amastigote-infected macrophages are ingested. 7. Within the gut of the sand fly, the amastigotes differentiate through the different promastigote stages. 8. The promastigotes differentiate into the infective metacyclic promastigote stage and migrate to the proboscis. (CDC, 2019).

Within the Mammalian host, the cycle begins with the bite of a female phlebotomine sandfly (Figure 1, point 1), either the *Phlebotomus* or *Lutzomyia* species dependent on the geographical location. Old World leishmaniasis, present in the Eastern hemisphere, primarily Asia, Africa and Southern Europe is transmitted by sandflies of the genus *Phlebotomus*. Whereas New World leishmaniasis is endemic in the Western hemisphere, particularly South America, and is spread by sandflies of the genus *Lutzomyia*. As only female sandflies are known pool feeders, the skin of the human host is broken in a cutting action and the superficial blood vessels damaged, to create a pool of blood to feed on (Bates, 2007). This blood meal begins the cycle and transfer of metacyclic promastigotes as well as promastigote secretory gel and sandfly saliva, into the bloodstream; which synergistically recruits host immune cells to the site of infection (Bates, 1994). The metacyclic promastigotes are then phagocytosed by the recruited immune cells, primarily macrophages (Figure 1, point 2) and within 72 hours metamorphosis occurs (Figure 1, point 3). The transforming into intracellular amastigotes occurs within vacuolar components (phagolysosomes) and is where the parasites are able to survive and reside. Metamorphosis is known to be induced upon exposure to the increased temperature and acidity of the macrophages and the phagolysosomes shown to minimise the exposure and provide protection from the harsh environment (Bates, 1994). Unlike the promastigote form, amastigotes have an extremely shortened flagellum but is not completely diminished. The reduced flagellum is believed to be involved in host-parasite signalling in contrast to the function associated with the promastigotes (Gluezn, Ginger and McKean, 2010). Once within host macrophages, amastigotes rapidly proliferate by binary fission. As a result of the subsequent rupture of the infected cells, amastigotes are then released into the bloodstream to infect further host cells (Figure 1, point 4) (Naderer and McConville, 2007). Naïve sandflies taking a meal from an infected host then ingest infected macrophages and free parasites in the blood (Figure 5, point 6).

Within the Sandfly vector, the *Leishmania* life cycle within the vector differs greatly and includes several promastigote morphologies. Within the sandfly, the life cycle duration is dependent on multiple factors, such as the species and temperature; as higher temperatures have shown to be proportional to a shortened life cycle (Torres-Guerrero, Quintanilla-Cedillo, Ruiz-Esmenjaud and Arenas, 2017). Within 12 to 18 hours of ingesting an infected blood meal, the amastigotes undergo transformation into flagellated procyclic promastigotes. This morphological change occurs due to the reduced temperature and increased pH of the sandfly; either midgut or hindgut depending on *Leishmania* subgenera. The procyclic promastigotes attach to the parasite-specific region of the gut epithelial cells through lipophosphoglycan (LPG), an abundant *Leishmania* surface molecule and rapidly proliferate (Figure 2b) (Pimenta et al., 1994). For 48 to 72 hours, there are multiple transformations into several intermediate promastigote forms before differentiating into the infective metacyclic promastigotes; as seen in Figures 2A and B. Such transformations include the expression of certain surface molecules, such as lipophosphoglycan. This molecule is known to be a stage-specific molecule that is abundant of the surface of promastigotes and is modified when present on metacyclic promastigotes but is almost absent on the amastigote forms (Coutinho-Abreu et al., 2020, Turco and Descoteaux, 1992).

Procyclic promastigotes first transform into nectomonads and cluster in the anterior of the abdominal midgut. Due to *Leishmania* chitinase activity, after three days the peritrophic membrane ruptures resulting in the access and migration of the parasites to the thoracic midgut and stomodeal valve (Pimenta et al., 1997; Rogers et al., 2008). Nectomonads are then able to transform into leptomonads and produce promastigote secretory gel (PSG), which consists of a *Leishmania*-unique glycoprotein named filamentous proteophosphoglycan (fPPG) (Rogers, Chance and Bates, 2002). Leptomonads replicate and proceed into a process named

metacyclogenesis, to transform into the infective metacyclic promastigotes. The process is induced and made favourable due to PSG blocking the anterior of the thoracic midgut. A further intermediate form is the haptomonad that remains and resides in the stomodeal valve of the sandfly through the attachment of the parasitic structure, hemidesmosome (Walters, Chaplin, Tesh and Modi, 1989). The metacyclic promastigotes however, prepare to be transmitted to another host by migrating, via osmotaxis, to the saliva in the sandfly proboscis (Figure 1, 8). PSG has also shown to aid the transmission of the infective *Leishmania* parasites through forcing the sandfly to regurgitate and feed longer (Rogers and Bates, 2007). The gel-like profile of fPPG does this due to the physical obstruction it causes and therefore preventing an adequate blood meal leading to regurgitation of the metacyclic promastigotes, enhances the transmission to the host (Rogers et al., 2004).

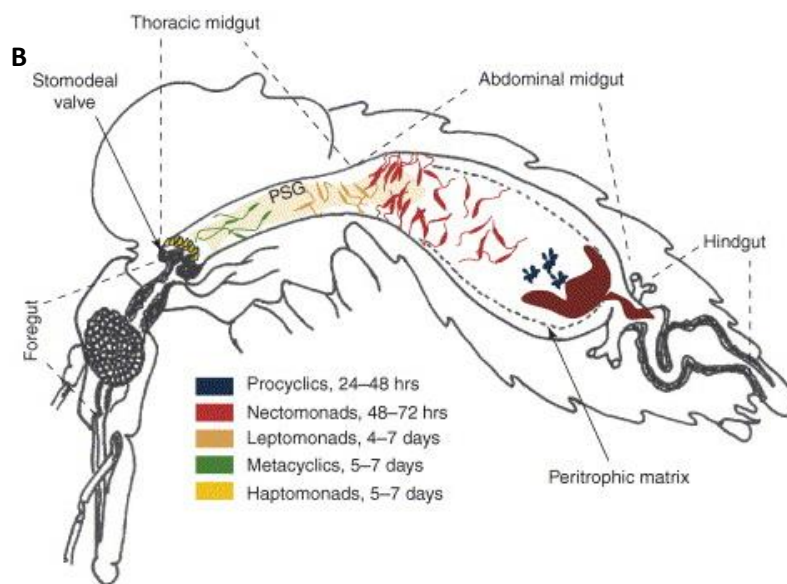
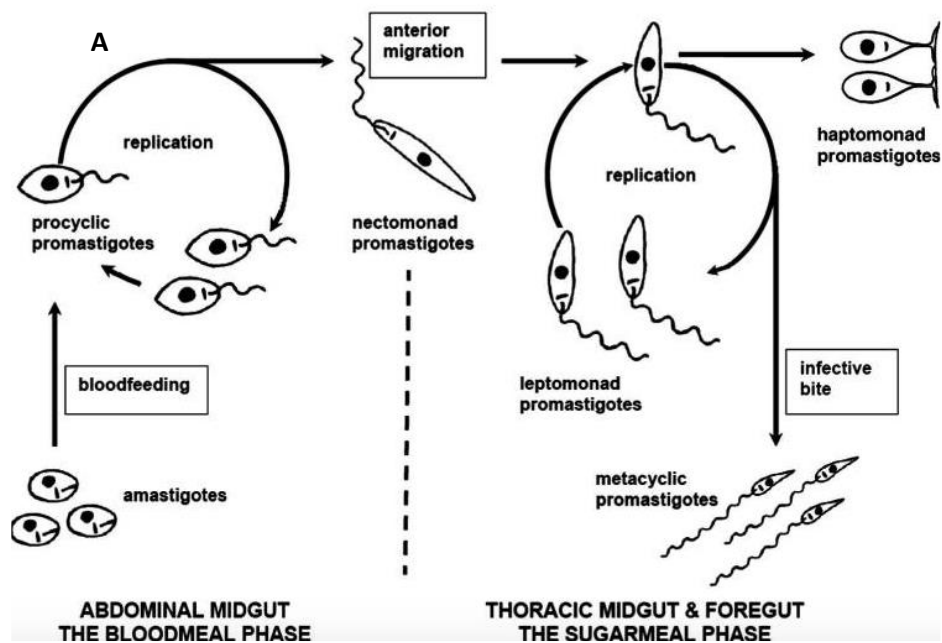


Figure 2 A-B *Leishmania* spp lifecycle within the sandfly vector. The *Leishmania* parasites undergo multiple transformations, from procyclic promastigotes to the infective metacyclic promastigotes (A). These various morphological changes occur within different areas of the sandfly (Figures sourced from Bates, 2007; Kamhawi, 2006).

1.1.2 Structure and gene expression

1.1.2.1 Structure

Leishmania parasites are unicellular eukaryotic organisms in which morphology, biochemistry and molecular changes enable cell survival in different environments and are linked to pathogenicity. The promastigote and amastigote morphologies both include several single-copy organelles. The organelles most widely studied and known include the: nucleus, mitochondrion, Golgi apparatus, kinetoplast and flagellum, as seen in figure 3 (Sunter and Gull, 2017).

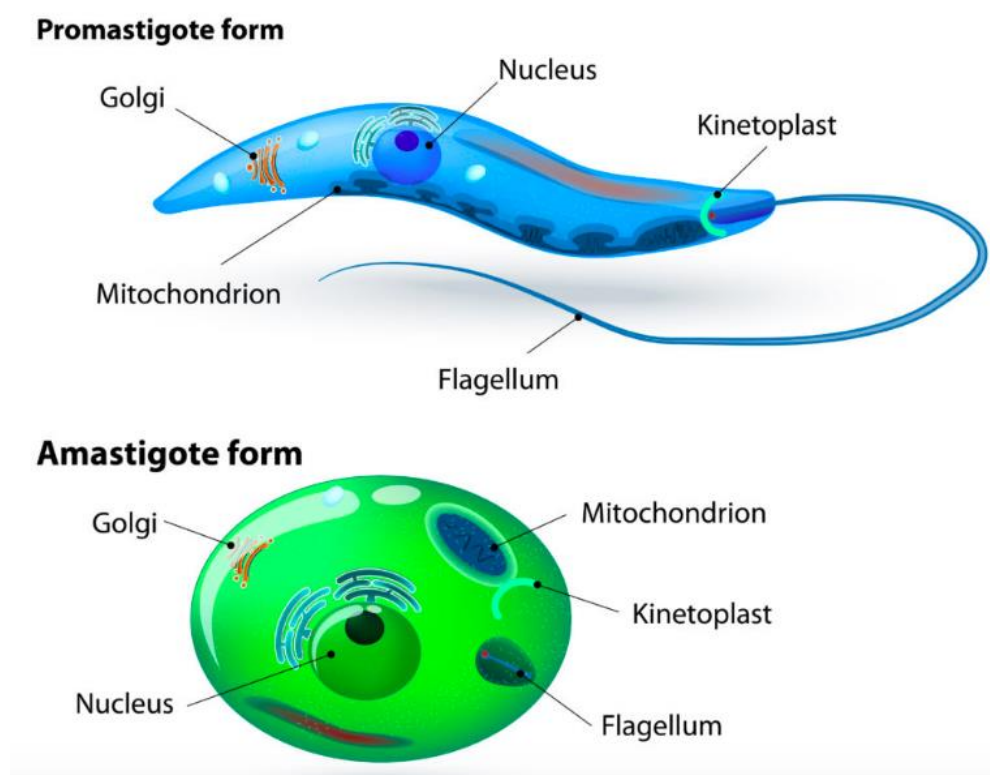


Figure 3 Schematic diagram showing the two forms of *Leishmania parasites*. The diagram shows the major organelles and structure of *Leishmania* promastigote (top) and amastigote (bottom) forms. (Leish@York.,2020).

The kinetoplast is located in close proximity to the nucleus and is found to directly interact with the parasite basal body; though the position of the kinetoplast varies depending on the position within the *Leishmania* life cycle. This disc-shaped granule contains a mass of circular kinetoplast DNA (kDNA), equivalent to that of mitochondrial DNA in other eukaryotes and is composed of 20 - 50 maxicircles and about 10,000 minicircles per parasite. The complicated kDNA network resembles a structure similar to that of chainmail through the interactions of minicircles and maxicircles. Through an individual interlock, each minicircle has been shown to connect with three other minicircles, whereas maxicircle catenanes form a rosette organisation. These separate networks are linked, which possesses a flexible, planar property (Shapiro, 1993).

Maxicircles are about 20-40 kb in size, similar to mitochondrial DNA. Through DNA sequencing, conserved regions of maxicircles have been found to encode proteins typically associated with the mitochondria, such as respiratory enzyme subunits (Camacho et al., 2019). Many of the mRNA transcripts undergo RNA editing, a process involving the addition or deletion of uridine residues from the mRNA. This editing ultimately alters the frameshift in the gene, determining the functionality of the protein-coding genes (Benne et al., 1986; Feagin, Abraham and Stuart, 1988).

Minicircles are about 1kb in size and are composed of many subclasses, conserved in different *Leishmania* species. The conserved region of minicircles is found throughout the genus *Leishmania* and have been found to be an ideal diagnostic target for PCR assays due to such a high copy number (Karamian et al., 2008). However, due to polymorphisms and sequence similarities, PCR assays designed on minicircle conserved regions have the potential to amplify more than one *Leishmania* species (Galluzzi et al., 2018; Mary, Faraut, Lascombe and Dumon, 2004; Rolão, Cortes, Rodrigues and Campino, 2004). Minicircles are essential for editing maxicircle transcripts and encode about four small non-coding RNAs for this function. These

short complementary transcripts, known as guide RNA (gRNA) are directly involved in directing the RNA editing process (Simpson and da Silva, 1971). The complementary section of gRNAs is termed the anchor sequence and are located at the 5' terminal, which then act as a template for uridine addition or deletion. A poly-U tail, either as a source for uridine addition or as a site for acceptance after uridine deletion, is located at the 3' terminal (Blum, Bakalara and Simpson, 1990). This accurate nucleotide mutation process has yet to be understood but possible models include: the cleavage-ligation pathway and the transesterification pathway (Sunter and Gull, 2017).

1.1.2.2 Gene expression in kinetoplastids

Leishmania parasites have a digenetic lifecycle with tightly regulated gene expression to effectively adapt to the two different host environments. These modifications occur both in the nucleus and cytosol and the mechanisms of regulation vary greatly from those typically seen in other eukaryotes.

Within the nucleus, protein-coding genes are found to be arranged into polycistronic transcription units. Regions of the genes marked with specific histone modifications initiate transcription by RNA polymerase II, where transcription is then terminated by the presence of genes to be transcribed by other RNA polymerases (Anderson et al., 2013; Reynolds et al., 2014). RNA polymerase II and several associated transcription factors also drive Splice Leader (mini exon) RNA transcription (Das, Banday and Bellofatto, 2007). From the precursor, the mRNAs are then co-transcriptionally processed. This includes the production of a capped 5' end via *trans* splicing, as well as evidence of cleavage and polyadenylation at the 3' end (Preusser, Jaé and Bindereif, 2012). This *trans-splicing* generates an identically capped sequence of 39 nucleotides at the SL, for each mRNA (Liang, Haritan, Uliel and Michaeli, 2003). RNA-binding proteins (RBPs)

can then form a messenger ribonucleoprotein particle (mRNP) by association with the regulatory sequences in the 3' untranslated region (UTR) of mature RNAs. These mRNPs can then be exported to the cytosol through nuclear pores (Gupta et al., 2014). It has been recently shown that *L. mexicana* has the ability to adapt to heat shock protein 90 (Hsp90) stress conditions by relying on several different protein-RNA interactions within the promastigote and amastigote life cycles (Kalesh et al., 2022).

Within the cytosol, ribosomes are recruited once there is association of mRNAs with translation initiation factors. The RBPs on the 3' (UTR) are often found to remain attached or replaced, indicating the importance of this region for trypanosome gene expression and RNA stability. Sequences associated with the 3'-UTRs have been shown to be very important and affect mRNA translation. The cysteine proteinase B 2.8 gene cluster is known to be highly expressed in the amastigote form of *L. mexicana* parasites. Green fluorescent protein (GFP) has been used to show how the stage-specific post-transcriptional modulation is dependent on the intergenic regions (IR) found 3' of the coding sequence (Misslitz, Mottram, Overath and Aebischer, 2000). Kinetoplastids are known to have five homologues of eIF4E and eIF4G with various phenotypic effects (Freire et al., 2014). This mRNA-binding complex eIF4E, is known to be an essential component in the regulation of translation initiation (Topisirovic, Svitkin, Sonenberg and Shatkin, 2010). The cap-binding initiation factor eIF4E4 has been shown to form complexes with eIF4G3, which are believed to have a significant function in translation and essential for viability (Moura et al., 2015). Some kinetoplastids have RNAi interference machinery; an RNA silencing mechanism found to regulate mutations created by mobile elements (Teixeira, Paiva, Kangussu-Marcolino and DaRocha, 2012). RNAi is absent in many *Leishmania* species, such as *L. major* but *L. braziliensis*, *L. guyanensis* and *L. panamensis* within the *Leishmania* subgenus *Viannia*, have demonstrated a functional RNAi pathway (Lye et al., 2010). Therefore, these *Leishmania* species

have retained key RNAi genes for functional RNAi-mediated regulation, as well as potential active retroposons and RNA viruses (Peacock et al., 2007). As a result of the extensive post-transcriptional regulation involved in kinetoplastid gene expression, the RNA levels often do not match the protein levels produced.

Tight regulation of gene expression in *Leishmania* is vital for the adaptations required in the sandfly and mammalian hosts; including the varying levels of proteins expressed within these environments and the morphological transformations that occur for survival.

1.2 Leishmaniasis

1.2.1 Leishmaniasis forms and pathology

With an estimated one million new *Leishmania* infections each year, the disease is most commonly associated with marginalised populations living in extreme poverty and is endemic in over 98 countries (Alvar et al., 2012). The cases and fatality figures published are often not an accurate representation but deaths from the leishmaniasis are reported to be between 20,000 and 40,000 annually (WHO, 2022).

The three major clinical forms of leishmaniasis are: cutaneous, mucocutaneous and visceral. With over thirty species of *Leishmania*, not all are pathogenic to humans with 15 of the species and subspecies that are pathogenic noted in Table 1, and the clinical form associated.

Localised cutaneous leishmaniasis (LCL) is the least severe but most common form of leishmaniasis with between 600,000 and 1 million new cases each year. CL is also the most widely distributed; with up to 75% of cases present in ten countries (see Table 1). The Old World species *L. (L.) aethiopica*, *L. (L.) major* and *L. (L.) tropica* are the predominant species to cause CL in the Eastern hemisphere. Whereas, *L. (L.) mexicana* and *L. (V.) braziliensis* are the main New World species to cause CL in the Western hemisphere (Alvar et al., 2012).

Usually the face, arms or legs are the site of a sandfly bite due to being areas of exposed skin. An infection will first present as a papule (a small swelling) at this site, within two months. This papule will then progress into the characteristic large, ulcerative lesions associated with

cutaneous leishmaniasis (Bilgic-Temel, Murrell and Uzun, 2019). Most lesions are known to spontaneously self-heal, although this process is relatively slow and depends on the *Leishmania* species (Burza, Croft and Boelaert, 2018; Uzun et al., 2018). Despite this being described as painless, these lesions may be uncomfortable if present near joints, carry psychological and social stigma and can result in life-long disfiguring scars (Bennis et al., 2017). For certain species, such as *L. mexicana* and *L. amazonensis*, it is not uncommon for satellite papules or nodules to appear around the primary lesion, which may indicate diffuse cutaneous leishmaniasis (DCL). Unlike LCL, the lesions associated with DCL rarely spontaneously self-heal and after treatment, relapses are also known to be more frequent (Christensen et al., 2019).

Table 3 The human pathogenic *Leishmania* species for the three main forms of leishmaniasis.

Three main clinical forms			
Cutaneous	Mucocutaneous	Visceral	
<i>L. (L.) aethiopica</i>			Old World species
<i>L. (L.) infantum</i>	<i>L. (L.) infantum</i>	<i>L. (L.) infantum (chagasi)</i>	
<i>L. (L.) major</i>	<i>L. (L.) major</i>		
<i>L. (L.) tropica</i>	<i>L. (L.) tropica</i>		
	<i>L. (L.) donovani</i>	<i>L. (L.) donovani</i>	
<i>L. (L.) amazonensis</i>	<i>L. (L.) amazonensis</i>		New World species
<i>L. (L.) chagasi</i>		<i>L. (L.) infantum (chagasi)</i>	
<i>L. (L.) mexicana</i>	<i>L. (L.) mexicana</i>		
<i>L. (L.) venezuelensis</i>			
<i>L. (V.) braziliensis</i>	<i>L. (V.) braziliensis</i>		
<i>L. (V.) guyanensis</i>	<i>L. (V.) guyanensis</i>		
<i>L. (V.) lainsoni</i>			
<i>L. (V.) naiffi</i>			
<i>L. (V.) panamensis</i>	<i>L. (V.) panamensis</i>		
<i>L. (V.) peruviana</i>			
<i>L. (V.) shawi</i>			
Afghanistan, Algeria, Brazil, Colombia, Iraq, Pakistan, Syrian Arab Republic	Bolivia, Brazil and Peru	Bangladesh, Brazil, Ethiopia, Eritrea, Kenya, India and Sudan, Chad, Iraq, Nepal, Somalia, Yemen	Countries with the highest number of reported cases

With 90% of mucocutaneous leishmaniasis (MCL) cases found in Brazil, Peru and Bolivia, this form of the disease is primarily associated with New World *Leishmania* species. The disease manifests more slowly than CL, with disease progression taking place over several years as opposed to months (Machado, Prates and Machado, 2019). This form occurs when parasites (often *Viannia* subgenera) from CL infections disseminate to mucosal tissue and target the destruction of the nasal and pharyngeal cavity membranes. Eventually these lesions, if left untreated, causes severe disfiguration and mutilation of the face, respiratory difficulties and are potentially fatal. As a result of exposed facial wounds due to MCL, secondary infections are also common, such as *Staphylococcus aureus*, with further implications for the patient and the treatment (Alvar et al., 2012).

Visceral leishmaniasis (VL) is the most severe form because, if left untreated, it is usually fatal within two years in over 95% of cases (WHO, 2020). The causative species for this disease are: *L. (L.) donovani* and *L. (L.) infantum*. *L. (L.) chagasi* was originally described to be the only New World species to cause VL but has since been identified as *L. (L.) infantum* and so, the two names are often used interchangeably (Torres-Guerrero, Quintanilla-Cedillo, Ruiz-Esmenjaud and Arenas, 2017). VL is prevalent in Africa, India, Mediterranean and the New World and is an estimated 50,000 to 90,000 of new VL cases annually; though accurate reports and data are difficult to obtain and it is estimated that only 45% of cases are reported (WHO, 2020).

The visceral form arises when the VL causative *Leishmania* parasites disseminate in the host and proliferate in the liver, bone marrow and spleen. This results in a number of symptoms including: a prolonged fever, weight loss, enlargement of the spleen (splenomegaly) and liver (hepatomegaly) and pancytopenia (McCall, Zhang and Matlashewski, 2013). As a result of the internal damage caused by the parasites, gastrointestinal bleeding and heart or liver failure are

the primary causes of death in those suffering from VL without effective treatment (Chappuis et al., 2007).

VL is also the form implicated with HIV co-infections, as the parasites act as opportunistic pathogens (Lindoso, Moreira, Cunha and Queiroz, 2018). According to the WHO, in 2020 there were an estimated 37.7 million people living with HIV, the majority of whom are in sub-Saharan African. A high *Leishmania* coinfection rate is seen in these prevalent areas where HIV and VL infections overlap, such as Southern Europe and Africa (Alvar et al., 2008). This coinfection is a major challenge for the treatment and control of VL as the *Leishmania* infection accelerates HIV replication and the immunosuppression caused by HIV provides an opportunity for *Leishmania* to successfully infect the host (Lindoso, Moreira, Cunha and Queiroz, 2018; WHO, 2022).

Despite only one of the three major forms of the disease being fatal, all clinical manifestations of leishmaniasis can result in life-long psychological and social stigma and debilitating chronic illness. Desjeux, 2004 reported that the disability-adjusted life years (DALYs), meaning the years estimated to have been lost, as a result of the ill health and deaths associated with leishmaniasis is 2.4 million. However, this generalised quantification of the impact inflicted by the disease does not consider the stigma or mental health effects attributed to all forms of leishmaniasis and is therefore likely to underestimate the true burden of this disease.

1.2.2 Epidemiology and Risk Factors

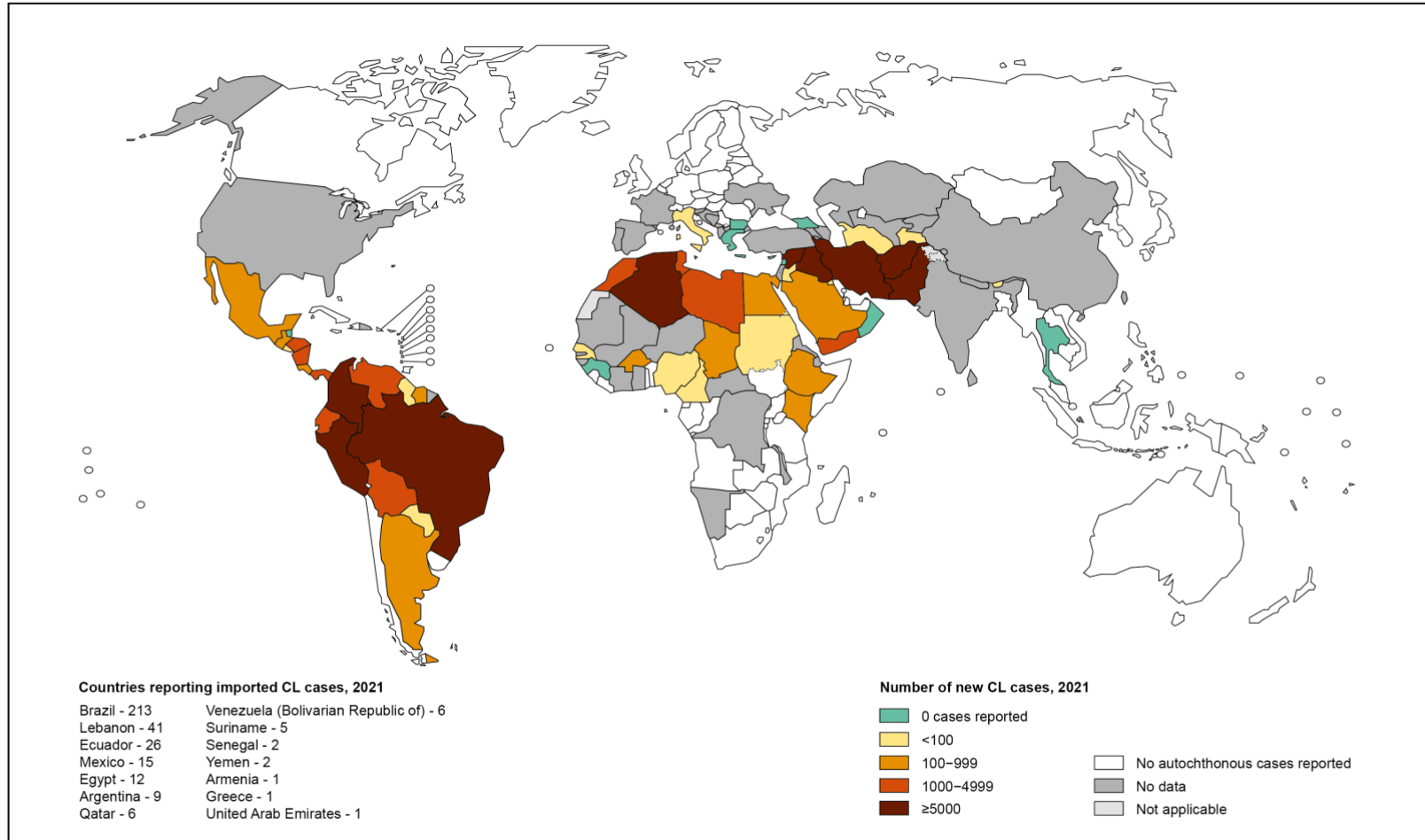
The distribution of leishmaniasis is shown in figures 4 A-B, although under reporting and misdiagnosis of the disease should be considered. Major risk factors that are responsible for the distribution of *Leishmania* infections include: socioeconomic conditions, malnutrition,

population mobility and environmental changes, such as climate change (González et al., 2010; Koch, Kochmann, Klimpel and Cunze, 2017).

Those residing in marginalised societies with inadequate sanitation, resources and housing are most at risk of *Leishmania* infections. These poor conditions, such as overcrowded living, open sewerage and sleeping without protection on the ground or outside creates a favourable environment for sandfly resting, breeding and blood meals (Okwor and Uzonna, 2016; Oryan and Akbari, 2016).

This risk has been increasingly evident with immigrants and within refugee camps. Increasing numbers of travellers and more significantly, population displacement as a result of conflict, have shown to impact the distribution of the disease. The over-population and poor temporary accommodation have resulted in CL epidemics due to such inadequate conditions (Fotakis et al., 2019). A significant increase in CL cases have been reported in Syria and surrounding areas following the beginning of the Syrian conflict in 2011; despite leishmaniasis being endemic in this area for over two centuries. An estimated 6.7 million Syrians have been internally displaced and a further 6.6 million Syrian refugees worldwide. As a result, the health care infrastructure is extremely poor due to the destruction of public hospitals and has resulted in temporary overcrowded living conditions for millions of people (Du, Hotez, Al-Salem and Acosta-Serrano, 2016).

A Status of endemicity of cutaneous leishmaniasis worldwide, 2021



The boundaries and names shown and the designations used on this map do not imply the expression of any opinion whatsoever on the part of the World Health Organization concerning the legal status of any country, territory, city or area or of its authorities, or concerning the delimitation of its frontiers or boundaries. Dotted lines on maps represent approximate border lines for which there may not yet be full agreement. © WHO 2022. All rights reserved

Data Source: World Health Organization
Map Production: Control of Neglected
Tropical Diseases (NTD)
World Health Organization



B Status of endemicity of visceral leishmaniasis worldwide, 2021

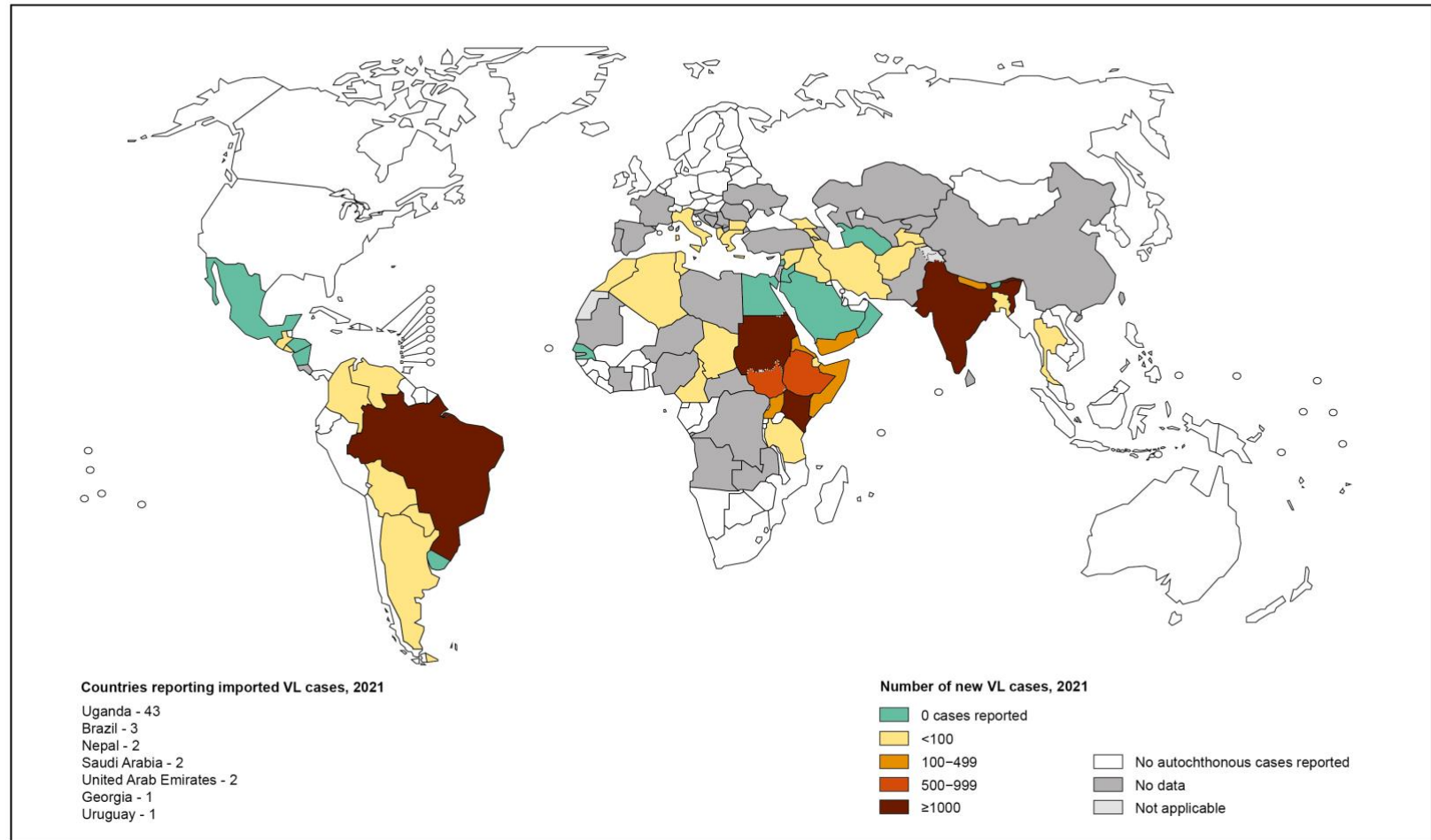


Figure 4 A-B Distribution maps of reported cases of cutaneous (A) and visceral (B) leishmaniasis in 2021 (WHO, 2022).

1.2.3 Immune response to *Leishmania*

1.2.3.1 Innate immune response

Leishmania-Neutrophil interaction

Neutrophils, or polymorphonuclear neutrophils (PMNs) are the first innate immune cells to rapidly migrate to the site of parasitic infection. These motile cells are essential for host defence against various pathogenic microorganisms, through the release of proteolytic enzymes and reactive oxygen species (ROS) production (Ribeiro-Gomes and Sacks, 2012). Neutrophils are present at the infection site within a few hours of tissue damage from *Leishmania* inoculation, either via a sandfly bite or needle injection (Peters et al., 2008). Around 80 to 90% of metacyclic promastigotes are phagocytosed by neutrophils within the first 24 hours of infection (Ribeiro-Gomes et al, 2012) to temporarily function as an intermediate host (figure 5) (Laufs et al., 2002).

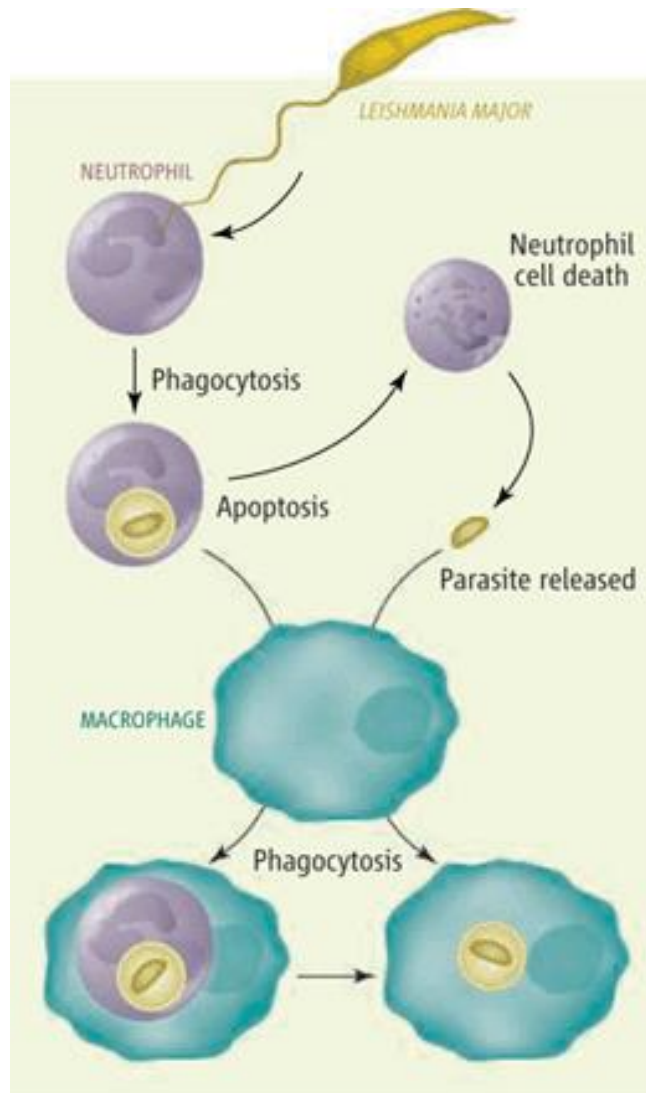


Figure 5 Trojan horse model of innate immune response to *Leishmania* infection. The phagocytosis of infective promastigotes by neutrophils, either results in apoptosis of the cell or phagocytosis by macrophages (John and Hunter, 2008).

The interaction of *Leishmania* with host neutrophils, promotes the production of numerous chemokines and microbicidal factors to eliminate the parasites and aid the immune response. Such mechanisms include; the production of ROS, the cytokines IL-8 and IL-12, the release of azurophilic granules (containing Neutrophil Elastase (NE) and myeloperoxidase (MPO)) and neutrophil

extracellular traps (NETs). *Leishmania* promastigotes produce the neutrophil chemotactic factor – LCF, which induces the secretion of IL-8 to amplify the recruitment of neutrophils to the site of infection (van Zandbergen et al., 2002) and the azurophilic granules release proteolytic enzymes, as well as defensins – increasing the permeability of the target cell membranes (Oualha et al., 2019). The filamentous structure of NETs is composed of chromatin DNA filaments coated with granular proteins and these structures have the ability to capture and kill microorganisms. The release of these structures induces a process similar to apoptosis and necrosis, known as NETosis – the mechanisms are triggered by *Leishmania* promastigotes either; through redox imbalance and elastase involvement or via an elastase-dependent and ROS-independent manner (Guimaraes-Costa et al., 2009; Rochael et al., 2015). Interestingly, although several studies have demonstrated the interaction and function of NETs with *Leishmania* species, evasion mechanisms have been shown; allowing these parasites to avoid NET-killing. The nuclease activity of promastigotes, specifically 3'-nucleotidase, allows for the cleaving of NETs by 3'NT/NU (enzyme 3'-nucleotidase/nuclease) (Guimarães-Costa et al., 2014).

The half-life of neutrophils is typically short, between 6 and 10 hours, before apoptosis spontaneously occurs. After two to three days, a second wave of monocytes arrive at the site of infection to phagocytose the apoptotic infected neutrophils (Thalhofer et al., 2011). However, *Leishmania* have shown the ability to delay the spontaneous apoptosis of the infected neutrophils by two to three days. Extending the neutrophil life span by inhibiting the apoptosis-inducing caspase, caspase-3, allows for the silent and unrecognisable internalisation of *Leishmania* into macrophages – the neutrophils effectively acting as a 'Trojan Horse' (Aga et al., 2002; Chaves et al., 2020; van Zandbergen et al., 2004).

Leishmania-macrophage interaction

Upon arrival at the site of infection, the monocytes recruited by chemokine (CCL3 and CCL4) secretion, differentiate into either macrophages or dendritic cells. *Leishmania* are either thought to infect macrophages via the 'Trojan Horse' process (figure 5), which has been studied using fluorescently-labelled cells *in vitro* or phagocytosed directly having left the apoptotic neutrophils, which has been studied using intravital microscopy and flow cytometry (Peters et al., 2008).

Macrophages are the primary host cells for *Leishmania* and the site of differentiation from promastigotes into amastigotes and therefore, integral for parasite persistence and infection. Shortly after phagocytosis, the process of phagolysosomal biogenesis occurs, during which a parasitophorous vacuole (PV) is formed in which the *Leishmania* reside (Courret et al., 2002). Produced through the fusion of the phagosome with lysosomes, *Leishmania* remodel and interrupt the phagosome-lysosome fusion to provide extended time for differentiation into amastigotes. This delay in phagosome maturation is attributed to the LPG expression on the metacyclic promastigote surface. This surface glycoconjugate has shown to inhibit proton-ATPase recruitment on the phagosome membrane. Once differentiated, amastigotes are hydrolase-resistant, therefore allowing for their intracellular survival and protection from the acid hydrolases present within the PV (Forestier et al., 2011; Moradin and Descoteaux, 2012).

Infected macrophages subsequently become activated by tumour necrosis factor (TNF) and primarily interferon (IFN)- γ , both produced by CD4⁺T lymphocytes and natural killer (NK) cells (Bogdan, 2012). This activation results in the increased generation of either: inducible nitric oxide (iNOS) or type 2 nitric oxide synthase (NOS2). iNOS or NOS2 catalyses the L-arginine to L-citrulline conversion, which also produces nitric oxide (Bogdan, Rollinghoff and Diefenbach, 2000; Müller et al., 2013). Nitric oxide (NO)

derived from iNOS is not only a potent effector against *Leishmania* but is also a central metabolite in Th1 cell signalling and response (Bogdan, 2015).

Leishmania-dendritic cell interaction

During *Leishmania* infections, monocyte-derived dendritic cells have a significant role in promoting antigen-specific Th1 responses and cytokine production (Petritus et al., 2012). DCs are highly involved in the adaptive immune response as they function to process *Leishmania* antigens and present them to T cells once migrated from the infection site to the draining lymph node (Ritter et al., 2004). Also, shown to be major IL-12 and iNOS producing cells, DCs therefore stimulate the Th1 cell formation and parasite killing; though IL-12 and iNOS suppression has been demonstrated in various species of *Leishmania* (Favila et al., 2014; McDowell et al., 2002; Petritus et al., 2012).

1.2.3.2 Adaptive immune response

The types of cytokines released by the innate immune cells shortly after a *Leishmania* infection fundamentally dictates the type of adaptive immune response; Th1 or Th2. The presented *Leishmania* antigens via the major histocompatibility complex (MHC) of DCs will either stimulate a CD8⁺ T cell response through the MHC class I pathway or a CD4⁺ Th cell response, through the MHC class II pathway. During a *Leishmania* infection, MHC class II is typically shown as the molecules present in this complex are mainly peptides derived from endocytosed microorganisms and therefore, the activation of CD4⁺ T cells primarily occurs (Muraille et al., 2010).

Th1 and Th2 are the two subsets of CD4⁺ Th cells and their activation are determined via the cytokines released from infected macrophages and DCs. The IL-12 production from the infected innate immune cells, consequentially forms Th1 cells via the activation of the STAT4 pathway (Rossi and Fasel, 2017).

The IFN- γ produced during the infection has shown to induce IL-12 production and Th1 cell formation

by effectively generating a positive feedback loop (Park, Hondonwicz and Scott, 2000). This Th1 response promotes cellular immunity and parasite elimination through the stimulation of macrophage-released toxic metabolites, such as iNOS production. Whereas the secretion of IL-4 and IL-13 from basophils, mast cells and eosinophils form Th2 cells through the activation of the STAT6 pathway. The secretion of IL-10 from Th2 cells also aids a Th2 focused response by inhibiting IFN- γ and therefore suppressing Th1 cell production (Schwarz et al., 2013). The Th2 response involves the production of *Leishmania*-specific antibodies by humoral immunity and B cell activation. This response has however been described to promote susceptibility and is insufficient for parasite clearance and control. However, *in vivo* studies have expanded on the adaptive immune responses and have demonstrated the complexity of the Th1/Th2 subsets as a heightened Th1 response, resulted from high TNF- α levels, actually favours metastatic development of DCL infections (Silveira et al., 2009).

However, *Leishmania* parasites have evolved to evade the complexities of the host immune system. The developed immune evasion mechanisms are employed to manipulate the host immune responses and pathways, in order to successfully adapt and survive. Although the evasion strategies still require further research to fully comprehend, they are known to involve the manipulation of specific signalling pathways. The pathways known to be repressed due to *Leishmania* infections include JAK/STAT, mitogen-activated protein kinases and Ca²⁺-dependent protein kinase C. The dysfunction of JAK2/STAT1 signalling, for example, results in disrupted macrophage function, such as the inhibition of IFN- γ -inducible functions, such as nitric oxide (NO) and IL-12 production (Olivier, Gregory and Forget, 2005).

Leishmania surface molecules are important in immune evasion, with the expression of several essential surface molecules being stage-specific and directly linked to pathogenicity. The most abundant surface molecule associated with metacyclic promastigotes is lipophosphoglycan (LPG) and

is found to coat the parasite surface, anchored to a dense glycocalyx jacket (Rossi and Fasel, 2017). LPG is found in all *Leishmania* promastigote species but varies in glycan side chains and composition of the core structure. LPG is known to have important interactions and contribution in the evasion of complement-driven lysis. The increased length of LPG on metacyclic promastigotes compared to procyclic promastigotes (Soares et al., 2002) inhibits C5b-C9 subunit attachment of the complement complex and *L. donovani* promastigotes have shown to attach to the inactive C3bi subunit, preventing C5 convertase formation (Puentes, Dwyer, Bates and Joiner, 1989). LPG also has a significant role in macrophage attachment, where metacyclic promastigotes interact with complement receptor 1 (CR1) transiently and complement receptor 3 (CR3) of macrophages through C3b and C3bi interactions (Gupta, Oghumu and Satoskar, 2013). Due to CR3 attachment, the usual oxidative burst during phagocytosis does not occur (Mosser and Edelson, 1987; Polando et al., 2013)).

The zinc metalloprotease, gp63 is a critical virulence factor and is also found throughout the surface of promastigotes but is less abundant than LPG. GP63 also has a significant role in *Leishmania* survival and evasion of the complement system. The surface glycoprotein is known to be responsible for the cleavage of C3b into the inactive, C3bi on the promastigote surface to reduce C5 convertase formation (Brittingham et al., 1995) and provide resistance against the complement-mediated lysis. The function of gp63 has shown to protect different *Leishmania* species and favouring opsonisation and internalisation of the parasites (Olivier, Gregory and Forget, 2005). Gp63 is also involved in the modulation of several cell signalling pathways. Gp63 has been shown to cleave protein tyrosine phosphatases within the macrophage cytoplasm, which in turn inhibits macrophage inflammatory functions and promotes parasite infection (Gomez et al., 2009). Multiple signalling pathways and proteins have also been reported to alter upon *Leishmania* infection of the macrophage, including JAK, MAP and IRAK-1 kinase pathways and mTORC1-dependent signalling, which in turn leads to the down regulation of protein synthesis (Isnard, Shio and Olivier, 2012).

Therefore, despite the harsh environment intracellular parasites are exposed to, they quickly adapt to resist host first-line defences.

1.2.4 Diagnosis of leishmaniasis

1.2.4.1 Microscopy

Microscopic observation remains the primary technique for diagnosing *Leishmania* infections. Detecting *Leishmania* parasites in suspected cases of CL involves a biopsy or dermal scraping of the active lesion; whereas for VL, aspirates of the bone marrow, spleen and lymph nodes are performed. These smear samples are Giemsa-stained and examined under a light microscope for the direct identification of amastigotes. This host-specific stage of *Leishmania* parasites are observed by the following characteristics; a rounded body between 2-4 μm in diameter and the presence of large nuclei and rod-like kinetoplasts. Under Giemsa-stained conditions, the cytoplasm of the amastigotes would appear pale blue, the nucleus red and the kinetoplast violet, shown in figure 6. Parasite density is then recorded in a logarithmic scale, ranging from 0 to +6, respective of 0 to >100 parasites per oil immersion field; resulting in a negative or positive score (Schallig et al., 2019).

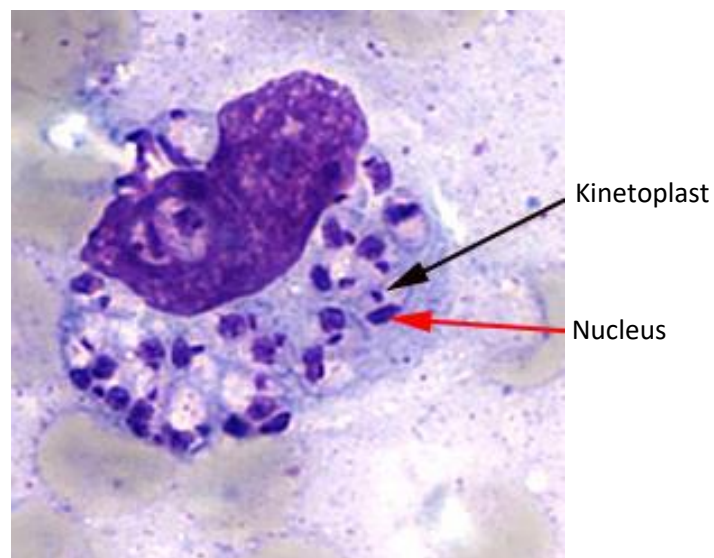


Figure 6 Light microscopic image of a Giemsa-stained infected macrophage (CDC, 2018).

Despite the frequent use of this procedure, it is an invasive method with variable sensitivity and limited information. Obtaining bone marrow and splenic aspirations is a skilled procedure that is not only invasive but uncomfortable and painful for the patient, with possible fatal complications. If splenic aspirations are incorrectly performed, there is an associated risk of fatal haemorrhage. Therefore, patients exhibiting a platelet count of less than 40,000 platelets/ μl should have samples obtained from elsewhere to avoid splenic puncture (Sundar and Rai, 2002).

Microscopic detection can determine parasite load but fails to distinguish between *Leishmania* species, which is necessary information for subsequent treatment of the patient. The sensitivity of diagnosis by this method varies greatly, including low sensitivity being demonstrated for HIV co-infected patients (Cota et al., 2012). Due to the dependency of parasite dispersion in the acquired samples and the experience of the personnel performing the examination, sensitivity of diagnosing *Leishmania* infections by microscopy have been reported to be between 42% and 95% (Aviles et al., 1999). The sensitivity of lymph node smears is low, between 50 and 80 %, bone marrow smears have shown 60 to 85% sensitivity and splenic smears have exceeding 90% sensitivity. As well as the variable of sample type, parasite species also affects the sensitivity of microscopic examination (Al-Hucheimi, Sultan and Al-Dhalimi, 2009).

Despite these limitations, this diagnostic practise is inexpensive, rapid and specific; providing a useful approach for endemic areas, where expertise and costly equipment is often absent.

1.2.4.2 Culturing

Culturing *Leishmania* parasites can be performed to provide an alternative or additional diagnostic method for a failed diagnosis or often to supplement routine methods. *Leishmania* cultures provide high specificity for parasite detection by producing sufficient parasite quantity, which can then be used for numerous diagnostic methods, such as immunological methods, microscopy or for *in vitro* drug screening.

The culture media used to maintain *Leishmania* strains varies depending on the purpose of parasitic culture. For primary isolation of *Leishmania*, a diphasic medium is used whereas for parasite amplification, a supplemented monophasic medium is typically used. *Leishmania* promastigotes are commonly maintained within Schneider's medium supplemented with heat-inactivated foetal calf serum, penicillin and streptomycin (Goto and Lindoso, 2010). One to two drops of obtained bone marrow or splenic aspirate is added to the supplemented Schneider's medium and the samples incubated between 22°C and 28 °C. Microscopic examination of the cultures, for *Leishmania* promastigote observation, is performed frequently for 4 weeks.

Rarely, *Leishmania* cultures may also be performed for further diagnostic studies *in vivo*. Intraperitoneal or intrasplenic inoculation of either promastigotes or amastigotes into animal subjects can be performed for *Leishmania* diagnosis. The infection is examined weekly for physical manifestations, such as lesions and hepatosplenomegaly. Splenic and liver biopsies are also taken to obtain amastigotes in tissue and confirm a *Leishmania* infection (Akhoundi et al., 2017). This procedure is very time-consuming as it could take many months for symptoms to arise and requires an extensive and expensive laboratory set up; it is therefore not commonly practiced for this purpose.

Amplifying *Leishmania* promastigotes by culturing can also be applied to species identification and a supplementary method for cellulose acetate electrophoresis. This technique is used to analyse the species-species isoenzyme pattern with a required large parasite load (Reithinger and Dujardin, 2016). However, this method is not high throughput and relied on cultured parasites and therefore could not be used for clinical samples (Rasti et al., 2016). The use of this practice is outdated and PCR-RFLP (restriction fragment length polymorphism) is now a more common alternative. PCR-RFLP allows for a faster and sensitive detection of specific *Leishmania* species through the use of species-species restriction sites (Akhoundi et al., 2017; Ben Abda et al., 2011).

1.2.4.3 Immunological tools for diagnosis

Immunological methods are often employed for the diagnosis of *Leishmania* due to the easiness and accuracy they offer. Despite the techniques often used, misdiagnosis is possible and there are limitations of its use due to cross reactions and implications in those who are immunosuppressed.

These limitations of immunological tools are known for the widely used Montenegro skin test (MST) but is still commonly used in endemic areas such as Brazil. MST suffers in accuracy for certain forms of the disease and in immunocompromised patients. As well as the variability in accuracy, the applicability of the method is far from what is desired also. Aside from cross-reactions, if patient cooperation is low, the risks of false positives are likely and the length of time for a retest is at least two years if necessary (de Paiva-Cavalcanti et al., 2015). Despite these, it has been used in association with indirect immunofluorescence assay (IFA) to successfully diagnose cutaneous leishmaniasis. As IFA is a method dependent on anti-*Leishmania* antibody detection, it is a technique with low specificity and inability to distinguish circulating antibody levels with the stage of disease (Szargiki et al., 2009).

Enzyme-Linked Immunosorbent Assays (ELISA) using highly specific and sensitive recombinant *Leishmania* antigens, have shown to be very successful in diagnosing. The most widely employed *Leishmania* antigen is the highly conserved, recombinant K39 (rK39) and has performed in VL diagnosis with 100% specificity and 96% sensitivity (Palatnik-de-Sousa et al., 1995), very rapidly. Patients who are co-infected with HIV are often difficult to diagnose VL, but this antigen is able to successfully diagnose the disease at point of care (de Paiva-Cavalcanti et al., 2015). Other candidates for this method include recombinant membrane glycoproteins, such as gp63, which can improve the sensitivity and specificity of ELISA (Oliveira et al., 2011). Cross-reactions with other antibodies are still a possibility and therefore false positives may result in healthy individuals receiving unnecessary antileishmanial treatment and is therefore a limitation of ELISA (Regli et al., 2017).

Rapid diagnostic tests (RDTs) are widely applied immunological kits, largely explored due to accessibility for field conditions. Also based on the detection of specific antibodies, RDTs are used for the quick detection of VL using serum (Vaish et al., 2012) or peripheral blood (Kumar et al., 2013). The rK39 rapid immunochromatic strip tests and direct agglutination test (DAT) are seen to be the main tool for VL (*L. donovani*) diagnosis in certain endemic countries, such as India, Nepal and Bangladesh (Cunningham et al., 2012). DAT is able to remain stable with the use of freeze-dried antigens and rK39 test strips are able to produce rapid results in 10 minutes; with both very easy to use and therefore facilitates their application in endemic areas with limited resources (Mohebbi et al., 2011). Like with all serological tests however, there is the possibility of cross-reaction as well as, the inability to accurately differentiate active and quiescent infections.

1.2.4.4 Molecular tools for diagnosis

Recent research advancements have resulted in the genome sequencing of a number of the *Leishmania* species and strains, providing valuable information on differences in gene content

between them (Franssen et al., 2020). This has provided a platform to develop further molecular diagnostics for leishmaniasis. Polymerase chain reaction (PCR) kits have proved to function as one of the most sensitive and specific techniques used for VL diagnosis (Singh and Sundar., 2015). The sensitivity of amplifying *Leishmania* DNA is dependent on where the biological sample was obtained, such as blood or bone marrow and the primers used, such as small subunit ribosomal rRNA or kDNA. Such high sensitivity has also shown to be effective for VL diagnosis for those co-infected with HIV as less than 100 parasites per ml are regularly observed (de Ruiter et al., 2014). PCR-based diagnostics however, often lack field applicability due to expensive equipment and a long time to produce results; therefore, a PCR-based technique known as Loop-mediated isothermal amplification (LAMP) has been developed (Nzelu, Kato and Peters, 2019).

The LAMP technique consists of a *Bacillus stearothermophilus* (*Bst*) DNA polymerase and a set of four primers. The two inner primers and two outer primers are highly specific as they recognise six target DNA sequences with two additional primers occasionally used to reduce the required reaction time by accelerating the amplification reaction (Nagamine, Hase and Notomi, 2002). Both species-specific and genus-specific assays have been established for VL based on the kDNA and 18S rRNA/ ITS1 genes respectively (Abbasi, Kirstein, Hailu and Warburg, 2016). LAMP is highly efficient, as within an hour it can amplify a few copies of DNA to 10^9 and does so in three main steps: initiation, cycling amplification and elongation (Notomi et al., 2000). The auto strand displacement properties of the *Bst* DNA polymerase means that constant temperature fluctuation through expensive thermal cyclers is not needed and the reaction can occur at a maintained temperature using simple equipment. Not only is available and cost-effective equipment such as, a water bath required, the results are quick and can be analysed using simple colorimetric visualisation and/or agarose gel electrophoresis (Nzelu et al., 2014) – providing an advantageous method for field application. As well as high sensitivity and specificity, performing at a similar standard to known PCR methods, 100% sensitivity and specificity has also been reported for patients suffering from both VL and HIV (Adams et al., 2018). This recent

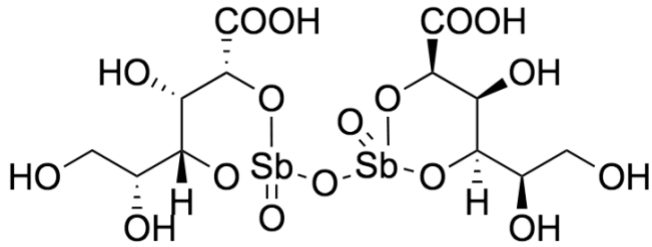
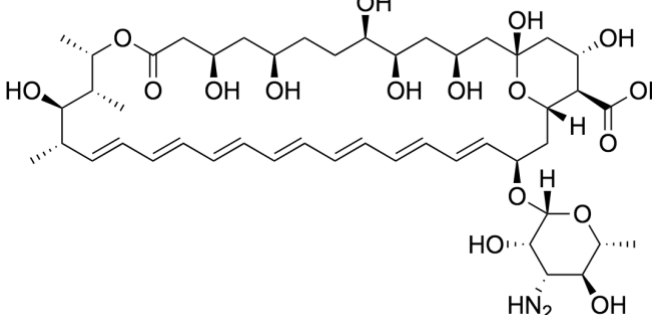
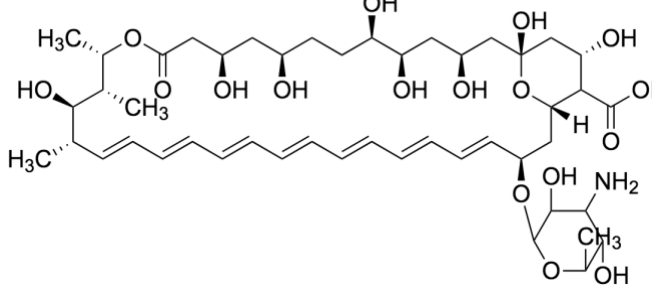
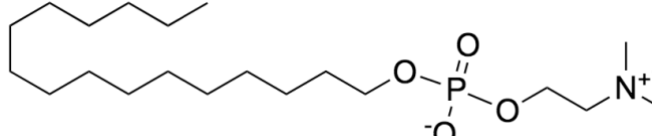
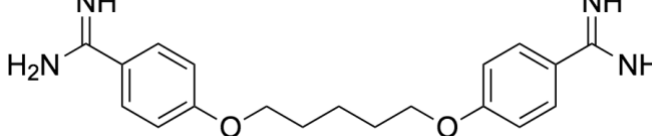
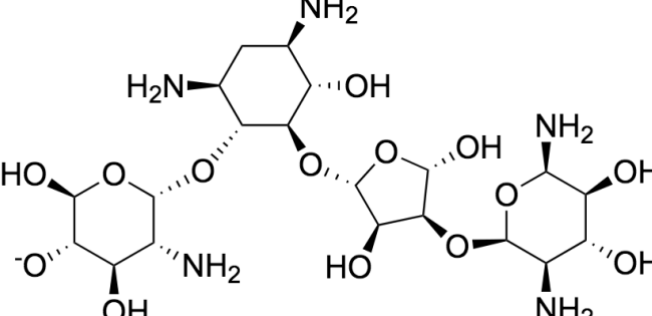
molecular tool has emerged as a promising point of care VL and PKDL diagnostic technique for those in endemic areas.

Despite the range of diagnostic tools and leishmaniasis known to mainly affect those living in extreme poverty, many of the techniques developed and used are not suitable for point of care diagnosis. However, with recent and ongoing research developments, field-adaptable tools are emerging where speed, expense and expertise are taken in consideration.

1.2.5 Treatments

Current treatments for the different forms of leishmaniasis are heavily dependent on chemotherapy, however the universal drug treatments employed are far from ideal, with the majority of drugs repurposed from other conditions or infections. Each of the therapeutic options currently in use are associated with major limitations, involving long and painful administration, toxic side effects and/or emerging issues with drug resistance. The chemical structures of the main anti leishmanial drugs discussed in this thesis are shown in Table 2.

Table 4 Structures of sodium stibogluconate, amphotericin B, AmBisome, miltefosine, pentamidine and paromomycin, drawn in ChemDraw JS.

Drug	Structure
Sodium stibogluconate	 <p>The structure shows a central antimony (Sb) atom coordinated to two gluconate rings and two oxygen atoms. Each gluconate ring is a six-membered ring with hydroxyl groups at various positions and a carboxylic acid group (COOH) at the C5 position.</p>
Amphotericin B	 <p>The structure features a long, unsaturated macrocyclic ring system with multiple hydroxyl groups. It is substituted with a diethylamino group (HN₂) and a glucose moiety at the C3 position, and a carboxylic acid group at the C12 position.</p>
AmBisome	 <p>The structure is similar to Amphotericin B but includes two methyl groups (H₃C) on the macrocyclic ring and a trimethylammonium group (N⁺CH₃)₃ on the glucose moiety.</p>
Miltefosine	 <p>The structure consists of a long, saturated alkyl chain (heptadecyl) attached to a phosphorus atom, which is also bonded to an oxygen atom and a trimethylammonium group (N⁺CH₃)₃.</p>
Pentamidine	 <p>The structure shows a central pentamidine chain (a 1,5-diazabicyclo[3.3.0]heptane derivative) with two phenyl rings attached at the 2 and 7 positions. Each phenyl ring has a guanidino group (NH₂C(=NH)-) at the para position.</p>
Paromomycin	 <p>The structure is a complex oligosaccharide consisting of several linked sugar rings, including a hexose and a pentose, with multiple hydroxyl groups and amino groups (NH₂) attached.</p>

1.2.5.1 Pentavalent antimonials

Pentavalent antimony compounds (Sb^V), such as sodium stibogluconate, SSG (Pentostam[®]) and meglumine antimoniate (Glucantime[®]) are frequently used as first-line therapy for cutaneous leishmaniasis. Antimonials were also a frontline treatment for VL but their use has been considerably restricted due to the toxicity and resistance. Variable cure rates have been observed, primarily in Bihar; a region of India (Rijal et al., 2010; Sundar et al., 2000; Thakur and Narayan, 2004) and areas of neighbouring countries (Lira et al., 1999), due to resistance. Such low efficacy of pentavalent antimonials in Bihar was found to be a result of chronic exposure to naturally occurring trivalent arsenic in the drinking water, therefore resulting in cross-resistance to VL treatment (Perry et al., 2013).

The administration regime for the antimonials has been modified over the years, with the recommended dose of sodium stibogluconate increasing from 10 mg/kg per day to 20 mg/kg per day in attempts to overcome emerging resistance (Olliaro et al., 2005; WHO., 1984). This dose is usually administered intravenously, over a 20-day period for CL. This treatment regime is costly, and hospitalisation is required (Uliana, Trinconi and Coelho., 2017). In addition to the expense and access, the systemic side effects are adverse and toxic (nausea, myalgia, vomiting, diarrhoea, hepatotoxicity and cardiotoxicity), with a long treatment duration needing multiple injections.

Despite its years of use, the mechanism of action and site of reduction for Sb^V is disputed and not entirely understood, although there are two models currently used: “pro-drug” model and “active Sb^V ” model.

Many studies have revealed that within mammalian tissues, Sb^V is reduced to an active but toxic trivalent form, Sb^{III} and is therefore considered a pro-drug (Goodwin and Page, 1943). The cause of this reduction is still unclear but numerous studies have indicated this conversion to occur within both; the macrophage of the host and the parasite itself (Ponte-Sucre et al., 2017). The thiols involved in this reaction are the four mono- and di-thiols: glutathione (GSH), cysteine (Cys), cysteine-glycine (Cys-Gly) and trypanothione ($T(SH)_2$), with the latter three mentioned having demonstrated to induce the conversion at 37°C in an acidic pH (dos Santos Ferreria et al., 2003). These conditions are representative and favourable of the intrinsic environment of *leishmania* amastigotes, which suggests that the reduction of Sb^V to occur within the parasite by these thiols (Shaked-Mishan et al., 2000). An overexpression and downregulation of the parasite membrane carrier, aquaglyceroporin (AQP1), resulted in the hypersensitivity and resistance of Sb^{III} in *L. donovani* isolates respectively (Mandal et al., 2010). AQP1 is therefore known to be the most significant and primary source of entry for Sb^V into the parasites once reduced within the host macrophage, whereas the entry for the unreduced Sb^V form is still unknown.

Following this “pro-drug” model, the active trivalent state forms complexes with the two significant thiols, GSH and $T(SH)_2$ as $Sb(GS)_3$ and T-Sb respectively (Sun, Yan and Cheng, 2000; Yan et al., 2003). These interactions are believed to result in apoptosis-like parasite death through the binding of the antimony-thiol complexes to either trypanothione reductase (TR) or a zinc finger peptide (Frézard, Demicheli and Ribeiro, 2009). The binding to the active site of TR is believed to result in apoptosis through the downstream inhibition of $T(SH)_2$; an essential intermediate for, thiol redox homeostasis (Wyllie, Cunningham and Fairlamb, 2004). This provides oxidative protection (Vickers and Fairlamb, 2004) and is involved in the integral parasitic phosphates required for DNA synthesis (Krauth-Siegel and Comini, 2008). This inhibition therefore increases parasite susceptibility to oxidative stress, as well

as, indirectly disrupting cell metabolism. Both this interaction and a study that exposed *Leishmania infantum* amastigotes to Sb^{III} have provided evidence of late stage apoptosis (Sereno et al., 2001).

The second, “active Sb^v” model, suggests that the mode of action of this class of drugs depends upon inhibiting DNA topoisomerase 1. It is hypothesised that Sb^v forms a complex with ribose-containing-biomolecules (Demicheli et al., 2002) to incur intrinsic anti-leishmanial activity through the interference of *Leishmania* purine pathways and metabolism and depletion of ATP and GTP (Haldar, Sen and Roy, 2011), though this is still unclear.

Relevant to such studies of Sb^{III} mode of action, increased thiol expression is strongly associated with both clinical and *in vitro* trivalent antimonial resistance. Disruption to the intracellular thiol homeostasis, has been shown to involve the decrease of glutathione (Carter et al., 2005) and trypanthione metabolic enzymes and AQP1 (Decuyper et al., 2005). An upregulation of the coding genes associated with ATP-binding cassette (ABC) transporters, and therefore an overexpression of the relevant proteins, such as MRP1, have also been largely associated in the resistance (El Fadili et al., 2005; Mukherjee et al., 2006). The amplified genes within *Leishmania* cells are related to the treatment failure due to the function of this transport system being to regulate the accumulation and efflux of numerous drugs (Rai et al., 2013).

1.2.5.2 Amphotericin B and AmBisome

Amphotericin B deoxycholate (AmB) was originally developed as an anti-fungal antibiotic in the 1950s but is has been used as a treatment against visceral leishmaniasis for HIV co-infected patients and in epidemic areas with antimony resistance (Sundar and Chakravarty, 2010). Administration of amphotericin B deoxycholate is via intravenous infusion with a low dose of 0.75 – 1.0 mg/kg depending

on body weight, due to the dose-limiting toxicity the therapy displays (Sundar et al., 2007a). The regime duration is long, and the infusion required daily or alternate days for between 15 and 20 days. Although, high cure rates for AmB have been recorded, the accompanied reactions are severe and highly toxic, with patients often exhibiting chills, fever, thrombophlebitis and occasionally nephrotoxicity and myocarditis (Stone et al., 2016). As a result, hospitalisation and constant renal observation are needed – a requirement that is not cost effective or accessible to many endemic areas. Therefore, the standard formulation of amphotericin B is rarely used due to the high levels of toxicity associated with the treatment and its use even halted in a phase 4 trial in Brazil. A study aimed to assess the safety of three anti-leishmanial therapies, led to the suspension of amphotericin B after an unplanned interim safety analysis (Romero et al., 2017).

Less toxic lipid formulations of amphotericin B were developed to reduce the severe side effects of the drug while maintaining efficacy. The new formulations were developed by the replacement of deoxycholate with different lipids, the primarily used and approved variety being liposomal amphotericin B, also known as AmBisome. This formulation was shown to have clinically similar treatment efficacy (Sundar et al., 2002) compared to AmB but with significantly lower recorded nephrotoxicity (Mistro et al., 2012). The AmBisome composition of 25% cholesterol and distearylphosphatidyl glycerol (DSPG), reduces the possibility of exposure to other organs, such as the kidneys, leading to a greater accumulation in the desired areas – liver, spleen and bone marrow (Sundar and Chakravarty, 2014). Increased tolerance of amphotericin B through this lipid formulation has allowed the administration of AmBisome in greater doses over a shorter time period; the dose and duration of which vary slightly depending on the patient and endemic region. AmBisome is currently a first-line treatment for visceral leishmaniasis in antimony-resistant *L. donovani* and *L. infantum* endemic regions, either at a daily dose of 3-5 mg/kg to a total of 15 mg/kg over a 3 to 5-day period, or as a single 10mg/kg dose (Sundar et al., 2004; Sundar et al., 2010). This modification to AmB, has

improved patient compliance with treatment, as well as having reduced health-care expenses in countries of socio-economic stability and wealth (Syriopoulou et al., 2013). This however, is not the case for those living in poverty in Low- and Middle-Income Countries (LMICs), as although AmBisome has been donated by pharma companies, access and storage conditions for this therapy still remain challenging (Gradoni et al., 2008; Kafetzis et al., 2005).

The mode of action of amphotericin B and the lipid formulations is not fully understood but involves the interactions on sterols; found on both *Leishmania* promastigotes and host macrophages (Paila, Saha and Chattopadhyay, 2010). The binding of AmB to *Leishmania* ergosterol, has shown to disrupt the cell permeability of the parasites by forming transmembrane channels and pores (Hartsel and Bolard, 1996); and at high concentrations, cell lysis occurs (Ramos et al., 1996). The binding with membrane cholesterol of the host macrophages is thought to be another mechanism of AmB, though is still uncertain. The AmB-cholesterol complex is suggested to consequently sequester within the membrane, to reduce cholesterol function in receptor pathways and *Leishmania* internalisation (Mouri et al., 2008).

Although liposomal amphotericin B resistance is not common, there are concerns that the single dose administration is a cause for developing resistance; of which combination therapy may reduce and combat that threat (Sundar et al., 2011). Studies investigating possible resistance mechanisms against liposomal amphotericin B, have shown changes in sterol content and disruption to the sterol pathway (Purkait et al., 2011).

1.2.5.3 Miltefosine

Miltefosine is an alkyl phospholipid and the only approved oral treatment for human leishmaniasis. Originally developed as an antineoplastic agent, miltefosine was used to treat VL in India, until liposomal amphotericin B replaced it. Miltefosine is currently used in combination regimens, CL and MCL. Miltefosine treatment is dependent on age and body weight, with children aged between 2 and 11 years, typically administered a dose of 2.5 mg/kg daily for 28 days. This dose increases with age and body weight; up to 150 mg daily for those exceeding 50 kg (Sundar et al., 2002). Relapses using miltefosine monotherapy has seen patients being retreated with combination therapy, usually AmBisome and treatment durations can last twice as long (Ware et al., 2020).

The side effects associated with this anti-leishmanial agent most commonly include nausea, diarrhoea, vomiting and anorexia. Of major concern, an embryotoxic and teratogenic risk has been identified within a study on a rodent model. Although these potential risks have not been documented within pregnant women, the treatment is strictly excluded from this group and also from women of childbearing age unless compulsory contraception is taken for three months post treatment (Sindermann and Engel, 2006).

Despite the general toxicity of miltefosine being lower than the current first-line and second-line treatments for CL and VL, it is not as widely distributed or as successful as first anticipated (Sunyoto, Potet and Boelaert, 2018). Unfortunately, a common limitation of drug accessibility and affordability for poverty-related diseases, is that it continues to exclude the most deprived populations in endemic areas. Therefore, due to high costs, teratogenic potential and emerging resistance, miltefosine is currently not a first-line drug for leishmaniasis. It is used as a second-line treatment for *L. donovani* infections, when co-administered with either: liposomal amphotericin B for 7 days, or paromomycin for 10 days (Monge-Maillo and Lopez-Velez, 2015; Seifert and Croft, 2005; Dorlo et al., 2012).

The mode of action of miltefosine against *Leishmania* parasites involves numerous targets, all of which indirectly induce cell death due to a mechanism similar to apoptosis (Marinho et al., 2011; Paris et al., 2004). Although not all targets of miltefosine are known, several have been identified and investigated. Phosphocholine cytidyltransferase is an enzyme essential in phosphatidylcholine biosynthesis. Treatment of *L. donovani* with miltefosine has shown phosphatidylcholine biosynthesis inhibition, which has consequentially resulted in cell death (Rakotomanga et al., 2007). Miltefosine action is also associated with disrupted mitochondrial function against trypanosomatids, via inhibiting cytochrome *c* oxidase (Luque-Ortega and Rivas, 2007). The activation of a sphingosine-activated Ca²⁺ channel in the *L. donovani* plasma membrane as a result of miltefosine presence has also been investigated. In addition to the cation channel opening, there is also an observed direct effect on acidocalcisomes. These combined actions, including the disruption to phosphatidylcholine synthesis and cytochrome *c* oxidase function, would result in parasitic apoptosis (Pinto-Martinez et al., 2017).

The emerging resistance to miltefosine, has been investigated and believed to be primarily due to: misuse and long treatment regime when used as monotherapy and long half-life. Not all mechanisms are known or understood but some resistance mechanisms have been studied, including reduced drug uptake and increased efflux by the parasites (Pérez-Victoria et al., 2006). Experimental point mutations targeting the genes of the miltefosine transporter, LdMT and protein LdRos3 (required for miltefosine uptake), generated amastigote lines that were less sensitive to miltefosine (Seifert et al., 2007). Reduced intracellular miltefosine has also been connected with miltefosine transporter (MT)-Ros3 mutations, affecting drug translocation and uptake (Fernandez-Prada et al., 2016). Increased efflux of the anti-leishmanial agent has been associated with an overexpression of *Leishmania* ABCB1, involved in the trafficking of alkyl phospholipids (Perez-Victoria et al., 2006).

1.2.5.4 Paromomycin

Paromomycin is an aminoglycoside antibiotic, used in combination as a first-line treatment against visceral leishmaniasis and as a local therapy for cutaneous leishmaniasis (Wiwanitkit, 2012). The dose and length of treatment has varied over the years, in order to reach a beneficial efficacy comparable to other first-line anti-leishmanial agents used. From a cure rate of 93% in India (Jha et al., 1998) to 46.7% in Sudan (Hailu et al., 2010), the approved and current treatment regime for paromomycin is in combination with liposomal amphotericin b to treat VL in India, and in combination with Sb^v therapy to treat VL in East Africa. Administered intramuscularly, the dosage of paromomycin against *L. donovani* infections in India is 15 mg/kg daily for 10 days and for East Africa, the duration is extended to 17 days (Musa et al., 2012).

Paromomycin has also been modified with the primary addition of methylbenzethonium, to be used topically as a CL treatment. This 15% paromomycin ointment is applied twice daily for 20 days for both old world and new world CL (Davidson, den Boer and Ritmeijer, 2009). Despite how long it has been used, the efficacy varies, with it marginally showing to be more beneficial than the self-healing lesions and actually showing to be less effective than Sb^v treatment (Khatami et al., 2007).

Adverse effects of paromomycin are primarily associated with the parenteral administration and the pain induced at injection site. There have also been reports of nephrotoxicity, though still demonstrates a safer toxicity profile than other chemotherapies used. Side effects associated with the topical form include tenderness, itching, oedema and rash-like appearances, although these are rare (Sundar et al., 2007b).

The mode of action of paromomycin has not been fully elucidated in *Leishmania* infections and is likely to be multifactorial. Several *in vitro* studies have however, identified *L. donovani* metabolism and mitochondrial respiration inhibition as a possible mechanism (Maarouf et al., 1998). Protein synthesis inhibition has been previously demonstrated in paromomycin exposed *L. donovani* due to the binding of the drug to the 50S and 30S mitochondrial ribosomal subunits (Jhingran et al., 2009; Maarouf et al., 1995).

Resistance to paromomycin has not yet been reported in the field but has been demonstrated numerous times *in vitro* and is likely to occur if used as monotherapy. Paromomycin resistant *L. donovani* (Maarouf et al., 1998), *L. major* (El-On, Sulitzeanu and Schnur, 1991), *L. tropica* (Fong et al., 1994) species have been induced and have shown a reduction in drug uptake but the mechanism needs further exploration.

Despite the low-cost and shorter treatment duration of paromomycin, it is still an inadequate treatment for all forms of leishmaniasis; due to the emerging resistance and parenteral administration.

1.2.5.5 Pentamidine

Pentamidine is an aromatic diamidine derivative, preferentially used as CL treatment and as a prophylaxis in HIV-VL infections. Pentamidine is used in cases of leishmaniasis in the form of pentamidine isethionate and was originally used as a treatment against Sb^v resistant VL in India. However, this application of pentamidine was stopped due to poor efficacy in those endemic areas and the high toxicity associated with the treatment. Pentamidine isethionate salt is also currently employed as systemic therapy for new world CL, specifically against *L. guyanensis* and *L. panamensis*

(Sundar and Chakravarty, 2014). The current treatment regime is a dose of 4 mg/kg every other day for three doses, administered intramuscularly (Delobel, 2003).

The adverse effects associated to pentamidine treatment are pain at the injection site, nausea, vomiting, headache, dizziness and more severely, diabetes mellitus and nephrotoxicity. Pentamidine-induced diabetes mellitus has however been linked to drug misuse, improper dosage and those with a family history of the disease, being at greater risk (Gadelha et al., 2018).

The mode of action of pentamidine has not been extensively researched in *Leishmania*, though it is believed to disrupt mitochondrial function. Several studies have identified the parasitic kinetoplast as a target of pentamidine, including kinetoplast DNA disruption (Croft and Brazil, 1982) and the collapse of the membrane potential of the mitochondria (Mehta and Shaha, 2003; Vercesi and Docampo, 1992). Despite the limited understanding of pentamidine mechanisms in *Leishmania*, these findings correlate with studies with other kinetoplastids; where accumulation of the compound within kinetoplasts of *Trypanosoma brucei* has been shown to depolarise the membrane potential (Lanteri, Tidwell and Meshnick, 2007; Mathis et al., 2007; Ward et al., 2011).

Increased efflux and reduced uptake of the compound have been identified as possible resistance mechanisms, in pentamidine-resistant *L. donovani* and *L. amazonensis* promastigotes (Basselin et al., 2002; Bray et al., 2003). A specific ABC transporter named, pentamidine resistance protein 1 (PRP1), has been characterised as having a possible involvement in reduced pentamidine uptake in resistance parasites; though much remains unclear (Coelho, Beverley and Cotrim, 2003).

1.2.6 Drug discovery for leishmaniasis

When evaluating the current drug treatments, the development of new and *Leishmania*-specific options are vital. The drug discovery process however, is long and complex that integrates multiple disciplines such as: biology, chemistry, pharmacokinetics, computer sciences and mathematical modelling. The process to discover more effective drugs has both scientific and non-scientific challenges and often follows the pipeline shown in Figure 7.

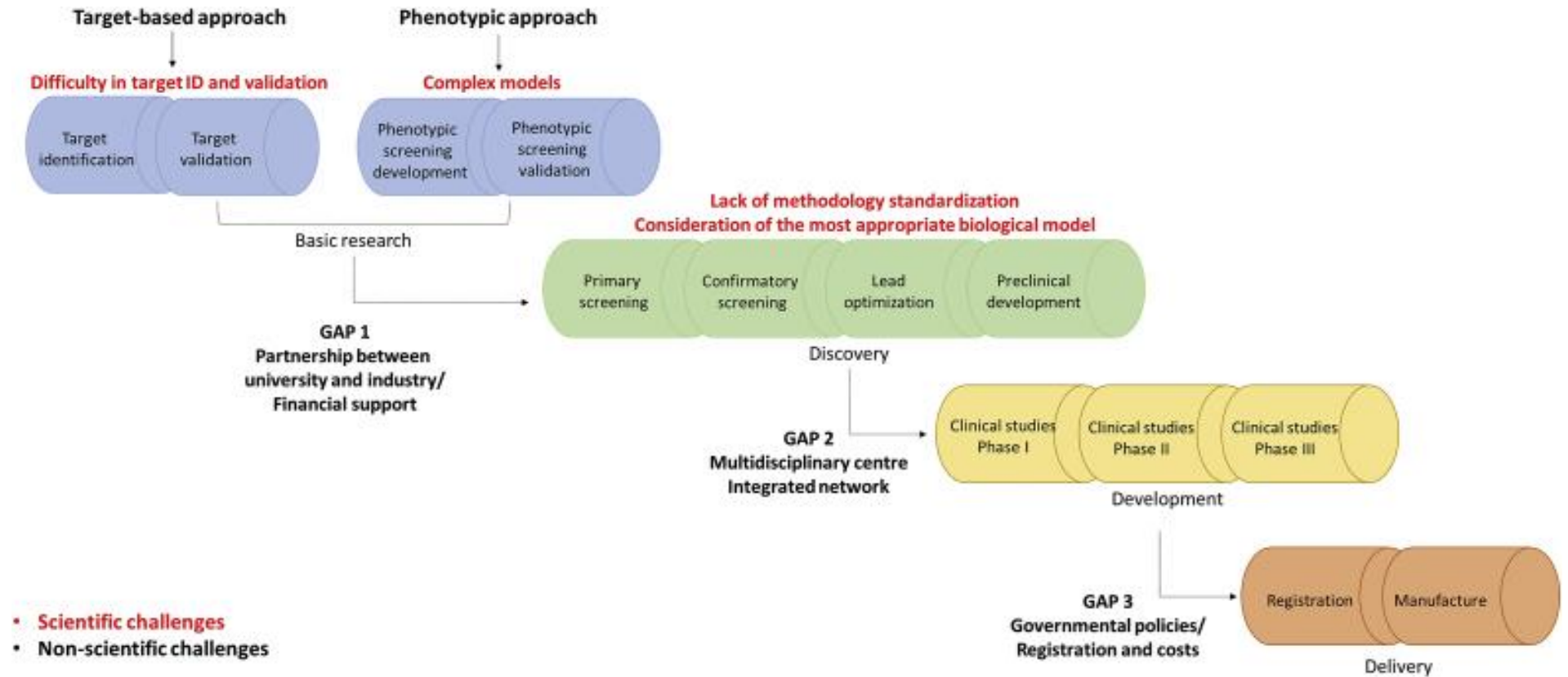


Figure 7 The general pathway of drug discovery (Alcântara, Ferreira, Gadelha and Miguel, 2018).

Drug discovery often begins with basic scientific research, to identify and validate a target or phenotypic assay. For leishmaniasis, the high throughput screen cell-based assays can be designed for a certain pathway or specific lifecycle stage. Phenotypic screening has been the traditional approach of drug discovery for leishmaniasis as it effectively demonstrates what impact the compound directly inflicts on parasite viability (Zulfiqar, Shelper and Avery, 2017). This approach defines the *Leishmania* parasite itself as the target, as opposed to a specific molecule or pathway as using target-based screening for leishmaniasis is associated with numerous challenges. The primary challenge includes the chemical properties required to produce a stable, effective compound within the acidic environment of the parasitophorous vacuole and the several host and parasitic membranes involved. This early research stage faces possible financial challenges and gaining the partnerships required between industry and research base to successfully begin.

Compounds found to be promising may proceed into a discovery phase where they are selected and optimised before they are then tested *in vivo* and the pharmacodynamics and pharmacokinetics evaluated. The target product profiles stated by DNDi are the standards needed in order for hit compounds to be selected as leishmaniasis drug treatments, a summarised version of these expectations for cutaneous and visceral leishmaniasis are presented in Tables 3 and 4. (DNDi, 2020). One of the expected criteria is that the potential hit must exhibit an EC₅₀ value (half maximal effective concentration) of less than 10 µM against intracellular amastigotes of *Leishmania* spp (Alcântara, Ferreira, Gadelha and Miguel, 2018).

The target product profile requirements stated by DNDi clearly and effectively compare where the standards of new treatments aspire to be and what the current accepted limits are.

Table 5 Target product profiles for cutaneous leishmaniasis. Information sourced from DNDi, 2020.

	Ideal	Acceptable
Target species	All species	<i>L. tropica</i> or <i>L. braziliensis</i>
Safety/tolerability	Well tolerated	Safety monitoring at primary health care level. <ul style="list-style-type: none"> • Systemic adverse reactions (AR) ≤ Grade 3 in <5% patients treated. • Local AR ≤ Grade 2 in <30% patients treated. • No treatment-induced mortality
Contraindications	None	Assessed at primary health care level.
Efficacy	<ul style="list-style-type: none"> • >95% patients with complete clinical cure, defined as 100% epithelialisation / flattening of lesion(s) at 3 months from treatment onset. • Minimal scar • No relapse or MCL development 	<ul style="list-style-type: none"> • 60% epithelialisation/flattening of lesion(s) for <i>L. tropica</i> and 70% for <i>L. braziliensis</i> patients with complete cure. • Scar no worse than natural healing. • <5% rate of relapse or MCL development at 1 year.
Formulation	Topical/oral	Non-parenteral or few doses if parenteral
Treatment regimen	Topical ≤14 days and oral < 7 days	Topical: 28 days, oral: twice daily for 28 days and parenteral ≤ 3 injections.
Target population	No restrictions	<ul style="list-style-type: none"> • >9 months of age. • No efficacy in immune-compromised patients. • Not for use in pregnancy
Stability	No cold chain. At least 3 years at 37° C	2 years at 4-8° C
Cost	To be defined	To be defined

Table 6 The treatment regimen target product profile for visceral leishmaniasis and visceral leishmaniasis combination therapies. Information sourced from DNDi, 2020.

	Treatment Regimen	
	Ideal	Acceptable
Visceral leishmaniasis	<ul style="list-style-type: none"> • Oral: 1/day for 10 days • Intramuscular: 3 injections over 10 days 	<ul style="list-style-type: none"> • Bid for < 10 days oral • >3 intramuscular injections over 10 days
Visceral leishmaniasis combination therapies	Single dose treatment or fixed-dose combination tablet/paediatric formulation up to 7 days	<ul style="list-style-type: none"> • Currently existing drugs: twice daily for ≤28 days oral • Intramuscular injections ≤14 days

The acceptable safety of new cutaneous leishmaniasis treatments is particularly astounding when comparing no treatment-induced morbidity with the ideal safe and tolerable aspirations. In addition to the wide safety margins for where treatments are currently accepted compared to the ideal standard, the treatment regimen is also needing considerable improvement. With cutaneous leishmaniasis in particular, the regimen for topical treatments is currently twice as long as where the ideal limit lies and for oral treatments, it is 4 x longer with multiple doses per day compared to just the once expected for an ideal treatment. These target product profiles highlight the significant improvement and development needed in new therapies and approaches to the drug discovery process. Therefore, using the target product profiles as guidelines for where to develop and improve the drug discovery for anti-leishmanial, this thesis aims to utilise an approach that could be beneficial to early compound screening in the aid to reduce the lengthy treatment regimen currently used.

The developmental step is then putting a targeted compound into the three phases of human clinical trials, where the compound is only considered a drug candidate if they perform to a satisfactory standard.

The final step that is the registration and manufacture of the compound as a treatment and is often challenged financially and by governmental policies (Zulfiqar, Shelper and Avery, 2017).

1.2.6.1 Current anti-leishmanial screening assays

There have been a number of *in vitro* screening assays developed over the years for leishmaniasis. The assays are developed based on the *Leishmania* parasites forms and what can be achieved *in vitro*. Therefore, the assays can be performed for *Leishmania* promastigotes, axenic amastigotes and/or intracellular amastigotes when applying an intramacrophage model. Screening assays available for promastigotes are not clinically relevant for disease progression as they are not the disease-causing form, however, do provide the options to compare the compound effectivity between the distinguished forms (Alcântara, Ferreira, Gadelha and Miguel, 2018). Although axenic amastigotes morphologically resemble the clinically relevant lifecycle stage, this form lacks the host environment and harsh conditions that they are usually exposed to and because of this limitation, results for drug sensitivity assays are often skewed and present high false-positive rates (De Rycker et al., 2013). The significance of early passaging of cultured *Leishmania* have also been shown. A loss of virulence and reduced conversion into virulent metacyclics has been observed due to genomic changes (Sinha et al., 2018). Axenic amastigote assays however more closely represent the metabolic and structural composition when compared to promastigotes and can provide useful information regarding the possible functions of the compounds. Exposing active compounds against intracellular amastigotes is the most complex model to establish but the most relevant and suitable assay for the purpose of drug discovery and predicting clinical activity (De Rycker et al., 2013; Siqueira-Neto., 2012).

1.2.6.2 Absorbance and Fluorescence-based assays

Several colorimetric and fluorescent assays have been used to detect the number of metabolically active *Leishmania* cells. These are either via reagents measuring the metabolism of the parasites, such as 3-(4,5-dimethyl thiazol-2-yl)-2,5-diphenyltetrazolium bromide assay (MTT) and resazurin (Bastos et al., 2017). Such assays are useful for the promastigote or axenic amastigote form but are ineffective for intramacrophage models as the metabolic reagents are unable to distinguish between metabolites

from host cells and parasites. AlamarBlue is a resazurin reagent that is often applied due to the affordability, reproducibility and simplicity it offers. AlamarBlue (resazurin) is a weakly fluorescent dye that is blue when visually observed. Once present in metabolically active cells, resazurin is reduced into the pink fluorescent product, resorufin, as seen in figure 8. This conversion is therefore proportional to aerobic respiration and reflects the number of metabolically active cells (Mikus and Steverding, 2000). The location of the conversion of resazurin to resorufin has been disputed but is now understood to only occur intracellularly (Chen, Steele and Stuckly, 2017). The reaction itself is believed to be as a result of several redox enzymes in the mitochondria and cytosol alongside the involvement of the coenzyme NADH (Chen, Steele and Stuckly, 2017). The cell number reflected by the assay can be recorded either by an absorbance reading (excited at 570 nm and emission at 600 nm) or reading the fluorescence (excited at 530-570 nm and emission at 580-590 nm) (Nakayama, Caton, Nova and Parandoosh). A limitation of resazurin-based assays for drug screenings is that the reaction is irreversible and requires an incubation period of four hours or longer. This could therefore lead to recording inaccurate parasite survival when drug treatments are administered.

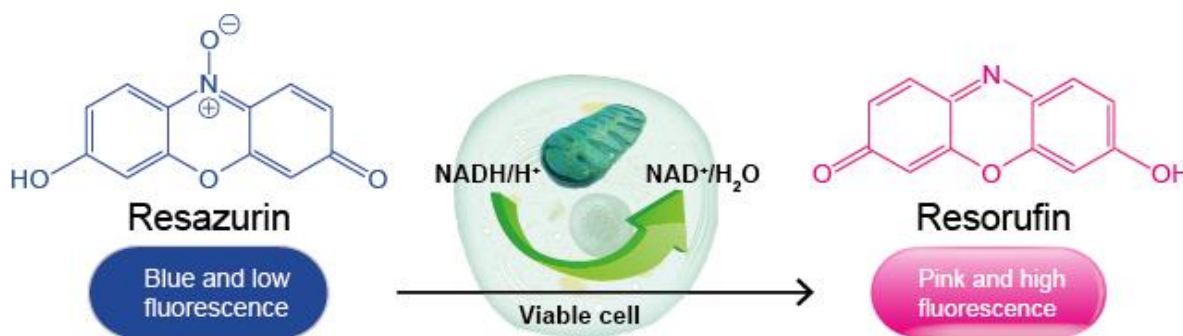


Figure 8 The mechanism of resazurin reduction into resorufin of resazurin-based assays, such as alamarBlue and Presto Blue (ABP Biosciences, 2020).

1.2.6.3 Bioluminescent transgenic parasites

The use of bioluminescence is a more recent development that has created considerable opportunities as a dynamic method and continues to show potential in the parasitology field. Bioluminescence technology exploits the light generating properties of luciferase reporter enzymes, using transgenic pathogens heterologously expressing one or more luciferase proteins. This technique can therefore offer the ability to not only determine the parasite viability but also the location in which the enzyme is tagged. Several luciferases that have been discovered and applied as reporters in drug screens for numerous infectious disease models, including for *Plasmodium falciparum* (Ullah, Sharma, Biagini and Horrocks, 2017) and kinetoplastid parasites (Sadeghi et al., 2015; Suganuma et al., 2014). Several luciferases, particularly those derived from *Photinus pyralis* (Firefly luciferase) and *Renilla reniformis* (*Renilla* luciferase) have been widely explored, however the recent discovery of NanoLuc is of current interest. The NanoLuc luciferase is one of the smallest luciferases (19.1 kDa) and is derived from *Oplophorus gracilirostris*, a deep-sea shrimp (England, Ehlerding and Cai, 2016). NanoLuc produces a high intensity, glow-type bioluminescence due to a chemical reaction between the enzyme and the corresponding substrate, furimazine, in the presence of molecular oxygen. This results in the products furimamide and light, as seen in Figure 9.

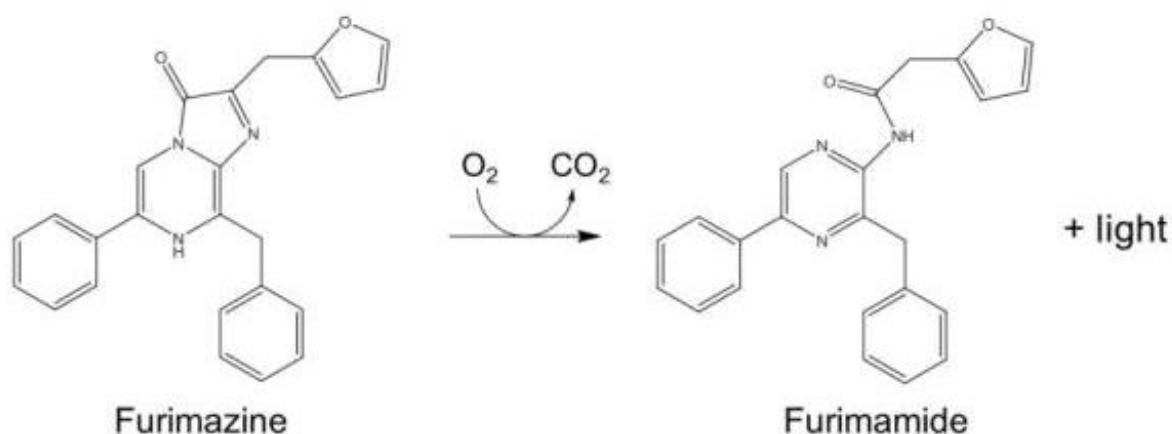


Figure 9 The mechanism of NanoLuc luciferase activity to produce bioluminescence (Modified from England, Ehlerding and Cai, 2016).

In cellular assays, the NanoLuc system provides high specificity and low background activity, due to the stable intracellular half-life (6 hours) but has shown to lack the ability to discriminate between live and dead parasites (Agostino et al., 2020). Therefore because of this limitation and its low emission maximum, NanoLuc is not optimal or ideal for *in vivo* investigations (England, Ehlerding and Cai, 2016).

Modified versions of NanoLuc have been produced which are better adapted to specific applications. One of particular interest is a destabilised form known as NanoLuc-PEST. In this form, the luciferase possesses a shorter intracellular half-life of about 20 minutes due to the addition of a PEST motif (England, Ehlerding and Cai, 2016). The PEST motif is a proline (P), glutamate (E), serine (S) and threonine (T) rich region, which is fused to the C-terminus of the NanoLuc and targets the luciferase to the proteasome for degradation (García-Alai et al., 2006). Recent studies have employed the use of NanoLuc-PEST in axenic- and intramacrophage-based drug potency assays. Measurement of bioluminescence in transgenic *Leishmania* cell lines has been demonstrated to be an effective indicator of cell viability with the potential for application in drug development (Berry et al., 2018).

1.2.7 Rate of Kill of the anti-leishmanial drugs pentamidine, miltefosine, amphotericin B and potassium antimonial tartrate

An understanding of the rate of kill for anti-leishmanial drugs is very limited and so a summary of these studies has been conducted to fully comprehend the knowledge gap for this area of *Leishmania* research. The drug discovery pathway has heavily focused on using target-based approaches for many years (Zheng, Thorne and McKew, 2013). These initial approaches rely on identifying the known targets and pathways essential for drug interaction within a model of interest. However, this methodology of identifying promising compounds is the first challenge when observing these properties against kinetoplastid parasites. There is a lack of knowledge about the mode of action and targets of the drugs currently used and renders this primary approach unsuitable for parasitic research (Frearson, Wyatt, Gilbert and Fairlamb, 2007). Drug discovery research for kinetoplastid parasites, such as *Leishmania*, has therefore traditionally evolved to phenotypic screenings. Instead, this process involves the *Leishmania* parasite itself as being the primary target, where the inhibition of cell viability against a drug is measured and used to characterise compounds with promising antiparasitic activity but with unknown targets.

When considering the target product profiles developed by the Drugs for Neglected Diseases initiative (DNDi) for new drug treatments for leishmaniasis, the acceptable requirements are far from ideal for people living with leishmaniasis. The acceptable criteria for cutaneous leishmaniasis involves accessing primary health care and a cold chain supply for treatment storage. These requirements are not possible or feasible for many people with neglected tropical diseases, including leishmaniasis. The acceptable efficacy for cutaneous treatment is currently defined as 60% and 70% epithelialisation for *L. tropica* and *L. braziliensis* respectively, whereas the ideal efficacy is 100% epithelialisation after 3 months of

treatment. This accepted percentage difference is another example of the extent that treatments for CL need to be very significantly improved. There is also a significant difference in the treatment duration between what would be ideal, and the regimes considered acceptable. Topical treatments currently have a duration of 28 days and oral treatments of twice a day for 28 days. Compared to the ideal 14-day treatment course for topical and less than 7 days for oral, these acceptable criteria require significant improvement. Combining the current treatment duration and access to primary health care, varied patient compliance and recovery is expected.

Little understanding of the mode of action and molecular targets of compounds are not the only limitations of phenotypic screenings for parasitic diseases and these result in further research gaps. One factor that is often overlooked is the speed at which the active compound kills the targeted parasite cells. For neglected infectious diseases, the understanding of the biochemistry and mechanisms involved with its pathogenicity is often limited and drug treatments employed are often repurposed and/or unspecific. This is seen with leishmaniasis, as many of the drugs currently used still require research to determine their exact mode of action within the parasites. Therefore, considering the current target product profiles and the phenotypic drug discovery approach, overlooked variables, such as the rate of kill (“rate of action” or “time to kill”) of a compound should be emphasised in research.

Recent studies have utilised transgenic malarial parasite lines that express a luciferase enzyme in bioluminescence relative rate of kill (BRRoK) assays, to study this knowledge gap (Ullah, Sharma, Biagini and Horrocks, 2017). Determining the rate of kill of current treatments should be considered during the drug development process as the employment of primary fast-acting drugs may improve patient welfare and compliance as treatment protocols could be shortened.

Studies on the rate of kill of amphotericin B for antifungal research has been documented due to its original use prior to its discovered anti-leishmanial properties (Spadari, Vila, Rozental and Ishida, 2018). Amphotericin B has been observed to have a species specific rate of kill in fungi. At four times the MIC, fungicidal endpoint (99.9% killing) was observed to be two hours for some species, but this rate increased with various species (Cantón et al., 2004).

The development of *in vitro* and *in vivo* rate-of-kill experiments has become more commonly employed in anti-leishmanial drug research over the last decade. Voak et al., 2017 assessed the effect of AmBisome at three concentrations (10, 2.5 and 0.6 mg/kg) in *L. donovani*-infected mice, assessing the parasite burden across four time points (1, 2, 3 and 7 days). The highest dose of AmBisome administered (10 mg/kg) showed >90% parasite growth inhibition in the liver within two days. This suggests that AmBisome is fast-acting and was consistent with drug distribution from blood to tissue.

Gupta et al., 2014 performed a ‘time-kill’ assay in order to identify a preclinical candidate for oral treatment for VL. *In vivo* mouse and hamster rate of kill assays determined the *R* enantiomer (DNDI-VL-2098) of a racemate, DNDI-VL-2001 (a racemate being a mixture of equal quantities of two enantiomers) to have the best leishmanicidal activity. In 2015 work on this drug candidate was discontinued due to toxicity issues. However, in 2019, Wijnant et al., 2019 evaluated the pharmacokinetics and pharmacodynamics of DNDI-0690, a structural analogue of DNDI-VL-2098 that progressed into phase I clinical trials for VL. Using *in vivo* CL mouse models with bioluminescent *L. major* and *L. mexicana* parasites, the new compound was observed to be as efficacious as an AmBisome control at the end of the 10-day treatment (>99%) after oral administration. Therefore, DNDI-0690 was shown to be fast-acting when comparing to AmBisome and considering the complexities of *in vivo* research. A high dose of drug was used to perform these studies (50 mg/kg) and so further dose fractionation studies will be needed. Identifying DNDI-0690 through a combination of

PK/PD studies, including rate of kill, has been significant data that will allow estimation of optimal dosing regimens.

Tegazzini et al., 2017 also used an adapted protocol to determine the rate of kill of novel compounds sourced from GSK "*L. donovani* box" against *L. donovani*-infected macrophages. This *in vitro* intramacrophage research was used to evaluate the potency of the compounds over four time points (24, 48, 72 and 92 hours), to help prioritise hit compounds in high throughput early drug screenings. Although there is limited understanding of the rate of kill for current treatments, amphotericin B and miltefosine have previously been determined as "fast-acting" and "slow-acting" respectively and so have been used as reference drugs in similar research, including Tegazzini et al., 2017. These compounds provided a standard benchmark to characterise novel compounds in relation to their rate of kill compared to the data obtained for amphotericin B and miltefosine. From this differentiation, cross-comparison between the rate of kill and chemical structure of the compounds revealed the same biological behaviour from the structures of compounds classified by their rate of kill. This approach may therefore reveal important biological and chemical connections to aid prioritising hit compounds.

1.2.8 Aims

This thesis aims to address the lack of research conducted on the rate of kill of several current anti-leishmanial drug treatments.

Understanding the recent development and potential of NanoLuc systems, the study aims to establish and evaluate a bioluminescence-based rate of kill assay using a transgenic line of *Leishmania mexicana* that expresses NanoLuc-PEST. This assay will then be used to establish the relative rate of kill for the anti-leishmanial drugs amphotericin B, miltefosine, pentamidine and potassium antimonyl tartrate in axenic promastigote- and amastigotes in comparison to a fluorescence-based assay.

This research aims to provide evidence of a novel molecular technique that can be used to aid the development of more predictive assays for early stages of drug discovery, addressing an important gap in drug discovery research.

Chapter 2 – Materials

2.1 Materials

All plasticware and glassware used were purchased from the following companies: ThermoFisher Scientific (Gibco©) (Loughborough, UK), VWR International (Lutterworth, UK), Star Lab (Milton Keynes, UK), Eppendorf (Cambridge, UK) and Greiner Bio-One (Solingen, Germany). All chemicals and reagents were purchased from ThermoFisher Scientific (Gibco©), Lonza (Basel, Switzerland) and Sigma-Aldrich (Merck) (Watford, UK).

2.1.1 Plasticware, glassware and equipment

ThermoFisher Scientific (Gibco©) (Loughborough, UK)	Nunc™ MicroWell™ 96-Well, Nunclon Delta-Treated, Flat-Bottom Microplates; BioLite 25cm ² Cell Culture Treated Flasks
VWR International (Lutterworth, UK)	24-well plates, flat bottom, TC-treated
StarLab (Milton Keynes, UK)	StarTub PS Reagent Reservoir; Graduated TipOne Filter Pipette Tips; CytoOne® Bottle Top Filtration Unit, Full Assembly, 0.2 µm
Greiner Bio-One (Solingen, Germany)	Serological Graduated Pipettes
3520 Advance bench pH meter	
GloMax® Multi Detection System Plate reader	

2.1.2 Chemicals and Reagents

ThermoFisher Scientific (Gibco®) (Loughborough, UK)	HyClone™ Amphotericin B (fungizone) solution; PrestoBlue®; Heat inactivated Foetal Bovine Serum
Sigma-Aldrich (Merck) (Watford, UK)	Paraformaldehyde; Miltefosine; Pentamidine isethionate salt; Potassium antimonyl tartrate trihydrate; Dimethyl sulphoxide
Lonza (Basel, Switzerland)	BioWhittaker® Pen-Strep (10 U/ml); Schneider's Drosophila Medium, Modified

2.1.3 Drug Stocks Preparation

Table 7 The preparation and storage conditions of Amphotericin B, Miltefosine, Pentamidine and

Potassium Antimonial Tartrate.

Drug	Stock concentration	Solvent	Storage
Amphotericin B	271 µM	N/A	All stocks stored at -20 °C until needed.
Miltefosine	1 mM	Distilled H ₂ O (dH ₂ O)	
Pentamidine isethionate salt	5 mM	DMSO	
Potassium Antimonyl Tartrate	10 mM	DMSO	

Chapter 3 – Methods

3.2.1 Cell culture of *L. mexicana*

Parasite culture and experimental work were conducted in Health and Safety Executive (HSE) approved Containment Level 2 and Containment Level 3 cell culture facilities.

Frozen samples of *L. mexicana* promastigotes (strain MNYC/BZ/62/M379) and previously transformed transgenic *L. mexicana* NanoLuc-PEST promastigotes (method described by Berry et al., 2018), were rapidly defrosted from liquid nitrogen and 1mL added to 10mL of complete Schneider's medium pH 7.0. The medium was supplemented with 10% Foetal Bovine Serum (FBS), 100 U/mL penicillin and 100 µg/mL streptomycin (complete Schneider's media pH7.0). These cultures were maintained as procyclic promastigotes at 26°C. Differentiation of promastigotes (approximately 10^7 cell density) into axenic amastigotes was performed by pipetting 0.5 mL of stationary phase promastigotes into 10 mL of Schneider's medium pH 5.5. Parasite growth was determined by preparation of a 1:10 dilution of parasite culture with 1% paraformaldehyde and counting cells using a Neubauer haemocytometer under light microscopy.

3.2.2 Nano-Glo Luciferase Expression and stability

Bioluminescence due to the activity of NanoLuc-PEST enzymes was detected using the Nano-Glo® Luciferase Assay Kit (Promega) following the manufacturer's protocol. Log phase NanoLuc-PEST parasites were diluted to 10^6 parasites per mL and a 10-fold dilution was carried out in media to get a $10^6 - 10^0$ parasite per mL range. 50 µl of diluted parasite were transferred to a white 96-well plate in triplicate, and 50 µl luciferase reagent (Luciferase Assay Buffer and Luciferase Assay substrate, 50:1) was added (1:1 (v/v)) to each well. The plate was homogenised by shaking and after three minutes, a GloMax® Multi Detection System (Promega) was used to measure bioluminescence. All data was

normalised against a sample containing only media (negative control), and assays performed in biological triplicate, n=3. Results were analysed using GraphPad Prism 8.0.

The stability of log-phase *L. mexicana* NanoLuc-PEST promastigotes was determined using a growth curve. A 1:10 dilution of promastigote culture in paraformaldehyde (PFA). Diluted promastigotes were counted every 24 hours for 120 hours using a haemocytometer and results normalised against a negative control (media) and analysed using GraphPad Prism 8.0.

3.2.3 PrestoBlue® Assay: Determining the EC₅₀ of amphotericin B, miltefosine, pentamidine and potassium pentavalent antimonial in *L. mexicana* cell lines

The preparation of parasites is consistent regardless of form and cell line. Log-phase promastigotes and amastigotes were counted, like described in 3.2.2 and diluted to a starting concentration of 1×10^6 cells per 10 mL. 100 μ L of diluted parasites were added in triplicate to 11 columns of a 96 well black plate.

The drug concentration ranges used to produce EC₅₀ curves were optimised to best plot the curve. The ranges were produced by a series of 2-fold dilution series dependent upon the drug. For amphotericin B, a 2-fold dilution was performed from a starting concentration of 12.5 μ M for promastigotes and 10 μ M for amastigotes in 24 well plates. 1 mL of the diluted stock concentration was serially diluted by continually taking 0.5 mL and further diluting with 0.5 mL of Schneider's media pH 7.0 for promastigotes and pH 5.5 for amastigotes, to produce 10 concentrations. 100 μ L of each diluted drug concentration was plated in triplicate 1:1 with the parasites (final parasite concentration 5×10^5 , final drug concentration half of originally prepared). Positive controls were included in triplicate for each assay. 5 μ M amphotericin B was used as the positive control as it is a supralethal kill dose, giving data

for 0% cell viability to normalise data. A negative control of untreated cells with media was used for 100% cell growth and also plated in triplicate.

For miltefosine, pentamidine and potassium antimonyl tartrate, the final drug concentration ranges in the EC₅₀ assays are described in Table 6.

Table 8 Table showing the preparation of amphotericin B, miltefosine, pentamidine and potassium antimonyl tartrate concentrations used for determining the EC₅₀ values. All stock concentrations were diluted to a top concentration at 1mL and diluted using Schneider's media pH5.5.

Parasite stage	Amphotericin B		Miltefosine		Pentamidine		Potassium Antimonyl tartrate	
	P	A	P	A	P	A	P	A
Final drug concentration ranges (µM)	6.25	5.00	15.00	10.00	50.00	25.00	125.00	200.00
	3.13	2.50	7.5	7.50	40.00	20.00	62.50	100.00
	1.56	1.25	3.75	5.00	25.00	15.00	50.00	50.00
	0.78	0.63	1.88	4.00	20.00	12.50	20.00	40.00
	0.39	0.31	0.94	3.75	15.00	10.00	17.50	30.00
	0.20	0.16	0.47	2.50	10.00	7.50	15.00	25.00
	0.10	0.08	0.23	2.00	5.00	5.00	10.00	20.00
	0.05	0.04	0.12	1.88	2.50	2.50	5.00	15.00
	0.02	0.02	0.06	1.25	1.25	1.25	2.50	12.50
	0.01	0.01	0.03	1.00	0.63	0.63	1.25	10.00
				0.5	0.31			5.00
				0.25	0.16			2.50
				0.13	0.08			1.25
								0.63
								0.31

The 96 well black plates containing 1:1 v/v treated parasites were then incubated at 26 degrees for 72 hours for promastigotes and at 32 degrees for 72 hours for amastigotes. Following this incubation period, 20 µL of PrestoBlue® (1:10 v/v) was added to each well, mixed via pipetting and incubated for a further 5 hours.

Plates were read on the GloMax® Multi Detection System and the fluorescence signal measured ($\lambda_{ex}/\lambda_{em} = 525/580-640$ nm), the percentage viability calculated as described by Berry et al., 2018 in Chapter 3.5.2 and data analysed using GraphPad Prism 8.0.

In GraphPad Prism 8.0, the EC₅₀ analysis was determined via a log transformed concentration versus normalised fluorescence or bioluminescence signal curve. Using the log concentration versus normalised response (variable slope) data, the data was plotted as a non-linear regression.

3.2.4 Statistical analysis used

Irrespective of assay, each assay was normalised and the Z' score calculated. All assays were performed in triplicate, with two biological replicates (n=6), unless stated otherwise. Positive, 0% growth, supralethal dose of 5 μ M Amphotericin B and negative, 100% growth (equivalent volume of relevant complete Schneider's medium) controls were included on each plate. The growth of parasites was calculated as: $100 \times [\mu_{(S)} - \mu_{(-)} / \mu_{(+)} - \mu_{(-)}]$, where $\mu_{(S)}$, $\mu_{(-)}$ and $\mu_{(+)}$ represents the means of the samples, the positive (0%) and negative (100%) controls respectively.

The Z' score was calculated as an assay quality parameter for all EC₅₀ and rate of kill assays performed to compare the robustness of bioluminescence and fluorescence-based assays. The Z' score was calculated as follows: $Z' = 1 - [3\sigma_{(+)} + 3\sigma_{(-)} / \mu_{(+)} - \mu_{(-)}]$, where $\mu_{(+)}$ and $\sigma_{(+)}$ are the mean and SD of the negative control respectively, and $\mu_{(-)}$ and $3\sigma_{(-)}$ are the mean and SD of the positive control respectively. The robustness of each method was determined as a value of 0.64 and greater (Hasenkamp et al., 2013), with a Z' value of >0.5 demonstrating a robust method.

3.2.5 Determining the Rate of Kill in *L. mexicana* cell lines

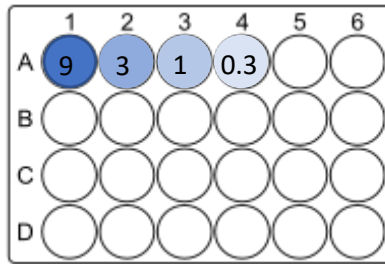
Multiples of the EC₅₀ values that were determined from the previous method, were used for the 4 concentrations needed to determine the relative rate of kill. 1.5 mL each of 0.3 X, 1 X, 3 X and 9 X the EC₅₀ per drug were prepared in 24 well plates and plated into 96 well plates in technical triplicate, as shown in Figure 10. 50 uL of each concentration was plated in black 96 well plates for fluorescence readings and 25 uL was added into white 96 well plates for bioluminescence-based readings. Positive (5 µM amphotericin B) and negative (Media, DMSO) controls were added in triplicate to each assay. 2 white 96 well plates were used in each bioluminescence based relative rate of kill assay as 4 incubation times were recorded: 4, 24, 48 and 72 hours. For the fluorescence approach, 1 black 96 well plates were used as the following 3 incubation times were recorded: 24, 48 and 72 hours.

L. mexicana amastigotes from log-phase cultures were counted and diluted to 1 x 10⁶ cells per mL as described in section 3.2.1 and 3.2.2. All amastigote assays were performed 24 hours after the transformation of promastigotes to amastigotes in culture. 50 uL of parasites at 1 x 10⁶ cells per mL were plated to all occupied wells in the black 96 well plates and 25 uL added to all occupied wells in the white 96 well plates, the layout is shown in Figure 10. Once cells and drug was plated, each plate was incubated for the relevant amount of time for each method.

For the PrestoBlue® assays, 10 uL of PrestoBlue® was added at every incubation interval; into each separate plate for the 24, 48- and 72-hour incubations and mixed via pipetting. Once added, the plate was incubated for a further 5 hours at 32 degrees. The plates were then read on the GloMax® Multi Detection System and the fluorescence signal measured ($\lambda_{ex}/\lambda_{em} = 525/580-640$ nm). Analysis was performed as described in 3.2.5.

For the luciferase assays, 25 uL of luciferase reagent (ratio shown in section 3.2.2) was added to all relevant wells after each incubation: every 4, 24, 48 and 72 hours. The plates were then shaken for 3 minutes prior luciferase reagent addition and the bioluminescence measured on the GloMax® Multi Detection System. Analysis was performed as described in section 3.2.4.

0.33 x, 1 x, 3 x and 9 x
fold-EC₅₀
concentration of drug



Fluorescence-based assay

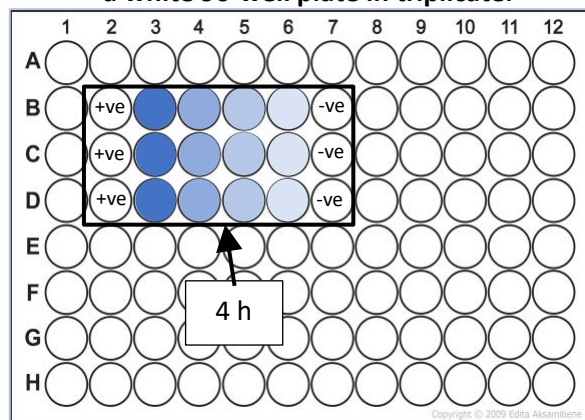
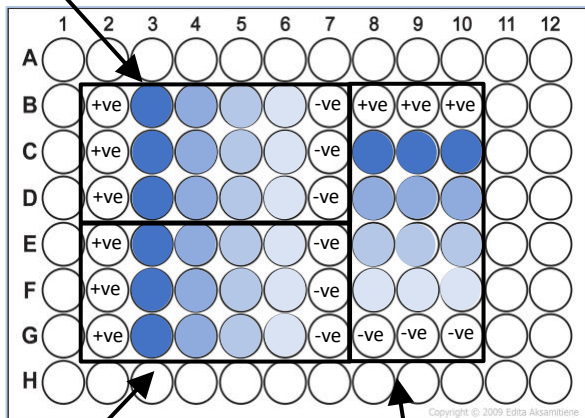
Bioluminescence-based assay

Prepared compounds were transferred onto

Prepared compounds were transferred onto

24 h a black 96-well plate in triplicate.

a white 96-well plate in triplicate.



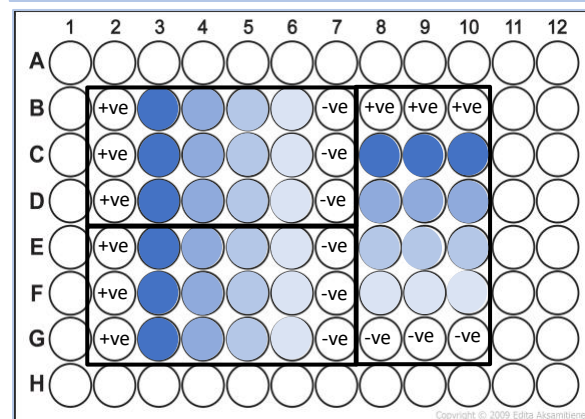
48 h

72 h

Incubated at 32°C for 24, 48 and 72 hours.

PrestoBlue® (1:10) was added after relevant time interval and further incubated for 5

hours and the fluorescence signal measured.



Incubated at 32°C for 4, 24, 48 and 72 hours.

Luciferase reagent (1:1) was added after the relevant time interval and the luciferase activity

Figure 10 Schematic diagram of the fluorescence and bioluminescence-based assays used to measure the rate of kill of drug compounds. 0.3 x-, 1x-, 3x- and 9x- the EC₅₀ were used as equipotent concentrations. 50 uL of each concentration was plated in triplicate three times into a black 96 well plate. 1 x 10⁶ parasites/mL were added to all occupied wells. This plate was incubated for 24, 48 and 72 hours where after each incubation 10 uL of PrestoBlue was added and the plate would be incubated for a further 5 hours. The fluorescence signal would then be measured. For the luciferase assay, 25 uL of each concentration was plated in triplicate four times into 2 white 96 well plates. 1 x 10⁶ parasites/mL were added to all occupied wells. The plates were then incubated for 4, 24, 48 and 72 hours where after each incubation, 25 uL of luciferase reagent was added, shaken for 3 minutes and the bioluminescence read. Positive control (0% growth) used was 5 uM amphotericin B and the negative control (100% growth) was untreated cells. All data was done in biological triplicate (n=3).

Chapter 4 - Results

4.1 Analysing the use of bioluminescence- and fluorescence-based assays for drug screening

An initial experiment was set up in order to characterise the cells and confirm their luciferase expression. A growth curve of *L. mexicana* NanoLuc-PEST promastigotes was first recorded, in which cells at a starting cell concentration of 1×10^5 were incubated in complete Schneider's medium (pH 7.0) at 27 degrees and counted every 24 hours over a five-day period. The promastigotes here showed to proliferate rapidly within the first 48 hours and then begin to plateau on day four. The rapid proliferation was expected due to the cell concentration and many dividing procyclic parasites in the initial counts, which reflects the early *Leishmania* morphology in the sandfly. As the number of procyclic parasites transform into the later stage morphologies, leptomonads and metacyclic promastigotes in days four and five, the cell concentration is expected to slow and peak. The growth curve graph produced (see Figure 11) from this experiment, confirms that the *L. mexicana* NanoLuc-PEST parasites were healthy and were growing normally, which was needed to proceed with the assays. This growth curve data also shows the optimal time period for differentiation into amastigotes. Metacyclic promastigotes are needed for successful differentiation from promastigotes and so, passaging and differentiating around day four or five would be optimal.

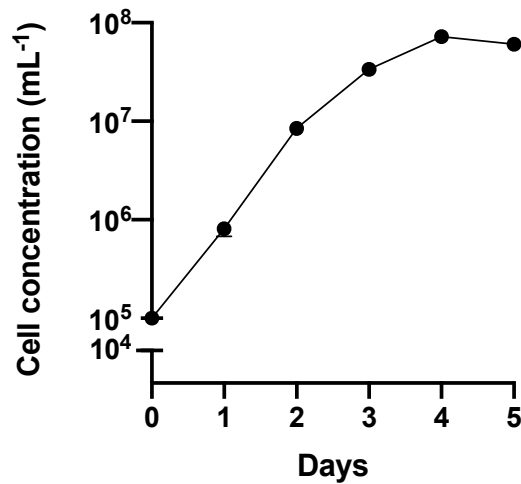


Figure 11 Growth curve of *L. mexicana* NanoLuc-PEST promastigotes. Cells were diluted to a starting concentration of 1×10^5 and monitored every 24 hours over five days. The growth curve was generated in and the Y-axis was transformed by \log_{10} . All mean values are shown as $n=3 \pm \text{SEM}$.

A secondary initial experiment was then conducted in order to confirm that the *L. mexicana* NanoLuc-PEST parasites were expressing the luciferase and if this was proportional to cell number. The parasites were serially diluted 10-fold from a cell density of 1×10^5 parasites to 1×10^1 and 1×10^0 for promastigote and amastigote parasites respectively, in complete Schneider's medium. Each dilution was incubated with luciferase reagent for three minutes before measuring the bioluminescence. Fluorescence-based assay analysis was also performed with WT promastigotes, in parallel to the bioluminescence-based assays for comparison. The WT promastigotes were serially diluted from a cell density of 1×10^6 parasites to 1×10^0 parasites in complete Schneider's medium (pH 7.0). Fluorescence was measured after incubating the cells with PrestoBlue for six hours. The graphs representing this data were created using GraphPad Prism and are shown in Figure 12.

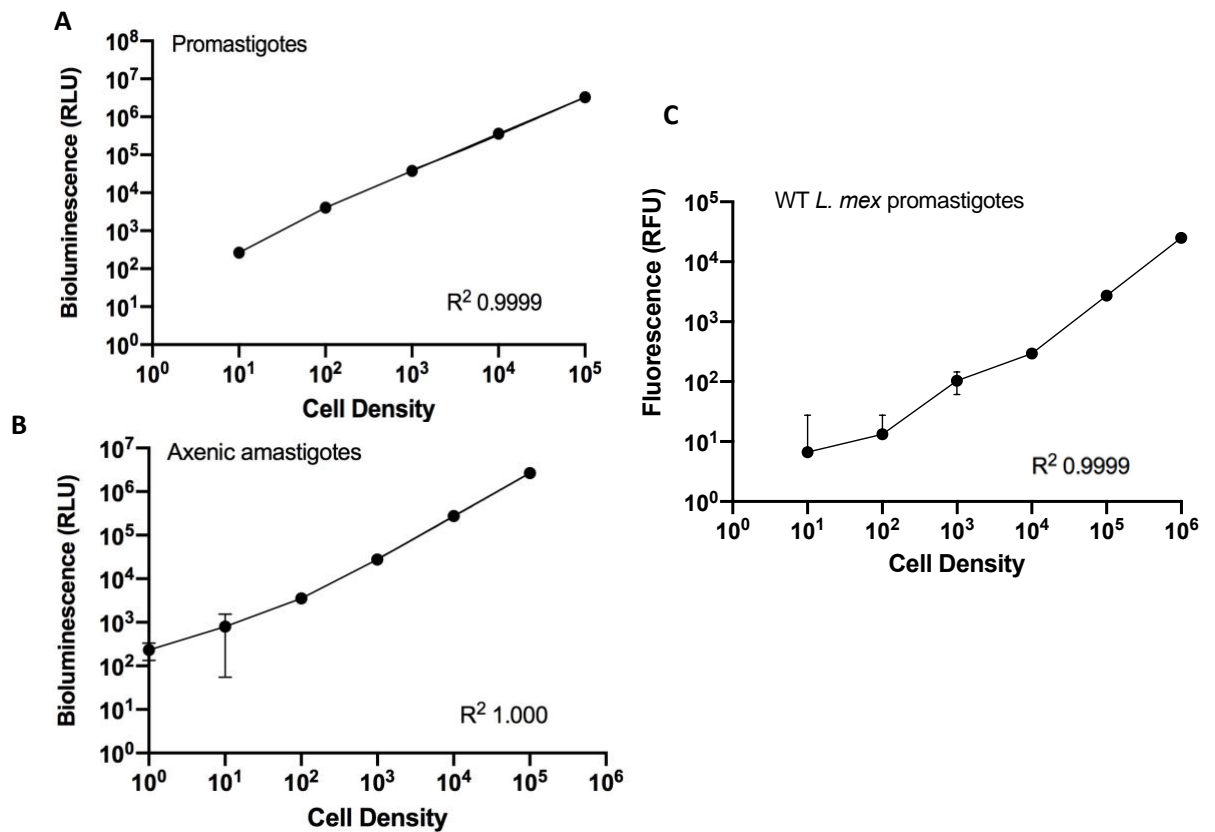


Figure 12 Initial analysis of luciferase-expressing *L. mexicana* transgenic cell line compared to fluorescence-based method. Cell density dilution series are plotted for the transgenic promastigote (A) and amastigote form (B) and on parental *L. mexicana* M379 promastigotes (C). Both X- and Y-axis were transformed by \log_{10} . All mean values are shown as $n=3 \pm \text{SEM}$.

The R^2 values obtained were 0.999 and 1.000 for NanoLuc-PEST expressing axenic promastigotes and amastigotes respectively and 0.999 for WT promastigotes, shown in Figure 12. The R^2 value is determined by using a nonlinear regression to fit the data to the equation $Y=\text{slope} \cdot X$. These R^2 values therefore show that the bioluminescence and fluorescence are proportional to the number of cells due to the strong linearity. This data also provides evidence that the transgenic parasites are expressing luciferase and that PrestoBlue is a fluorescence-based assay that can be used as comparison. The linearity of the graphs can be compared in the form of orders when compared to blanks. In Figure 12A, 4 orders can be seen as strong linearity, Figure 12B, 3.5 orders and Figure 12C, 2.5 orders. Therefore, the plateau seen from $10^1 - 10^2$ in the fluorescence graph suggests lower

sensitivity compared to the bioluminescence data. However, the R^2 data does not show a huge difference in sensitivity between the two methods as only a difference of 1.5 orders between the fluorescence and bioluminescence data.

4.2 Determining the EC₅₀ of Amphotericin B, Miltefosine, Pentamidine and Potassium Antimony Tartrate

The potency of a compound is expressed as the EC₅₀ (maximal effective concentration) and is the concentration of a drug that induces a response halfway between the baseline and maximum (Singh et al., 2020). This is a significant value that can be determined easily and is used to compare drug potencies. The EC₅₀ of each anti-leishmanial drug was therefore measured so that relevant concentrations could be determined for the rate-of-kill assays. The EC₅₀ for each anti-leishmanial drug was determined for NanoLuc-PEST expressing and WT strains of *L. mexicana*. The EC₅₀ values were obtained in promastigotes and axenic amastigotes in both cell lines using only the fluorescence-based method. This approach was used to ensure the transgenic cell line did not significantly differ from the wild type.

To determine the EC₅₀ of each drug, the parasites were incubated in a range of concentrations of each drug for 72 hours. The parasite viability and number of metabolically active cells were then measured after an appropriate incubation period with either luciferase reagent or PrestoBlue for the bioluminescence-based and fluorescence-based assays respectively. These values were generated in GraphPad Prism, using a log concentration versus normalised response curve, where the values are shown in Table 8 and the EC₅₀ curves in Figure 13. 5 µM of amphotericin B was used as a supralethal dose ensuring 0% growth and was used as a positive control in these assays. Untreated parasites were used as the negative control for 100% growth and used to normalise the data. Each assay was performed in biological triplicate and technical duplicate (n=3) for all EC₅₀ assays performed.

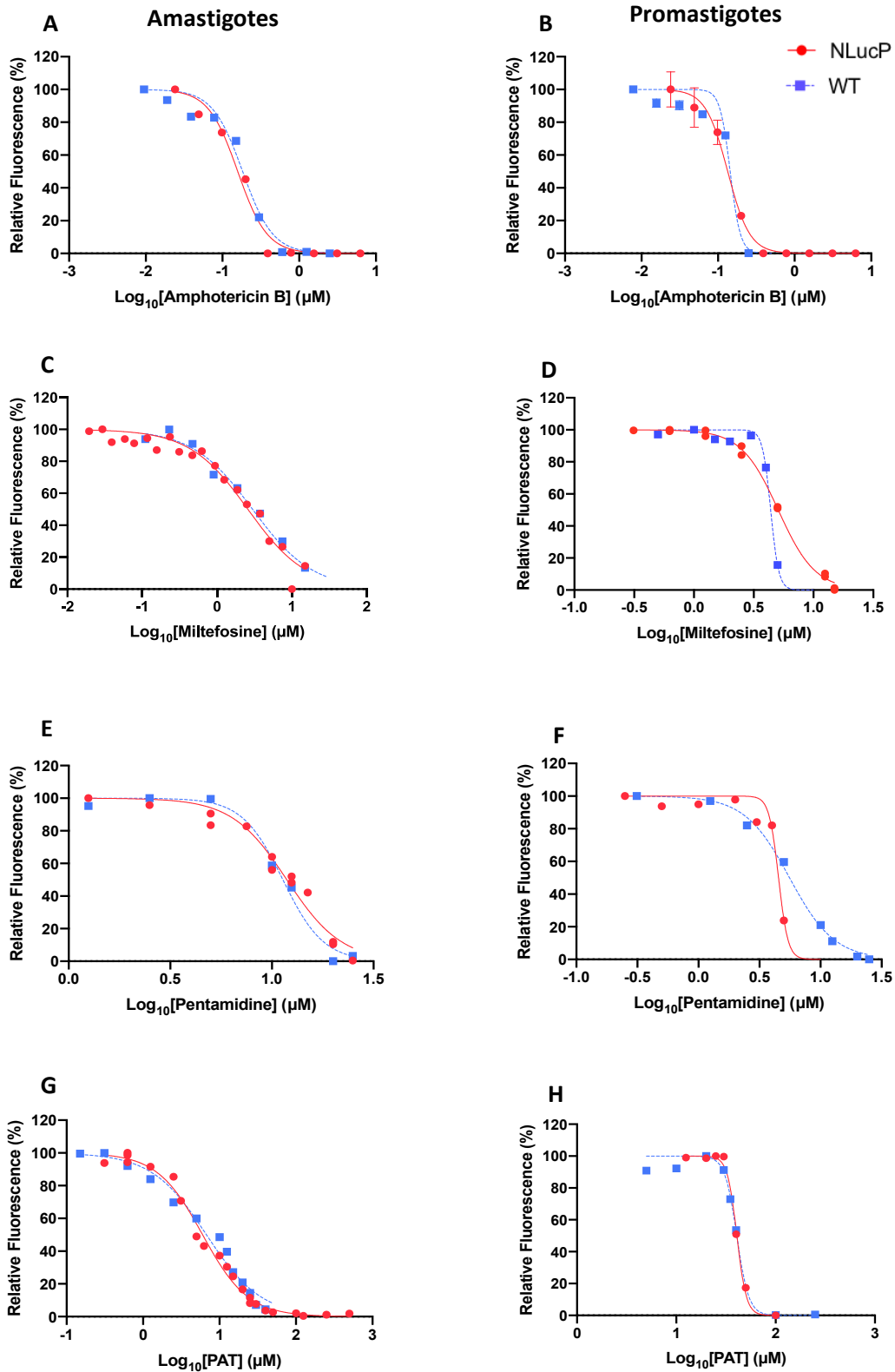


Figure 13 EC50 curves of amphotericin B, miltefosine, pentamidine and potassium antimonyl tartrate against (blue) wild type and (red) NanoLuc-PEST expressing *L. mexicana* axenic amastigotes (A,C,E,G) and promastigotes (B,D,F,H). Data represents n=3 with SEM error bar.

The parental and NanoLuc-PEST strains appear to have very similar susceptibility to each of the drugs using two different assays. Table 8 shows the EC₅₀ values from this study and Table 7 shows the EC₅₀ values obtained from other studies. Amphotericin B and Miltefosine values correspond with those determined in previous studies (Berry et al., 2018, Callahan, Portal, Devereaux and Groggl, 1997). It was difficult to compare the of pentamidine and potassium antimonyl tartrate EC₅₀ values obtained in this study, with literature values. The EC₅₀ of trivalent antimonial compounds have been studied but the majority of research was performed *in vivo*, using Old World visceral *Leishmania* species. The little *in vitro* studies that there are, use *L. infantum* or *L. major* species, which is again looking at a different causative species, see Table 7. The data from pentamidine and potassium antimonyl tartrate therefore does differ compared to these literature sources but not only are different species investigated, the methods used to determine the 50% inhibitory effect varies, as well as the routine experimental factors, such as the media used. Therefore, not only was the data not comparable with causative species but the amount of drug used was dependent on weight and not a directly comparable value.

Despite the differences in each study, this thesis therefore provides *in vitro* EC₅₀ data for drug treatments that have been routinely used for several years and confirms the similarity in EC₅₀ values for the amphotericin B and miltefosine, which have been investigated more thoroughly. It also shows the differences in EC₅₀ data that can be obtained from different experimental approaches, such as methods used to determine EC₅₀ values.

The Z' values shown in Table 8 for the EC₅₀ obtained from this study shows not only the robustness of the PrestoBlue assay as the Z' value is 0.78-0.88, much greater than the 0.5 reference value of an acceptable robust method. This statistical value is determined from the positive and negative controls and is calculated from the difference between them. Therefore, such a high Z' value shows that the positive (0% growth) and negative (100% growth) controls work.

Table 9 Table collating the EC50 values in literature for Amphotericin B, Miltefosine, Pentamidine and Potassium Antimonyl Tartrate. All studies show EC50 values against *L. mexicana* strain M379 unless stated otherwise in the table.

Drug	Strain	Form	Method	EC ₅₀ (μM) ± SEM	95% CI	Study
Amphotericin B	Wild-type	Axenic amastigote	Fluorescence	0.23	0.23-0.29	Berry et al., 2018
	NanoLuc-PEST	Axenic amastigote	Fluorescence	0.27	0.27-0.28	
	NanoLuc-PEST	Axenic amastigote	Bioluminescence	0.20	0.18-0.20	
	Wild-type	Axenic amastigote	Counting	0.28±0.02 ug/ml		Callahan, Portal, Devereaux and Grogl, 1997
Promastigote		0.14 ±0.02 ug/ml				
Miltefosine	Wild-type	Axenic amastigote	Fluorescence	1.11	0.99-1.16	Berry et al., 2018
	NanoLuc-PEST	Axenic amastigote	Fluorescence	1.99	1.80-2.06	
	NanoLuc-PEST	Axenic amastigote	Bioluminescence	2.19	2.07-2.35	
Pentamidine	Wild-type	Promastigote	Counting	0.67±0.1 ug/ml		Callahan, Portal, Devereaux and Grogl, 1997
	Wild-type	Axenic amastigote	Counting	5.0±0.8 ug/ml		
	Wild type	Promastigote	MTT assay	0.5 ±0.1		Basselin et al., 2002
Potassium Antimonyl Tartrate	<i>L. infantum</i> Wild-type	Axenic amastigote	MTT assay	1.32 ug/ml		Sereno et al., 1998
	<i>L. major</i> Wild type	Promastigotes	MTT assay	17.87 ug/ml		Mirzaie, Nosratabadi, Derakhshanfar, Sharifi, 2007

Table 10 EC₅₀ values of amphotericin B, miltefosine, pentamidine and potassium antimonyl tartrate.

These values were determined for wild type and NanoLuc-expressing *L. mexicana* axenic amastigotes and promastigotes using a fluorescence-based assay. Treated cells were incubated in triplicate for 72 hours in the dark with positive (5 μM amphotericin B) and negative (Schneider's medium) controls. Calculated Z' score and 95% CI for each assay is presented. All data represents n=6 as assay was performed in biological triplicate and technical duplicate.

Strain	Drug	Parasite stage	EC ₅₀ (μM)	95% CI	Z'
Wild Type	Amphotericin B	Promastigote	0.14	0.13 – 0.16	0.78 – 0.88
		Amastigote	0.18	0.17 – 0.20	
	Miltefosine	Promastigote	4.39	4.30 – 4.47	
		Amastigote	2.99	2.68 – 3.33	
	Pentamidine	Promastigote	4.74	4.27 – 5.24	
		Amastigote	10.89	9.72 – 11.48	
	Potassium Antimonyl	Promastigote	40.66	39.85 – 41.71	
		Amastigote	6.75	6.02 – 7.52	
NanoLuc-PEST	Amphotericin B	Promastigote	0.13	0.12 – 0.15	
		Amastigote	0.16	0.14 – 0.17	
	Miltefosine	Promastigote	5.07	4.89 – 5.25	
		Amastigote	2.58	2.27 – 2.94	
	Pentamidine	Promastigote	4.53	4.39 – 4.67	
		Amastigote	11.84	11.27 – 12.41	
	Potassium Antimonyl	Promastigote	40.72	40.04 – 41.42	
		Amastigote	6.01	5.53 – 6.51	

4.3 Determining the Rate of Kill of Amphotericin B, Miltefosine, Pentamidine and Potassium Antimony Tartrate

The determined EC_{50} values for the drugs (see Table 8) were used to calculate the four concentrations required to complete a 72-hour rate of kill assay. The rate of kill assay is relative that requires cells to be exposed to equipotent EC_{50} concentrations in order to compare any cytotoxic effects of amphotericin b, miltefosine, pentamidine and potassium antimonyl tartrate. A dilution range of $9 \times EC_{50}$, $3 \times EC_{50}$, $1 \times EC_{50}$ and $0.33 \times EC_{50}$ was used to measure the initial activity of the compounds against NanoLuc-PEST parasites, specifically only targeting the amastigote stage. The axenic amastigotes were only used to determine the EC_{50} values as they are the most clinically relevant form to research as the promastigote form is only present in a host for a very limited time before transforming into amastigotes. The parasite viability determined using bioluminescence-based assay was measured after 4, 24, 48 and 72 hours and the fluorescence-based assay was measured after 24, 48 and 72 hours.

Amphotericin B appears to be a fast-acting drug, as with the bioluminescence-based assay (Figure 14a), there were no viable parasites detected at $1 \times EC_{50}$ after 24 hours and the four-hour data showing no viable parasites detected at $1 \times$, $3 \times$ and $9 \times EC_{50}$. This can be seen by the rapid decline in the in 4, 24- and 48-hour lines to 0% relative bioluminescence. The fluorescence-based assay also shows that there were no metabolically active parasites detected at $3 \times EC_{50}$ regardless of time interval, as seen in Figure 14b by the rapid decline of the 24, 48- and 72-hour lines to 0%. The 24 hour (blue) data in the bioluminescence graph is seen to have higher parasite viability compared to the pink 4 hour data, where 0% viability is already seen at $1 \times EC_{50}$. This could be due to numerous reasons; the most likely possibility is human error. Each rate of kill assay was performed in biological triplicate and so, variations are likely without further technical repeats. Miltefosine, on the other hand, was shown to be a slow-acting drug, as seen in Figure 14C and D). Regardless of time, concentration or assay used,

miltefosine fails to eliminate all amastigotes. This is seen in Figure 14C and D by the slow decline and flatter profiles, showing much slower drug-induced effect on cell viability. Amphotericin B and miltefosine have been found in previous studies to also be fast- and slow-acting drugs respectively. As the relative rate of kill for amphotericin B and miltefosine had been determined using the *L. mexicana* NanoLuc-PEST cell line, these were used as benchmarks to characterise the rate of kill of pentamidine and potassium antimonyl tartrate.

Pentamidine and potassium antimonyl tartrate both exhibit an intermediate, moderate rate of kill in comparison to amphotericin B and miltefosine. Pentamidine shows to eventually reach the maximal effect at the highest concentration by 72 hours. Within the first 4 hours using the bioluminescence-based assay, pentamidine is shown to not to be effective as parasite viability appears consistent regardless of concentration. Potassium antimonyl tartrate shows to fully eliminate all parasites using the bioluminescence-based assay at $9 \times EC_{50}$ by 72 hours, as seen in Figure 14g. In comparison to pentamidine, the 4-hour data shows that potassium antimonyl tartrate acts slightly faster due to the concentration dependent decline in relative bioluminescence.

Therefore, these results appear to show the following relative rate of kill order: amphotericin B > potassium antimonyl tartrate > pentamidine > miltefosine, with both amphotericin B and miltefosine showing comparable results with other studies.

All assays had a Z' factor value of ≥ 0.5 , providing statistical evidence of the robustness of each assay (Table 9). The table shows the similarity and strong robustness of both the fluorescence and bioluminescence-based methods.

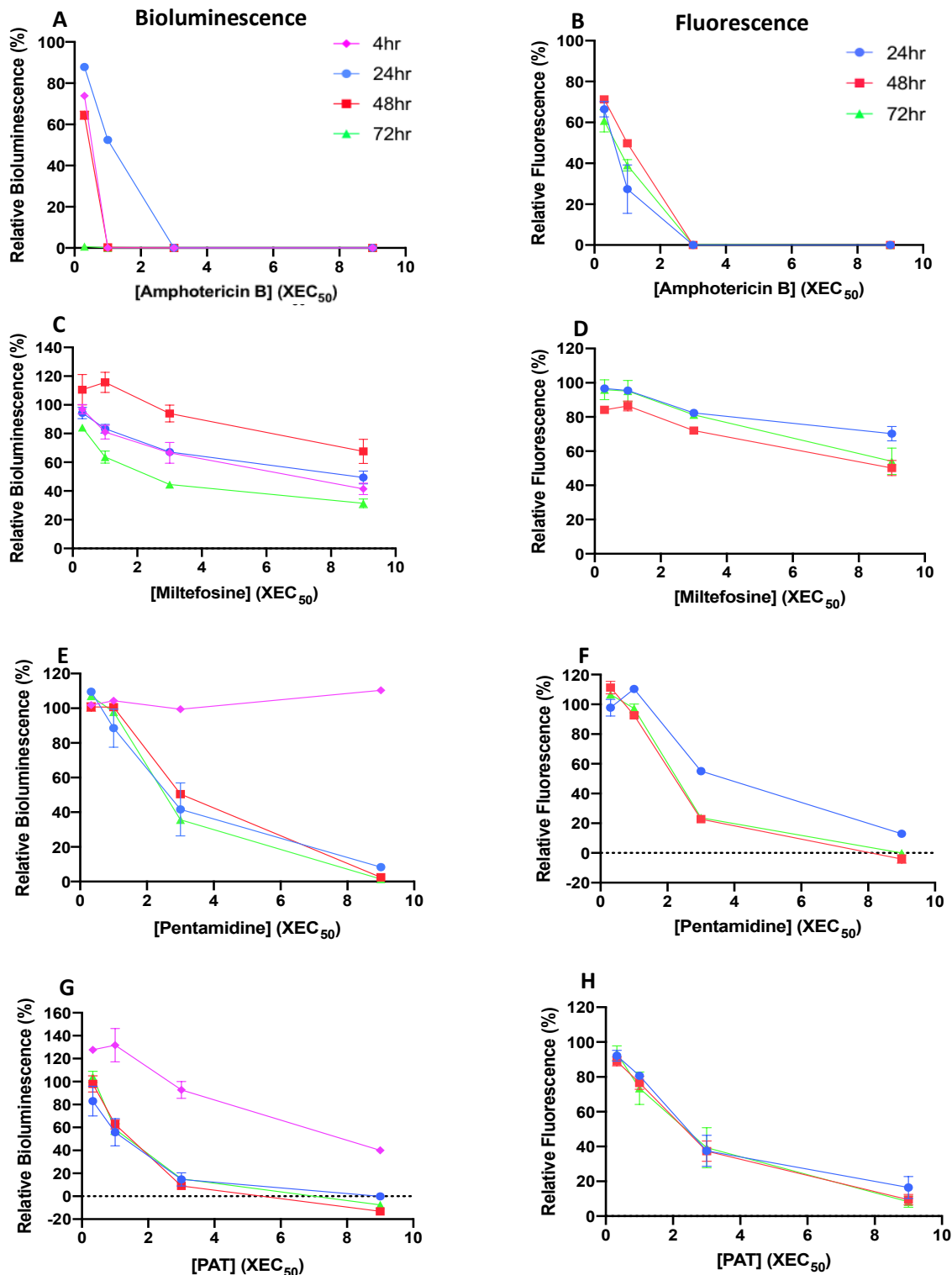


Figure 14 Rate of kill curves of amphotericin B, miltefosine, pentamidine and potassium antimonyl tartrate against the NanoLuc-PEST *L. mexicana* amastigotes. The normalised bioluminescence signal (a,c,e,g) and fluorescence signal (b,d,e,f) after 4, 24, 48 and 72 hours and 24, 48 and 72 hours of exposure respectively, is plotted as $n=3 \pm \text{SEM}$ error bars.

Table 9 Assay parameter, Z' factor values calculated for the rate of kill of amphotericin B, miltefosine, pentamidine and potassium antimonyl tartrate, for the PrestoBlue and the luciferase assays.

Drug	Assay	Z'
Amphotericin B	Fluorescence	0.72-0.88
Miltefosine		
Pentamidine		
Potassium Antimonyl Tartrate		
Amphotericin B	Bioluminescence	0.73-0.89
Miltefosine		
Pentamidine		
Potassium Antimonyl Tartrate		

Chapter 5 - Discussion

5.1 Rate of kill: Fast- or slow-acting compounds

The rate of kill for antileishmanial drugs is a significant gap in research and the use of a transgenic *Leishmania* expressing NanoLuc-PEST cell line is a novel approach for early drug discovery research. In this thesis, the relative rate of kill was determined for the antileishmanial drugs amphotericin B, miltefosine, pentamidine and potassium antimonyl tartrate, using an adaption of the BRRoK assay established by Ullah et al., 2017. This study demonstrated a robust format to monitor and rank the relative rate of kill for 372 antimalarial compounds. This assay used a transgenic *P. falciparum* cell line that expressed a luciferase (Dd2^{luc}) and measured the loss of bioluminescence signal within 6 hours following exposure to antimalarial drugs. Modifications were made and applied from this study such as, number of time intervals and concentrations monitored. Sanz et al., 2012 suggested that saturation of rate of kill at a 10x IC₅₀ concentration or greater occurs, meaning the maximal rate of in vitro kill, where any concentration-dependent parasite kill is unchanged. Ullah et al., 2017, confirmed these findings when using and so a maximum of 9xEC₅₀ concentration was used in this thesis and no saturation at the highest concentration was evident. The saturation point mentioned in both Ullah et al., 2017 and Sanz et al., 2012 may be worth revisiting in this relative rate of kill assay as the concentrations used were selected to best represent and modelled from *P. falciparum*. May be worth analysing the effects of 27 X EC₅₀ concentration too see if there is a saturation point, similar to that seen using *P. falciparum* parasites.

Ullah et al., 2017 conducted their BRRoK assay using drugs with known relative rate of kill data to firstly determine that the assay produces results comparable to literature and to then utilise them as benchmarks for the 372 screening compounds. Using the novel NanoLuc-PEST luciferase and shorter half-life manipulated by the PEST region, the ant-leishmanial drugs were monitored over 4 time points, with the first results recorded after just 4 hours, unlike the 6-hour timepoint used in previous research. Amphotericin B was observed to achieve maximal effect within 4 hours at concentrations over 3 x EC₅₀

using the luciferase expressing assay but showed to act much slower when using the resazurin-based assay, where maximum effect was seen at 3 x and 9 x EC₅₀. Amphotericin B has demonstrated slower killing rate in *in vivo* studies compared to the rapid four hours observed in this study. Although there are more differences than similarities in this study, at a high dose (10 mg/kg), over 90% inhibition was observed within two days (Voak et al., 2017). Within an animal model, the drug has a complex system to navigate and variables, such as; (i) the absorption (A) into the bloodstream, (ii) the distribution (D) around the host, (iii) how quickly it is metabolised (M) and (iiii) the excretion (E) and passing of the compound out of the host. As well as ADME factors to consider, there are extensive host and parasitic membranes to overcome prior to a drugs function. Therefore, the rate of kill defined as days in *in vivo* research, as opposed to a matter of hours seen *in vitro* is a variable to consider when comparing the time taken for a compound to be effective in more complex systems. Despite the clear differences between axenic practices compared to animal models, it would be unethical to test early drug discovery screenings in vivo first and this study shows a simple way of distinguishing relative rate of kill then can be used to discriminate promising compounds.

Miltefosine failed to kill all amastigotes, with detectable cell viability remaining after 72 hours of drug exposure. Long exposure of miltefosine in leishmaniasis treatments has been demonstrated. In previous studies, it took at least 168 hours at 2 x IC₅₀ (10 µM) for miltefosine to kill all *L. infantum* amastigotes in infected macrophages (Maes et al., 2016). Amphotericin B and miltefosine were therefore confirmed fast-acting and slow-acting anti-leishmanial drugs, in both the bioluminescence- and fluorescence-based assay and were used as benchmarks to discriminate the relative rate of kill for pentamidine and potassium antimonial tartrate.

The potassium antimonyl tartrate data indicates a moderate rate of kill in comparison to amphotericin B and miltefosine. Pentavalent antimonial drugs have been documented as slow releasing, with a

common explanation being the intracellular reduction of the pentavalent form into the trivalent form within acidic compartments of mammalian cells (dos Santos Ferreira et al., 2003). The inactive form has shown to fail reaching maximum cidal efficacy against *L. donovani*-infected macrophages within 240 hours. However, this would not be the case in this study as this model was not used, but it does provide an explanation for the differences in results obtained for potassium antimonyl tartrate EC₅₀ data and such, due to the complex mechanism involved. Potassium antimonyl tartrate demonstrated a definite concentration-dependent loss of both bioluminescence and fluorescence signal, where full cytotoxic effect was observed within 24 hours of exposure at 9 x EC₅₀. Maes et al., 2016 performed a time-to-kill assay of trivalent antimony against *L. donovani*- and *L. infantum*-infected macrophages and found that maximum effect was reached within 92 hours at 2 x IC₅₀ against *L. infantum* amastigotes. Although both results cannot be directly compared due to the different cellular models used, it can be noted that the rate of kill for trivalent antimony was slower than amphotericin B but acted faster than miltefosine (Maes et al., 2016). Therefore, the trivalent form did exhibit concentration-dependent cytotoxic effects and showed greatest potency at higher fold EC₅₀ concentrations. Intra-macrophage based assays however, have more membranes and biologically relevant environments to interact with compared to *in vitro* axenic assays.

For pentamidine, very little knowledge is documented about its rate of kill properties. From this work however, the relative parasite viability was significantly reduced at 9 x EC₅₀ with the maximal kill reached within 48 hours. It can therefore be suggested to fall between the fast- and slow-acting standards, acting slightly slower compared to potassium antimonyl tartrate.

This rate of kill assay demonstrated in this thesis is relative, providing only a qualitative outcome and broad interpretation of the order in which drugs effect cell viability in relation to known controls. Therefore, the order in which the drugs investigated within this study appear as, is: amphotericin B >

potassium antimonyl tartrate > pentamidine > miltefosine. With these results and relative observations, it provides amphotericin B and miltefosine as two very useful controls for future work as they clearly show extremely fast and extremely slow acting qualities respectively. As an approach to potentially categorise new drugs based on their relative rate of kill, amphotericin B and miltefosine set very clear boundaries for comparisons.

The mode of action for the anti-leishmanial drugs used in this study is limited and largely based on theories. However, there are strongly supported ideas that the rate of kill for anti-parasitic drugs are dictated by their mode of action. Applying that to the results of this thesis, it can be proposed that due to the similar rate of kill displayed by pentamidine and potassium antimonial tartrate, these two compounds may inhibit or interact with some of the same molecular targets or cellular pathways. Miltefosine displays a relatively slow rate of kill, with viable parasites detected after 72 hours. Again, the mode of action for miltefosine is limited, but it is known that it involves a number of targets that indirectly induces cell death. It is just a theory that the non-specific targets for leishmania cell death inflicted by miltefosine, may reflect the slow rate of kill shown. Amphotericin B is known to disrupt cell permeability resulting in membrane damage and cell death. An idea to support the fast rate of kill observed with amphotericin B could be that the mode of action is the specific membrane target that is the first point of contact with the amastigote once within the macrophage.

Using this rate of kill assay as a high throughput approach to categorise compounds on their cytotoxic effect on *Leishmania* cells and to aid in the identification of possible drug candidates is one useful quality of this assay. Another key parameter is the potential to connect the rate of kill and mode of action of a compound. Ullah et al., 2020 used this approach for *P. falciparum* studies and provided this approach that offers proof that the rate of kill of compound is related to its mode of action. Using only 2 incubation times of 6 and 48 hours, they compared the rate of kill of 370 compounds from the

Medicine for Malaria Venture (MMV) Malaria Box. By using a 6-hour incubation, compounds exhibiting a rapid rate of kill are easily distinguishable and as a result of a 48-hour incubation, any compounds showing intermediate effects or lags can be separately categorised and their mode of action compared to compounds exhibiting a similar rate of kill. From their study, they have highlighted scaffolds that offer a strong connection between the rate of kill, mode of action and structure of the possible candidates.

A limitation of this study, as Ullah et al., 2017 previously described is that despite the high-speed potential of this assay to determine the initial rate of kill, the preliminary EC₅₀ determination of the drugs took 72 hours compared to the 4-hour initial results obtained using the bioluminescence-based assay. However, there is significant potential for this assay to be a high-throughput screening. It was also suggested the opportunity of using stage-specific parasites to explore the rate of kill dynamics on the different *P. falciparum* stages. Whilst *Leishmania* has two stages, promastigotes are only found in the host for a very short period of time, meaning amastigotes would be the clinically-relevant *Leishmania* stage to consider and explore further rate of kill research.

Therefore, scaling this rate of kill assay to screen for potential anti-leishmanial candidates could be an exciting and promising approach for future work, though some modifications will need to be made for high throughput studies.

5.2 Evaluation of experimental approaches

5.2.1 Bioluminescence vs fluorescence

Determining the rate of kill for hit compounds in other protozoan parasites has seen increasing efforts in research. There are a number of *in vitro* techniques that have developed for *P. falciparum*, *T. brucei* and *T. cruzi* that have the common objective to measure parasite viability. These include parasite counting by microscopy and the activity of specific enzymes or metabolites to measure parasite growth inhibition. Limitations of such assays include how the sensitivity and application varies across each approach. The approaches used to measure parasite viability, ranging from metabolic activity to microscopic observation, provide a significant opportunity for misinterpretation or obtaining differing results. Challenging interpretation has been previously documented, with assays measuring viable cells dead due to parasites arrested in specific life cycle stages and therefore displaying to be metabolically inactive. Extended metabolic expression displayed by dying parasites and compounds that induce delayed parasite death are also likely to lead to conflicted results and assumptions (Cancino-Faure et al., 2016, Dahl and Rosenthal, 2007).

The resazurin-based PrestoBlue® approach is dependent upon the metabolic activity of the cell and the enzymatic activity required to reduce resazurin into resorufin. For the conversion of the resazurin substrate into a fluorescent marker of cell viability to occur, incubation with the compound of interest is required. For this study, each assay involved an incubation time of five hours once exposed to the compound, in order to adequately develop above background. Therefore, whilst advantages of this approach include visual observation of the reaction and being relatively inexpensive, there are limitations. A significant disadvantage of this assay is the lag when incubating the cells with the samples. The irreversible reduction to the fluorescent signal could result in the measurement of metabolically inactive or non-viable cells as viable and provide inaccurate results. This could provide a

partial explanation as to the differences in relative cell viability between the results obtained in this study, using the bioluminescence-based assay in comparison with the fluorescence-based method. A slightly higher normalised fluorescence reading is recorded in the fluorescence rate of kill curves, a possible reason for this being the viable cells included in the measured fluorescence signal that would be excluded if measured with a much shorter incubation period.

Therefore, as a counter-action to this limitation, the use of luciferase-expressing *Leishmania* were used, which produce a bioluminescence signal by generating light in the presence of a substrate. This reaction is dependent upon ATP within living cells and the reagents are incubated for three minutes before the bioluminescence measured. This is a much more dynamic assay: almost immediate measurement and no lag provides a greater accuracy when determining the cell viability at a desired time point. The “real-time” perspective combined a high sensitivity, provides an extremely promising and dynamic method. Berry et al., 2018, discussed and evaluated the robustness of the bioluminescence approach. All assays were robust and showed a Z' value of equal or greater than 0.64, all values clear of the 0.5 lower limit, similar to the results of this thesis shown in Tables 8 and 9. The signal to background (S:B) (or signal to noise) ratio was also calculated for each assay and displayed between a 50- and 100-fold higher S:B ratio compared to the fluorescence-based assay used as a comparison. This is a parameter that assesses the strength of the desired signal, bioluminescence or fluorescence for example, relative to undesired background noise. The high ratio observed for the NanoLuc-PEST cell line relates to the modified luciferase with the addition of the PEST sequence, providing the reporter with high enzymatic activity and short half-life. The sensitivity of using this dynamic approach can be seen in this thesis in Figure 12.

The bioluminescence-based assay explored in this thesis, therefore does not provide a direct quantitative measurement of the rate of kill but does indirectly report the viability of the parasites.

Unlike the possibility of reporting metabolically inactive cells using the fluorescence-based approach, using luciferase-expressing parasites relies on the inability of dead and dying parasites to synthesis new luciferase.

Whilst this thesis has shown the advantages of the luciferase transgenic line and the bioluminescence-based approach, it has also demonstrated unquestionable agreement with both the EC_{50} and rate of kill data obtained. There is no significant difference between the sensitivity of each assay, with the bioluminescence method being slightly greater (Figure 12) and the robustness and function of controls for each method showing extremely similar high quality, see Table 8 and 9. The greatest advantage I can conclude from using bioluminescence-based assays would be the ability to immediately read the results, which, for an experiment that is time dependent, can be such a crucial and beneficial tool.

Interestingly however, variability within the 24 hour time point and later is greater within the bioluminescence assay format and there is also no further valuable data that is obtained that we do not observe using the fluorescence method, see Figure 14. The variability seen, particularly within the amphotericin B and miltefosine data, is likely due to experimental and human error. Smaller volumes are used for the bioluminescence assays, and the rate of kill data was only performed in biological triplicate. It could also be as simple is insufficient mixing of the luciferase reagent as the plates are read almost immediately. Therefore, no data sourced from separate experimental conditions have contributed to confirm the variability, which will need to be done in future work. Another possibility is that noise may be contributing to the data in the later time points and skewing the results to give some of the unrealistic and higher values seen in the rate of kill graphs.

5.2.2 Evaluating experimental test models for rate of kill research

The most appropriate *in vitro* test model used for exploring drug activity is considered to be the intracellular amastigote model, yet conflicting interpretation is common. The type of macrophage host cell used for drug activity (Seifert, Escobar and Croft, 2010) and the rate of promastigote infectivity of the macrophage cells (Inocêncio da Luz et al., 2009), are two examples of variability found in research. However, this model for drug testing does provide a model that is more physiologically relevant to axenic *in vitro* studies and is more readily accessible and cost-effective compared to *in vivo* and clinical studies.

Clinical studies for pharmacodynamics in cutaneous and visceral leishmaniasis have been conducted but are largely restricted to geographic location and are also challenged with species-specific variation. For the majority of VL research on miltefosine, clinical trials have taken place in the state of Bihar, India – VL endemic area. Data from these clinical studies are therefore likely going to be primarily clinically relevant to that area of study and not comparable to other VL endemic areas that are of equal importance (Hailu et al., 2010). For CL, the quality and number of clinical studies is considerably poor and also shows large species variation (Soto et al., 2008). A reasoning behind such a lack of CL clinical studies is the self-healing ability that this form of leishmaniasis exhibits and is therefore not as emphasised as VL. The limited PD research performed in clinical studies has therefore focused on drug efficacy and toxicity and no rate of kill data has been reported, to my knowledge.

Using the host cell-free parasite is a common approach for compound screening as these models are easier to handle and inexpensive in comparison to *in vivo* and cellular based models. The biological relevance of this strategy is scrutinised given several limitations. Virulence attenuation has been observed in axenic *in vitro* cultures and could be linked with a decreased capacity of promastigote

differentiation, as well as the genomic instability of serially passaged *Leishmania* cultures (Ali, Rees, Terrell-Nield and Ali, 2013, Moreira et al., 2012, Sinha et al., 2018). Therefore, attention to the number of times an active culture is passaged is crucial for relevant and accurate data.

Studying the pharmacodynamics of anti-leishmanial drugs is challenging regardless of the experimental model as there are variables that prove challenging across all research. Variability in drug susceptibility across *Leishmania* species (Escobar, Matu, Marques and Croft, 2002), strains and clinical isolates (Yardley et al., 2005) prove challenging to compare and improve drug screening research.

Therefore, considering all approaches, applying the bioluminescence-based method in macrophage-infected *in vitro* models would be an exciting and optimal approach. The mechanism of the adapted BRRoK assay is parasite-specific, therefore able to differentiate between parasite and host cells unlike the fluorescence options. Performing early drug screening in *Leishmania*-infected macrophage host cells would provide a more suitable test model compared to the axenic methods. The limitations of this approach however, would include the optimisation and generation of transgenic cell lines and expense of the reagents.

5.3 The relevance of rate of kill

The clinical pharmacodynamics of current anti-leishmanial drugs are limited and are not documented in great detail. Evaluating and prioritising the rate of kill of promising compounds would provide beneficial information regarding the mode of action and evaluation of the treatment duration required.

5.3.1 Possible use for improving treatment duration regimens

A significant and common drawback of anti-leishmanial treatments is the toxic effects on the patient, leading to adverse effects (AE) and severe adverse effects (SAE). The rate of kill is a measure of the length of time required for a compound to reach its maximum effect at a threshold concentration and provides a very important quality that can help determine the length of treatment required in clinical use. A short duration of drug exposure is an ideal parameter of drug therapies, particularly for drugs that exhibit toxic effects on the patient.

The current treatment regimens for leishmaniasis are much longer and require greater cooperation than what the ideal standard stated by DNDi, this is shown in Tables 3 and 4.

The treatment regimen for miltefosine is to take a 50 mg oral capsule twice a day for 28 consecutive days if you are over the age of 12 and weigh from 30 to 44 kg. That treatment is an incredibly lengthy plan, requiring a lot of patient cooperation to follow it. The slow rate of kill of miltefosine combined with a long terminal half-life (Dorlo et al., 2008) and extensive accumulation is an explanation for the required long treatment regimen of twice daily injections or oral capsules for 28 days.

When used as a parenteral therapy for cutaneous leishmaniasis, liposomal amphotericin B treatment is administered by IV infusion and typically includes receiving 3 mg/kg daily for 6 or more doses. The treatment duration for amphotericin B is therefore much shorter than that of miltefosine. The correlation between these two variables is strong, as the ideal monotherapy is fast-acting compounds that would then require shorter treatments. These qualities benefit those suffering from leishmaniasis due to a reduced need to attend primary health care settings as often, shorter exposure to the toxic side effects and reduced risk of emerging resistance. Fast renal and faecal excretion of amphotericin B could explain why the treatment duration is longer than expected and compared to other drugs with slower rate of kill, such as pentamidine.

From the results of this study, both pentamidine and potassium antimonyl tartrate exhibit a relatively an intermediate rate of action. Further work to consolidate this would be required however, as comparable results from previous studies were difficult to find. The longer rate of kill and long half-life of active trivalent antimony however, could again offer a discussion around the resistance shown against pentavalent antimony treatment and long treatment regimen. For pentavalent antimony therapy, the standard dose is 20 mg/kg for typically 20 days. Once again, it is a long treatment plan which has suffered from emerging resistance. Pentamidine pharmacokinetic and pharmacodynamic data is also largely unreported.

Based on this rate of kill study and literature, improved chemotherapy treatments are desperately needed, and the clinical PK/PD properties evaluated. Not one of the drugs currently available and active in anti-leishmanial treatments are ideal. Evaluating the initial rate of kill data in early drug discovery and discriminating between fast- and slow-acting compounds would be extremely valuable. In endemic areas showing emerging resistance, HIV/VL co-infection and relapses in immunocompetent

patients, combined therapy practices between fast- and slower-acting drugs are highly considered for future treatment.

When reviewing the miltefosine results obtained and the slow rate of kill it demonstrates, combination therapy with a faster acting drug that has a different mode of action, would be advantageous to explore and has been studied. This approach would lower the doses of drug required, result in a shorter duration of treatment due to increased efficacy and delay emerging drug-resistant parasites.

Combination therapy of liposomal amphotericin B and miltefosine is found to be highly efficient and exceed miltefosine monotherapy results, through a long-term follow up study in visceral leishmaniasis (Goswami et al., 2020). Further studies involving combination with amphotericin and liposomal amphotericin B, characterised as fast-acting, has showed high efficacy and reduced treatment duration (161, 20, 182). Regarding the toxicity observed and undetermined drug-drug interactions, researching combination therapies for a disease such as leishmaniasis, is challenging.

Research into the rate of kill of initial drug screenings can provide essential data and help to improve clinical outcomes by informed dosing and combination therapy, particularly to combat visceral leishmaniasis.

5.4 Future work

Rate of kill is only one of the parameters needed to define a compound as successful but measuring this will provide relevant and extremely useful information that derives from its structure and mode of action. The sensitivity and results obtained from the bioluminescence-based assay as a dynamic approach for compound discrimination requires further work, but initial findings show some promise.

The axenic *in vitro* application of this assay was able to distinguish the rate of kill and showed good sensitivity in the bioluminescence-based approach. Therefore, following this study, the assay can be optimised and performed in an intra-macrophage model to better represent the physiological conditions and better compare against current research and the results obtained *in vitro*. This assay can then be used to measure the rate of kill of experimental compounds that have previously shown activity against *Leishmania* parasites. This research only displayed the relative rate of kill as the data was not quantified. In future research, parameters such as the lag phase, *in vitro* parasite reduction ratio (PPR) and parasite clearance time (PCT) values can be calculated.

The discrimination of compounds could then be based upon the rate of kill, chemical structure, proposed mode of action and therefore aid in the suggestion of treatment regimens, as shown in Ullah et al., 2019 study. With a larger number of compounds to screen, a comparison and analysis of the compound structures would provide significantly greater insight to possible active groups and conformations that exhibit the same relative rate of kill and therefore, possible mode of action.

Therefore, an ideal future avenue to explore would be a mass screening of numerous compounds, similar to Ullah et al., 2019 such as the Pathogen Box library (Tadele, M., Abay, S., Makonnen, E. and

Hailu, A., 2020). There is extremely promising potential to refine this rate of kill assay for high throughput screening purposes in the very early drug discovery pipeline. Modifications to the current method in this thesis would be required to streamline and quicken the process. One of the longest processes is determining the EC₅₀ value of a compound and scaling the approach to hundreds of compounds that would require modification. A possibility would be to choose one concentration for all compounds to eliminate that initial 72-hour experiment. A second refinement would be the concentrations used in the assay, much like Ullah et al., 2019 altered. As seen in Figure 14, there is no valuable information that was shown after the 24-hour incubation and ideal drug candidates are fast-acting to avoid accumulation, resistance and long treatment regimens. Therefore, cutting the longer incubation times and proceeding with just the 4-hour and either 24-hour or 48-hour incubation would save time, expense and effort. Finally, from this thesis amphotericin B and miltefosine would make ideal controls for anti-leishmanial drug screening due to consistent results and would provide a fast-acting and slow-acting benchmark control.

Conclusion

The work done in this thesis identified the relative rate of kill, using a luciferase-expressing system, of amphotericin B, miltefosine, pentamidine and potassium antimonyl tartrate. Amphotericin B and miltefosine were identified as fast- and slow- acting drugs whereas pentamidine and potassium antimonyl tartrate showed an intermediate rate of kill. The novel approach of using NanoLuc-PEST expressing *Leishmania* showed to be a sensitive and dynamic reporter for parasite viability. Further work will need to be carried out to further optimise and evaluate the novel bioluminescence-based assay in a macrophage-infected model. This data in this thesis has identified the pharmacodynamic research gaps in early drug discovery of anti-leishmanial compounds and shows a promising novel bioluminescence-based approach.

References

Abbasi, I., Kirstein, O., Hailu, A. and Warburg, A., (2016). Optimization of loop-mediated isothermal amplification (LAMP) assays for the detection of Leishmania DNA in human blood samples. *Acta Tropica*, 162, pp.20-26.

ABP Biosciences., (2020). *Cell Viability Assay Based On Metabolic Activity | ABP Biosciences*. [online] Abpbio.com. Available at: <<http://www.abpbio.com/product/cell-viability-assay-based-on-metabolic-activity/>> [Accessed 19 April 2020].

Adams, E., Schoone, G., Versteeg, I., Gomez, M., Diro, E., Mori, Y., Perlee, D., Downing, T., Saravia, N., Assaye, A., Hailu, A., Albertini, A., Ndung'u, J. and Schallig, H., (2018). Development and evaluation of a novel loop-mediated isothermal amplification assay for diagnosis of cutaneous and visceral leishmaniasis. *Journal of Clinical Microbiology*, 56(7).

Aga, E., Katschinski, D., van Zandbergen, G., Laufs, H., Hansen, B., Müller, K., Solbach, W. and Laskay, T. (2002). Inhibition of the spontaneous apoptosis of neutrophil granulocytes by the intracellular parasite *Leishmania major*. *The Journal of Immunology*, 169(2), pp.898-905.

Agostino, V., Trinconi, C., Galuppo, M., Price, H. and Uliana, S., 2020. Evaluation of NanoLuc, RedLuc and Luc2 as bioluminescent reporters in a cutaneous leishmaniasis model. *Acta Tropica*, 206, p.105444.

Akhoundi, M., Downing, T., Votýpka, J., Kuhls, K., Lukeš, J., Cannet, A., Ravel, C., Marty, P., Delaunay, P., Kasbari, M., Granouillac, B., Gradoni, L. and Sereno, D. (2017). Leishmania infections: Molecular targets and diagnosis. *Molecular Aspects of Medicine*, 57, pp.1-29.

Al-Hucheimi, S., Sultan, B. and Al-Dhalimi, M. (2009). A comparative study of the diagnosis of Old World cutaneous leishmaniasis in Iraq by polymerase chain reaction and microbiologic and histopathologic methods. *International Journal of Dermatology*, 48(4), pp.404-408.

Ali, K., Rees, R., Terrell-Nield, C. and Ali, S., 2013. Virulence loss and amastigote transformation failure determine host cell responses to *Leishmania mexicana*. *Parasite Immunology*, 35(12), pp.441-456.

Alvar, J., Aparicio, P., Aseffa, A., Den Boer, M., Canavate, C., Dedet, J., Gradoni, L., Ter Horst, R., Lopez-Velez, R. and Moreno, J. (2008). The Relationship between Leishmaniasis and AIDS: the Second 10 Years. *Clinical Microbiology Reviews*, 21(2), pp.334-359.

Alvar, J., Vélez, I., Bern, C., Herrero, M., Desjeux, P., Cano, J., Jannin, J. and Boer, M., 2012. Leishmaniasis Worldwide and Global Estimates of Its Incidence. *PLoS ONE*, 7(5), p.e35671.

Anderson, B., Wong, I., Baugh, L., Ramasamy, G., Myler, P. and Beverley, S., 2013. Kinetoplastid-specific histone variant functions are conserved in *Leishmania major*. *Molecular and Biochemical Parasitology*, 191(2), pp.53-57.

Aviles, H., Belli, A., Armijos, R., Monroy, F. and Harris, E. (1999). PCR detection and identification of *Leishmania* parasites in clinical specimens in Ecuador: A comparison with classical diagnostic methods. *The Journal of Parasitology*, 85(2), p.181.

Basselin, M., Denise, H., Coombs, G. and Barrett, M. (2002). Resistance to pentamidine in *Leishmania mexicana* involves exclusion of the drug from the mitochondrion. *Antimicrobial Agents and Chemotherapy*, 46(12), pp.3731-3738.

Bates, P. (1994). Complete developmental cycle of *Leishmania mexicana* in axenic culture. *Parasitology*, 108(01), p.178-184.

Bates, P. (2007). Transmission of *Leishmania* metacyclic promastigotes by phlebotomine sand flies. *International Journal for Parasitology*, 37(10), pp.1097-1106.

Ben Abda, I., de Monbrison, F., Bousslimi, N., Aoun, K., Bouratbine, A. and Picot, S., 2011. Advantages and limits of real-time PCR assay and PCR-restriction fragment length polymorphism for the identification of cutaneous *Leishmania* species in Tunisia. *Transactions of the Royal Society of Tropical Medicine and Hygiene*, 105(1), pp.17-22.

Benne, R., Van Den Burg, J., Brakenhoff, J., Sloof, P., Van Boom, J. and Tromp, M., 1986. Major transcript of the frameshifted *coxII* gene from trypanosome mitochondria contains four nucleotides that are not encoded in the DNA. *Cell*, 46(6), pp.819-826.

Bennis, I., Thys, S., Filali, H., De Brouwere, V., Sahibi, H. and Boelaert, M., 2017. Psychosocial impact of scars due to cutaneous leishmaniasis on high school students in Errachidia province, Morocco. *Infectious Diseases of Poverty*, 6(1).

Berry, S., Hameed, H., Thomason, A., Maciej-Hulme, M., Saif Abou-Akkada, S., Horrocks, P. and Price, H. (2018). Development of NanoLuc-PEST expressing *Leishmania mexicana* as a new drug discovery tool for axenic- and intramacrophage-based assays. *PLOS Neglected Tropical Diseases*, 12(7), p.e0006639.

Berman, J., Waddell, D. and Hanson, B. (1985). Biochemical mechanisms of the antileishmanial activity of sodium stibogluconate. *Antimicrobial Agents and Chemotherapy*, 27(6), pp.916-920.

Bilgic-Temel, A., Murrell, D. and Uzun, S., 2019. Cutaneous leishmaniasis: A neglected disfiguring disease for women. *International Journal of Women's Dermatology*, 5(3), pp.158-165.

Blum, B., Bakalara, N. and Simpson, L., 1990. A model for RNA editing in kinetoplastid mitochondria: RNA molecules transcribed from maxicircle DNA provide the edited information. *Cell*, 60(2), pp.189-198.

Bogdan, C. (2012). Natural killer cells in experimental and human leishmaniasis. *Frontiers in Cellular and Infection Microbiology*, 2.

Bogdan, C. (2015). Nitric oxide synthase in innate and adaptive immunity: an update. *Trends in Immunology*, 36(3), pp.161-178.

Bogdan, C., Rollinghoff, M. and Diefenbach, A. (2000). The role of nitric oxide in innate immunity. *Immunological Reviews*, 173(1), pp.17-26.

Bray, P., Barrett, M., Ward, S. and de Koning, H. (2003). Pentamidine uptake and resistance in pathogenic protozoa: past, present and future. *Trends in Parasitology*, 19(5), pp.232-239.

Brittingham, A., Morrison, C., McMaster, W., McGwire, B., Chang, K. and Mosser, D., 1995. Role of the Leishmania surface protease gp63 in complement fixation, cell adhesion, and resistance to complement-mediated lysis. *Parasitology Today*, 11(12), pp.445-446.

Burza, S., Croft, S. and Boelaert, M., 2018. Leishmaniasis. *The Lancet*, 392(10151), pp.951-970.

Callahan, H., Portal, A., Devereaux, R. and Grogil, M., 1997. An axenic amastigote system for drug screening. *Antimicrobial Agents and Chemotherapy*, 41(4), pp.818-822.

Camacho, E., Rastrojo, A., Sanchiz, Á., González-de la Fuente, S., Aguado, B. and Requena, J., 2019. Leishmania mitochondrial genomes: Maxicircle structure and heterogeneity of minicircles. *Genes*, 10(10), p.758.

Cancino-Faure, B., Alcover, M., Fisa, R., Jimenez-Marco, T. and Riera, C., 2016. Detection and quantification of viable and nonviable *Trypanosoma cruzi* parasites by a propidium monoazide real-time polymerase chain reaction assay. *The American Journal of Tropical Medicine and Hygiene*, 94(6), pp.1282-1289.

Cantón, E., Pemán, J., Gobernado, M., Viudes, A. and Espinel-Ingroff, A., 2004. Patterns of amphotericin B killing kinetics against seven *Candida* species. *Antimicrobial Agents and Chemotherapy*, 48(7), pp.2477-2482.

Carter, K., Hutchison, S., Henriquez, F., Legare, D., Ouellette, M., Roberts, C. and Mullen, A. (2005). Resistance of *Leishmania donovani* to sodium stibogluconate is related to the expression of host and parasite -glutamylcysteine synthetase. *Antimicrobial Agents and Chemotherapy*, 50(1), pp.88-95.

Chagas, A., Oliveira, F., Debrabant, A., Valenzuela, J., Ribeiro, J. and Calvo, E. (2014). Lundepe, a sand fly salivary endonuclease increases *Leishmania* parasite survival in neutrophils and inhibits XIla contact activation in human plasma. *PLoS Pathogens*, 10(2), p.e1003923.

Chakravarty, J. and Sundar, S. (2010). Drug resistance in leishmaniasis. *Journal of Global Infectious Diseases*, 2(2), p.167.

Chappuis, F., Sundar, S., Hailu, A., Ghalib, H., Rijal, S., Peeling, R., Alvar, J. and Boelaert, M. (2007). Visceral leishmaniasis: what are the needs for diagnosis, treatment and control?. *Nature Reviews Microbiology*, 5(11), pp.873-882.

Chaves, M., Lee, S., Kamenyeva, O., Ghosh, K., Peters, N. and Sacks, D., 2020. The role of dermis resident macrophages and their interaction with neutrophils in the early establishment of *Leishmania major* infection transmitted by sand fly bite. *PLOS Pathogens*, 16(11), p.e1008674.

Chen, J., Steele, T. and Stuckey, D., 2017. Metabolic reduction of resazurin; location within the cell for cytotoxicity assays. *Biotechnology and Bioengineering*, 115(2), pp.351-358.

Christensen, S., Belew, A., El-Sayed, N., Tafuri, W., Silveira, F. and Mosser, D., 2019. Host and parasite responses in human diffuse cutaneous leishmaniasis caused by *L. amazonensis*. *PLOS Neglected Tropical Diseases*, 13(3), p.e0007152.

Coelho, A., Beverley, S. and Cotrim, P. (2003). Functional genetic identification of PRP1, an ABC transporter superfamily member conferring pentamidine resistance in *Leishmania major*. *Molecular and Biochemical Parasitology*, 130(2), pp.83-90.

Cota, G., de Sousa, M., Demarqui, F. and Rabello, A. (2012). The diagnostic accuracy of serologic and molecular methods for detecting visceral leishmaniasis in HIV infected patients: Meta-analysis. *PLoS Neglected Tropical Diseases*, 6(5), p.e1665.

Courret, N., Fréhel, C., Gouhier, N., Pouchelet, M., Prina, E., Roux, P., Antoine, J.C., (2002) Biogenesis of Leishmania-harboring parasitophorous vacuoles following phagocytosis of the metacyclic promastigote or amastigote stages of the parasites. *J Cell Sci* 115, 2303–2316.

Coutinho-Abreu, I., Oristian, J., de Castro, W., Wilson, T., Meneses, C., Soares, R., Borges, V., Descoteaux, A., Kamhawi, S. and Valenzuela, J., 2020. Binding of *Leishmania infantum* LPG to the midgut is not sufficient to define vector competence in *Lutzomyia longipalpis* sand flies. *mSphere*, 5(5), pp.594-620.

Cunningham, J., Hasker, E., Das, P., El Safi, S., Goto, H., Mondal, D., Mbuchi, M., Mukhtar, M., Rabello, A., Rijal, S., Sundar, S., Wasunna, M., Adams, E., Menten, J., Peeling, R. and Boelaert, M., (2012). A global comparative evaluation of commercial immunochromatographic rapid diagnostic tests for visceral leishmaniasis. *Clinical Infectious Diseases*, 55(10), pp.1312-1319.

Dahl, E. and Rosenthal, P., 2007. Multiple antibiotics exert delayed effects against the *Plasmodium falciparum* apicoplast. *Antimicrobial Agents and Chemotherapy*, 51(10), pp.3485-3490.

Das, A., Banday, M. and Bellofatto, V., 2007. RNA polymerase transcription machinery in Trypanosomes. *Eukaryotic Cell*, 7(3), pp.429-434.

Davidson, R., den Boer, M. and Ritmeijer, K. (2009). Paromomycin. *Transactions of the Royal Society of Tropical Medicine and Hygiene*, 103(7), pp.653-660.

Decuypere, S., Rijal, S., Yardley, V., De Doncker, S., Laurent, T., Khanal, B., Chappuis, F. and Dujardin, J. (2005). Gene expression analysis of the mechanism of natural Sb(V) resistance in *Leishmania donovani* isolates from Nepal. *Antimicrobial Agents and Chemotherapy*, 49(11), pp.4616-4621.

Delobel, P. (2003). Rhabdomyolysis associated with pentamidine isethionate therapy for American cutaneous leishmaniasis. *Journal of Antimicrobial Chemotherapy*, 51(5), pp.1319-1320.

Demicheli, C., Frézard, F., Lecouvey, M. and Garnier-Suillerot, A. (2002). Antimony(V) complex formation with adenine nucleosides in aqueous solution. *Biochimica et Biophysica Acta (BBA) - General Subjects*, 1570(3), pp.192-198.

de Paiva-Cavalcanti, M., de Morais, R., Pessoa-e-Silva, R., Trajano-Silva, L., Gonçalves-de-Albuquerque, S., Tavares, D., Brelaz-de-Castro, M., Silva, R. and Pereira, V., 2015. Leishmaniasis diagnosis: an update on the use of immunological and molecular tools. *Cell & Bioscience*, 5(1), pp. 531-541.

de Ruiter, C., van der Veer, C., Leeflang, M., Deborggraeve, S., Lucas, C. and Adams, E. (2014). Molecular tools for diagnosis of visceral leishmaniasis: Systematic review and meta-analysis of diagnostic test accuracy. *Journal of Clinical Microbiology*, 52(9), pp.3147-3155.

De Rycker, M., Hallyburton, I., Thomas, J., Campbell, L., Wyllie, S., Joshi, D., Cameron, S., Gilbert, I., Wyatt, P., Frearson, J., Fairlamb, A. and Gray, D., 2013. Comparison of a high-throughput high-content intracellular *Leishmania donovani* assay with an axenic amastigote assay. *Antimicrobial Agents and Chemotherapy*, 57(7), pp.2913-2922.

Desjeux, P. (2001). The increase in risk factors for leishmaniasis worldwide. *Transactions of the Royal Society of Tropical Medicine and Hygiene*, 95(3), pp.238-243.

Desjeux, P., 2004. Focus: Leishmaniasis. *Nature Reviews Microbiology*, 2(9), pp.692-692.

Dorlo, T., Balasegaram, M., Beijnen, J. and de Vries, P. (2012). Miltefosine: a review of its pharmacology and therapeutic efficacy in the treatment of leishmaniasis. *Journal of Antimicrobial Chemotherapy*, 67(11), pp.2576-2597.

dos Santos Ferreira, C., Silveira Martins, P., Demicheli, C., Brochu, C., Ouellette, M. and Frézard, F. (2003). *BioMetals*, 16(3), pp.441-446.

Drugs for Neglected Diseases initiative (DNDi). 2022. *Target product profile for cutaneous leishmaniasis, DNDi*. [online] Available at: <https://dndi.org/diseases/cutaneous-leishmaniasis/target-product-profile/> [Accessed 18 April 2022].

Du, R., Hotez, P., Al-Salem, W. and Acosta-Serrano, A., 2016. Old world cutaneous leishmaniasis and refugee crises in the Middle East and north Africa. *PLOS Neglected Tropical Diseases*, 10(5), p.e0004545.

El Fadili, K., Messier, N., Leprohon, P., Roy, G., Guimond, C., Trudel, N., Saravia, N., Papadopoulou, B., Legare, D. and Ouellette, M. (2005). Role of the ABC transporter MRPA (PGPA) in antimony resistance in *Leishmania infantum* axenic and intracellular amastigotes. *Antimicrobial Agents and Chemotherapy*, 49(5), pp.1988-1993.

El-On, J., Sulitzeanu, A. and Schnur, L. (1991). *Leishmania major*: resistance of promastigotes to paromomycin, and susceptibility of amastigotes to paromomycin-methylbenzethonium chloride ointment. *Annals of Tropical Medicine & Parasitology*, 85(3), pp.323-328.

England, C., Ehlerding, E. and Cai, W., 2016. NanoLuc: A small luciferase is brightening up the field of bioluminescence. *Bioconjugate Chemistry*, 27(5), pp.1175-1187.

Escobar, P., Matu, S., Marques, C. and Croft, S., 2002. Sensitivities of *Leishmania* species to hexadecylphosphocholine (miltefosine), ET-18-OCH₃ (edelfosine) and amphotericin B. *Acta Tropica*, 81(2), pp.151-157.

Favila, M.A., Geraci, N.S., Zeng, E., Harker, B., Condon, D., Cotton, R.N., Jayakumar, A., Tripathi, V., McDowell, M.A. (2014) Human dendritic cells exhibit a pronounced type I IFN signature following *Leishmania major* infection that is required for IL-12 induction. *The Journal of Immunology* 192, 5863-5872

Feagin, J., Abraham, J. and Stuart, K., 1988. Extensive editing of the cytochrome c oxidase III transcript in *Trypanosoma brucei*. *Cell*, 53(3), pp.413-422.

Fernandez-Prada, C., Vincent, I., Brotherton, M., Roberts, M., Roy, G., Rivas, L., Leprohon, P., Smith, T. and Ouellette, M. (2016). Different mutations in a P-type ATPase transporter in *Leishmania* parasites are associated with cross-resistance to two leading drugs by distinct mechanisms. *PLOS Neglected Tropical Diseases*, 10(12), p.e0005171.

Fong, D., Gately, L., Grogl, M., Rodriguez, R., Berman, J. and Chan, M. (1994). Paromomycin resistance in *Leishmania tropica*: Lack of correlation with mutation in the small subunit ribosomal RNA gene. *The American Journal of Tropical Medicine and Hygiene*, 51(6), pp.758-766.

Forestier, C., Machu, C., Loussert, C., Pescher, P. and Späth, G. (2011). Imaging host cell-*Leishmania* interaction dynamics implicates parasite motility, lysosome recruitment, and host cell wounding in the infection process. *Cell Host & Microbe*, 9(4), pp.319-330.

Franssen, S., Durrant, C., Stark, O., Moser, B., Downing, T., Imamura, H., Dujardin, J., Sanders, M., Mauricio, I., Miles, M., Schnur, L., Jaffe, C., Nasereddin, A., Schallig, H., Yeo, M., Bhattacharyya, T., Alam, M., Berriman, M., Wirth, T., Schönian, G. and Cotton, J., 2020. Global genome diversity of the *Leishmania donovani* complex. *eLife*, 9.

Frearson, J., Wyatt, P., Gilbert, I. and Fairlamb, A., 2007. Target assessment for antiparasitic drug discovery. *Trends in Parasitology*, 23(12), pp.589-595.

Freire, E., Vashisht, A., Malvezzi, A., Zuberek, J., Langousis, G., Saada, E., Nascimento, J., Stepinski, J., Darzynkiewicz, E., Hill, K., De Melo Neto, O., Wohlschlegel, J., Sturm, N. and Campbell, D., 2014. eIF4F-like complexes formed by cap-binding homolog TbEIF4E5 with TbEIF4G1 or TbEIF4G2 are implicated in post-transcriptional regulation in *Trypanosoma brucei*. *RNA*, 20(8), pp.1272-1286.

Frézard, F., Demicheli, C. and Ribeiro, R. (2009). Pentavalent antimonials: New perspectives for old drugs. *Molecules*, 14(7), pp.2317-2336.

Gadelha, E., Ramasawmy, R., da Costa Oliveira, B., Morais Rocha, N., de Oliveira Guerra, J., Allan Villa Rouco da Silva, G., Gabrielle Ramos de Mesquita, T., Chrusciak Talhari Cortez, C. and Chrusciak

Goodwin, L. and Page, J. (1943). A study of the excretion of organic antimonials using a polarographic procedure. *Biochemical Journal*, 37(2), pp.198-209.

Galluzzi, L., Ceccarelli, M., Diotallevi, A., Menotta, M. and Magnani, M., 2018. Real-time PCR applications for diagnosis of leishmaniasis. *Parasites & Vectors*, 11(273), pp.218-231.

García-Alai, M., Gallo, M., Salame, M., Wetzler, D., McBride, A., Paci, M., Cicero, D. and de Prat-Gay, G., 2006. Molecular basis for phosphorylation-dependent, PEST-mediated protein turnover. *Structure*, 14(2), pp.309-319.

Ghodratollah, S., Hushang, R., Mojtaba, M., Abdolghayoum, M., Abdolmajid, F. and Ali, M. (2015). Identification of *Leishmania* species by kinetoplast DNA-polymerase chain reaction for the first time in Khaf district, Khorasan-e-Razavi province, Iran. *Tropical Parasitology*, 5(1), p.50.

Gluezn, E., Ginger, M. and McKean, P., 2010. Flagellum assembly and function during the Leishmania life cycle. *Current Opinion in Microbiology*, 13(4), pp.473-479.

Gomez, M., Contreras, I., Hallé, M., Tremblay, M., McMaster, R. and Olivier, M., 2009. Leishmania GP63 alters host signaling through cleavage-activated protein tyrosine phosphatases. *Science Signaling*, 2(90).

González, C., Wang, O., Strutz, S., González-Salazar, C., Sánchez-Cordero, V. and Sarkar, S., 2010. Climate change and risk of leishmaniasis in north America: Predictions from ecological niche models of vector and reservoir species. *PLoS Neglected Tropical Diseases*, 4(1), p.e585.

Goto, H. and Lindoso, J. (2010). Current diagnosis and treatment of cutaneous and mucocutaneous leishmaniasis. *Expert Review of Anti-infective Therapy*, 8(4), pp.419-433.

Gradoni, L., Soteriadou, K., Louzir, H., Dakkak, A., Toz, S., Jaffe, C., Dedet, J., Campino, L., Cañavate, C. and Dujardin, J. (2008). Drug regimens for visceral leishmaniasis in Mediterranean countries. *Tropical Medicine & International Health*, 13(10), pp.1272-1276.

Guimarães-Costa, A., DeSouza-Vieira, T., Paletta-Silva, R., Freitas-Mesquita, A., Meyer-Fernandes, J. and Saraiva, E. (2014). 3'-Nucleotidase/nuclease activity allows Leishmania parasites to escape killing by neutrophil extracellular traps. *Infection and Immunity*, 82(4), pp.1732-1740.

Guimaraes-Costa, A., Nascimento, M., Froment, G., Soares, R., Morgado, F., Conceicao-Silva, F. and Saraiva, E. (2009). Leishmania amazonensis promastigotes induce and are killed by neutrophil extracellular traps. *Proceedings of the National Academy of Sciences*, 106(16), pp.6748-6753.

Gupta, G., Oghumu, S. and Satoskar, A., 2013. Mechanisms of Immune Evasion in Leishmaniasis. *Advances in Applied Microbiology*, pp.155-184.

Gupta, S., Chikne, V., Eliaz, D., Tkacz, I., Naboishchikov, I., Carmi, S., Waldman Ben-Asher, H. and Michaeli, S., 2014. Two splicing factors carrying serine-arginine motifs, TSR1 and TSR1IP, regulate splicing, mRNA stability, and rRNA processing in *Trypanosoma brucei*. *RNA Biology*, 11(6), pp.715-731.

Gupta, S., Yardley, V., Vishwakarma, P., Shivahare, R., Sharma, B., Launay, D., Martin, D. and Puri, S., 2014. Nitroimidazo-oxazole compound DNDI-VL-2098: an orally effective preclinical drug candidate for the treatment of visceral leishmaniasis. *Journal of Antimicrobial Chemotherapy*, 70(2), pp.518-527.

Hailu, A., Musa, A., Wasunna, M., Balasegaram, M., Yifru, S., Mengistu, G., Hurissa, Z., Hailu, W., Weldegebreal, T., Tesfaye, S., Makonnen, E., Khalil, E., Ahmed, O., Fadlalla, A., El-Hassan, A., Raheem, M., Mueller, M., Koummuki, Y., Rashid, J., Mbui, J., Mucee, G., Njoroge, S., Manduku, V., Musibi, A., Mutuma, G., Kirui, F., Lodenyo, H., Mutea, D., Kirigi, G., Edwards, T., Smith, P., Muthami, L., Royce, C., Ellis, S., Aloba, M., Omollo, R., Kesusu, J., Owiti, R. and Kinuthia, J. (2010). Geographical variation in the response of visceral leishmaniasis to paromomycin in east Africa: A multicentre, open-label, randomized trial. *PLoS Neglected Tropical Diseases*, 4(10), p.e709.

Haldar, A., Sen, P. and Roy, S., 2011. Use of Antimony in the Treatment of Leishmaniasis: Current status and future directions. *Molecular Biology International*, 2011, pp.1-23.

Hartsel, S. and Bolard, J. (1996). Amphotericin B: new life for an old drug. *Trends in Pharmacological Sciences*, 17(12), pp.445-449.

Hasenkamp, S., Sidaway, A., Devine, O., Roye, R. and Horrocks, P., 2013. Evaluation of bioluminescence-based assays of anti-malarial drug activity. *Malaria Journal*, 12(1).

Herman, J., Gallalee, J. and Best, J. (1987). Sodium stibogluconate (pentostam) inhibition of glucose catabolism via the glycolytic pathway, and fatty acid β -oxidation in leishmania mexicana amastigotes. *Biochemical Pharmacology*, 36(2), pp.197-201.

Inocêncio da Luz, R., Vermeersch, M., Dujardin, J., Cos, P. and Maes, L., 2009. In vitro sensitivity testing of Leishmania clinical field isolates: Preconditioning of promastigotes enhances infectivity for macrophage host cells. *Antimicrobial Agents and Chemotherapy*, 53(12), pp.5197-5203.

Isnard, A., Shio, M. and Olivier, M., 2012. Impact of Leishmania metalloprotease GP63 on macrophage signaling. *Frontiers in Cellular and Infection Microbiology*, 2.

Jha, T., Olliaro, P., Thakur, C., Kanyok, T., Singhania, B., Singh, I., Singh, N., Akhoury, S., Jha, S. and Lockwood, D. (1998). Randomised controlled trial of aminosidine (paromomycin) v sodium stibogluconate for treating visceral leishmaniasis in North Bihar, India Commentary: Some good news for treatment of visceral leishmaniasis in Bihar. *British Medical Journal*, 316(7139), pp.1200-1205.

Jhingran, A., Chawla, B., Saxena, S., Barrett, M. and Madhubala, R. (2009). Paromomycin: Uptake and resistance in *Leishmania donovani*. *Molecular and Biochemical Parasitology*, 164(2), pp.111-117.

John, B. and Hunter, C., 2008. IMMUNOLOGY: Neutrophil soldiers or trojan horses?. *Science*, 321(5891), pp.917-918.

Kafetzis, D., Velissariou, I., Stabouli, S., Mavrikou, M., Delis, D. and Liapi, G. (2005). Treatment of paediatric visceral leishmaniasis: amphotericin B or pentavalent antimony compounds?. *International Journal of Antimicrobial Agents*, 25(1), pp.26-30.

Kalesh, K., Wei, W., Mantilla, B., Roumeliotis, T., Choudhary, J. and Denny, P., 2022. Transcriptome-wide identification of coding and noncoding RNA-binding proteins defines the comprehensive RNA interactome of *Leishmania mexicana*. *Microbiology Spectrum*, 10(1), pp2422-2434

Kamhawi, S., 2006. Phlebotomine sand flies and *Leishmania* parasites: friends or foes?. *Trends in Parasitology*, 22(9), pp.439-445.

Karamian, M., Motazedian, M., Fakhar, M., Pakshir, K., Jowkar, F. and Rezanezhad, H., 2008. Atypical presentation of Old-World cutaneous leishmaniasis, diagnosis and species identification by PCR. *Journal of the European Academy of Dermatology and Venereology*, 22(8), pp.958-962.

Karl, S., Wong, R., St Pierre, T. and Davis, T., 2009. A comparative study of a flow-cytometry-based assessment of in vitro Plasmodium falciparum drug sensitivity. *Malaria Journal*, 8(1).

Khatami, A., Firooz, A., Gorouhi, F. and Dowlati, Y. (2007). Treatment of acute Old World cutaneous leishmaniasis: A systematic review of the randomized controlled trials. *Journal of the American Academy of Dermatology*, 57(2), pp.335.e1-335.e29.

Koch, L., Kochmann, J., Klimpel, S. and Cunze, S., 2017. Modeling the climatic suitability of leishmaniasis vector species in Europe. *Scientific Reports*, 7(1).

Krauth-Siegel, R. and Comini, M. (2008). Redox control in trypanosomatids, parasitic protozoa with trypanothione-based thiol metabolism. *Biochimica et Biophysica Acta (BBA) - General Subjects*, 1780(11), pp.1236-1248.

Kumar, D., Khanal, B., Tiwary, P., Mudavath, S., Tiwary, N., Singh, R., Koirala, K., Boelaert, M., Rijal, S. and Sundar, S. (2013). Comparative evaluation of blood and serum samples in rapid immunochromatographic tests for visceral leishmaniasis. *Journal of Clinical Microbiology*, 51(12), pp.3955-3959.

Lainson, R., Ward, R. and Shaw, J., 1977. Leishmania in phlebotomid sandflies: VI. Importance of hindgut development in distinguishing between parasites of the *Leishmania mexicana* and *L. braziliensis* complexes. *Proceedings of the Royal Society of London. Series B. Biological Sciences*, 199(1135), pp.309-320.

Lanteri, C., Tidwell, R. and Meshnick, S. (2007). The mitochondrion is a site of trypanocidal action of the aromatic diamidine DB75 in bloodstream forms of *Trypanosoma brucei*. *Antimicrobial Agents and Chemotherapy*, 52(3), pp.875-882.

Laufs, H., Müller, K., Fleischer, J., Reiling, N., Jahnke, N., Jensenius, J.C., Solbach, W., Laskay, T. (2002) Intracellular survival of *Leishmania major* in neutrophil granulocytes after uptake in the absence of heat-labile serum factors. *Infection and Immunity* 70(2), 826–835.

Liang, X., Haritan, A., Uliel, S. and Michaeli, S., 2003. trans and cis Splicing in Trypanosomatids: Mechanism, Factors, and Regulation. *Eukaryotic Cell*, 2(5), pp.830-840.

Lindoso, J., Moreira, C., Cunha, M. and Queiroz, I., 2018. Visceral leishmaniasis and HIV coinfection: current perspectives. *HIV/AIDS - Research and Palliative Care*, Volume 10, pp.193-201.

Lira, R., Sundar, S., Makharia, A., Kenney, R., Gam, A., Saraiva, E. and Sacks, D. (1999). Evidence that the high incidence of treatment failures in Indian Kala-Azar is due to the emergence of antimony-resistant strains of *Leishmania donovani*. *The Journal of Infectious Diseases*, 180(2), pp.564-567.

Luque-Ortega, J. and Rivas, L. (2007). Miltefosine (hexadecylphosphocholine) inhibits cytochrome c oxidase in *Leishmania donovani* promastigotes. *Antimicrobial Agents and Chemotherapy*, 51(4), pp.1327-1332.

Lye, L., Owens, K., Shi, H., Murta, S., Vieira, A., Turco, S., Tschudi, C., Ullu, E. and Beverley, S., 2010. Retention and loss of RNA interference pathways in trypanosomatid protozoans. *PLoS Pathogens*, 6(10), p.e1001161.

Maarouf, M., Adeline, M., Solignac, M., Vautrin, D. and Robert-Gero, M. (1998). Development and characterization of paromomycin-resistant *Leishmania donovani* promastigotes. *Parasite*, 5(2), pp.167-173.

Maarouf, M., Lawrence, F., Croft, S. and Robert-Gero, M. (1995). Ribosomes of *Leishmania* are a target for the aminoglycosides. *Parasitology Research*, 81(5), pp.421-425.

Machado, G., Prates, F. and Machado, P. (2019). Disseminated leishmaniasis: clinical, pathogenic, and therapeutic aspects. *Anais Brasileiros de Dermatologia*, 94(1), pp.9-16.

Maes, L., Beyers, J., Mondelaers, A., Van den Kerkhof, M., Eberhardt, E., Caljon, G. and Hendrickx, S., 2016. In vitro 'time-to-kill' assay to assess the cidal activity dynamics of current reference drugs against *Leishmania donovani* and *Leishmania infantum*. *Journal of Antimicrobial Chemotherapy*, 72(2), pp.428-430.

Magalhães, R., Duarte, M., Mattos, E., Martins, V., Lage, P., Chávez-Fumagalli, M., Lage, D., Menezes-Souza, D., Régis, W., Manso Alves, M., Soto, M., Tavares, C., Nagen, R. and Coelho, E., 2014. Identification of differentially expressed proteins from *Leishmania amazonensis* associated with the loss of virulence of the parasites. *PLoS Neglected Tropical Diseases*, 8(4), p.e2764.

Mandal, S., Maharjan, M., Singh, S., Chatterjee, M. and Madhubala, R. (2010). Assessing aquaglyceroporin gene status and expression profile in antimony-susceptible and -resistant clinical isolates of *Leishmania donovani* from India. *Journal of Antimicrobial Chemotherapy*, 65(3), pp.496-507.

Marinho, F., Gonçalves, K., Oliveira, S., Oliveira, A., Bellio, M., d'Avila-Levy, C., Santos, A. and Branquinha, M. (2011). Miltefosine induces programmed cell death in *Leishmania amazonensis* promastigotes. *Memórias do Instituto Oswaldo Cruz*, 106(4), pp.507-509.

Mary, C., Faraut, F., Lascombe, L. and Dumon, H., 2004. Quantification of *Leishmania infantum* DNA by a real-time PCR assay with high sensitivity. *Journal of Clinical Microbiology*, 42(11), pp.5249-5255.

Mathis, A., Bridges, A., Ismail, M., Kumar, A., Francesconi, I., Anbazhagan, M., Hu, Q., Tanious, F., Wenzler, T., Saulter, J., Wilson, W., Brun, R., Boykin, D., Tidwell, R. and Hall, J. (2007). Diphenyl furans and aza analogs: Effects of structural modification on in vitro activity, DNA binding, and accumulation and distribution in trypanosomes. *Antimicrobial Agents and Chemotherapy*, 51(8), pp.2801-2810.

McCall, L., Zhang, W. and Matlashewski, G. (2013). Determinants for the development of visceral leishmaniasis disease. *PLoS Pathogens*, 9(1), p.e1003053.

McDowell, M.A., Marovich, M., Lira, R., Braun, M., Sacks, D. (2002) Leishmania priming of human dendritic cells for CD40 ligand-induced interleukin-12p70 secretion is strain and species dependent. *Infection and Immunity* 70(8),pp.3994–4001.

Mehta, A. and Shaha, C. (2003). Apoptotic death in *Leishmania donovani* promastigotes in response to respiratory chain inhibition. *Journal of Biological Chemistry*, 279(12), pp.11798-11813.

Mikus, J. and Steverding, D., 2000. A simple colorimetric method to screen drug cytotoxicity against *Leishmania* using the dye Alamar Blue®. *Parasitology International*, 48(3), pp.265-269.

Misslitz, A., Mottram, J., Overath, P. and Aebischer, T., 2000. Targeted integration into a rRNA locus results in uniform and high level expression of transgenes in *Leishmania* amastigotes. *Molecular and Biochemical Parasitology*, 107(2), pp.251-261.

Mistro, S., Maciel, I., de Menezes, R., Maia, Z., Schooley, R. and Badaro, R. (2012). Does lipid emulsion reduce amphotericin B nephrotoxicity? A systematic review and meta-analysis. *Clinical Infectious Diseases*, 54(12), pp.1774-1777.

Mohebbali, M., Edrissian, G., Shirzadi, M., Akhoundi, B., Hajjaran, H., Zarei, Z., Molaei, S., Sharifi, I., Mamishi, S., Mahmoudvand, H., Torabi, V., Moshfe, A., Malmasi, A., Motazedian, M. and Fakhar, M. (2011). An observational study on the current distribution of visceral leishmaniasis in different

geographical zones of Iran and implication to health policy. *Travel Medicine and Infectious Disease*, 9(2), pp.67-74.

Monge-Maillo, B. and Lopez-Velez, R. (2015). Miltefosine for visceral and cutaneous leishmaniasis: Drug characteristics and evidence-based treatment recommendations. *Clinical Infectious Diseases*, 60(9), pp.1398-1404.

Moore, K., de Waal Malefyt, R., Coffman, R. and O'Garra, A. (2001). Interleukin-10 and the interleukin-10 receptor. *Annual Review of Immunology*, 19(1), pp.683-765.

Moradin, N. and Descoteaux, A. (2012). Leishmania promastigotes: building a safe niche within macrophages. *Frontiers in Cellular and Infection Microbiology*, 121(2), pp.56-63

Moreira, D., Santarém, N., Loureiro, I., Tavares, J., Silva, A., Amorim, A., Ouaiissi, A., Cordeiro-da-Silva, A. and Silvestre, R., 2012. Impact of continuous axenic cultivation in *Leishmania infantum* virulence. *PLoS Neglected Tropical Diseases*, 6(1), p.e1469.

Moura, D., Reis, C., Xavier, C., da Costa Lima, T., Lima, R., Carrington, M. and de Melo Neto, O., 2015. Two related trypanosomatid eIF4G homologues have functional differences compatible with distinct roles during translation initiation. *RNA Biology*, 12(3), pp.305-319.

Mouri, R., Konoki, K., Matsumori, N., Oishi, T. and Murata, M. (2008). Complex formation of amphotericin B in sterol-containing membranes as evidenced by surface plasmon resonance†. *Biochemistry*, 47(30), pp.7807-7815.

Mukherjee, A., Padmanabhan, P., Singh, S., Roy, G., Girard, I., Chatterjee, M., Ouellette, M. and Madhubala, R. (2006). Role of ABC transporter MRPA, -glutamylcysteine synthetase and ornithine decarboxylase in natural antimony-resistant isolates of *Leishmania donovani*. *Journal of Antimicrobial Chemotherapy*, 59(2), pp.204-211.

Müller, A., Aeschlimann, S., Olekhnovitch, R., Dacher, M., Späth, G. and Bousso, P. (2013). Photoconvertible pathogen labeling reveals nitric oxide control of *Leishmania major* infection in vivo via dampening of parasite metabolism. *Cell Host & Microbe*, 14(4), pp.460-467.

Muraille, E., Gounon, P., Cazareth, J., Hoebeke, J., Lippuner, C., Davalos-Miszlitz, A., Aebischer, T., Muller, S., Glaichenhaus, N. and Mougneau, E. (2010). Direct visualization of peptide/MHC complexes at the surface and in the intracellular compartments of cells infected in vivo by *Leishmania major*. *PLoS Pathogens*, 6(10), p.e1001154.

Musa, A., Khalil, E., Hailu, A., Olobo, J., Balasegaram, M., Omollo, R., Edwards, T., Rashid, J., Mbui, J., Musa, B., Abuzaid, A., Ahmed, O., Fadlalla, A., El-Hassan, A., Mueller, M., Mucee, G., Njoroge, S., Manduku, V., Mutuma, G., Apadet, L., Lodenyo, H., Mutea, D., Kirigi, G., Yifru, S., Mengistu, G., Hurissa, Z., Hailu, W., Weldegebreal, T., Tafes, H., Mekonnen, Y., Makonnen, E., Ndegwa, S., Sagaki, P., Kimutai, R., Kesusu, J., Owiti, R., Ellis, S. and Wasunna, M. (2012). Sodium stibogluconate (SSG) & paromomycin

combination compared to SSG for visceral leishmaniasis in east Africa: A randomised controlled trial. *PLoS Neglected Tropical Diseases*, 6(6), p.e1674.

Naderer, T. and McConville, M. (2007). The Leishmania-macrophage interaction: a metabolic perspective. *Cellular Microbiology*, 10(2), pp.301-308.

Nagamine, K., Hase, T. and Notomi, T., 2002. Accelerated reaction by loop-mediated isothermal amplification using loop primers. *Molecular and Cellular Probes*, 16(3), pp.223-229.

Nakayama, G., Caton, M., Nova, M. and Parandoosh, Z., 1997. Assessment of the Alamar Blue assay for cellular growth and viability in vitro. *Journal of Immunological Methods*, 204(2), pp.205-208.

Notomi, T., Okayama, H., Masubuchi, H., Yonekawa, T., Watanabe, K., Amino, N. and Hase, T., 2000. Loop-mediated isothermal amplification of DNA. *Nucleic Acids Research*, 28(12), pp.63e-63.

Nzelu, C., Gomez, E., Cáceres, A., Sakurai, T., Martini-Robles, L., Uezato, H., Mimori, T., Katakura, K., Hashiguchi, Y. and Kato, H., 2014. Development of a loop-mediated isothermal amplification method for rapid mass-screening of sand flies for Leishmania infection. *Acta Tropica*, 132, pp.1-6.

Nzelu, C., Kato, H. and Peters, N., 2019. Loop-mediated isothermal amplification (LAMP): An advanced molecular point-of-care technique for the detection of Leishmania infection. *PLOS Neglected Tropical Diseases*, 13(11), p.e0007698.

Okwor, I. and Uzonna, J., 2016. Social and economic burden of human leishmaniasis. *The American Journal of Tropical Medicine and Hygiene*, 94(3), pp.489-493.

Oliveira, G., Magalhães, F., Teixeira, M., dos-Santos, W., Pereira, A., Gomes, Y., Pinheiro, C., Moreira, E., Brito, M., Pontes de Carvalho, L., Santos, L., de Melo Neto, O., Nascimento, M., Bedor, C. and Albuquerque, A., 2011. Characterization of novel *Leishmania infantum* recombinant proteins encoded by genes from five families with distinct capacities for serodiagnosis of canine and human visceral leishmaniasis. *The American Journal of Tropical Medicine and Hygiene*, 85(6), pp.1025-1034.

Olivier, M., Gregory, D. and Forget, G., 2005. Subversion mechanisms by which *Leishmania* parasites can escape the host immune response: a signaling point of view. *Clinical Microbiology Reviews*, 18(2), pp.293-305.

Olliaro, P., Guerin, P., Gerstl, S., Haaskjold, A., Rottingen, J. and Sundar, S. (2005). Treatment options for visceral leishmaniasis: a systematic review of clinical studies done in India, 1980–2004. *The Lancet Infectious Diseases*, 5(12), pp.763-774.

Oryan, A. and Akbari, M. (2016). Worldwide risk factors in leishmaniasis. *Asian Pacific Journal of Tropical Medicine*, 9(10), pp.925-932.

Oualha, R., Barhoumi, M., Marzouki, S., Harigua-Souiai, E., Ben Ahmed, M. and Guizani, I. (2019). Infection of human neutrophils with *Leishmania infantum* or *Leishmania major* strains triggers activation and differential cytokines release. *Frontiers in Cellular and Infection Microbiology*, 9.

Paila, Y., Saha, B. and Chattopadhyay, A. (2010). Amphotericin B inhibits entry of *Leishmania donovani* into primary macrophages. *Biochemical and Biophysical Research Communications*, 399(3), pp.429-433.

Palatnik-de-Sousa, C., Gomes, E., Paraguai-de-Souza, E., Palatnik, M., Luz, K. and Borojevic, R., 1995. *Leishmania donovani*: titration of antibodies to the fucose-mannose ligand as an aid in diagnosis and prognosis of visceral leishmaniasis. *Transactions of the Royal Society of Tropical Medicine and Hygiene*, 89(4), pp.390-393.

Paris, C., Loiseau, P., Bories, C. and Breard, J. (2004). Miltefosine induces apoptosis-Like death in *Leishmania donovani* promastigotes. *Antimicrobial Agents and Chemotherapy*, 48(3), pp.852-859.

Park, A., Hondowicz, B. and Scott, P. (2000). IL-12 is required to maintain a Th1 response during *Leishmania major* infection. *The Journal of Immunology*, 165(2), pp.896-902.

Peacock, C., Seeger, K., Harris, D., Murphy, L., Ruiz, J., Quail, M., Peters, N., Adlem, E., Tivey, A., Aslett, M., Kerhornou, A., Ivens, A., Fraser, A., Rajandream, M., Carver, T., Norbertczak, H., Chillingworth, T., Hance, Z., Jagels, K., Moule, S., Ormond, D., Rutter, S., Squares, R., Whitehead, S., Rabbinowitsch, E., Arrowsmith, C., White, B., Thurston, S., Bringaud, F., Baldauf, S., Faulconbridge, A., Jeffares, D.,

Depledge, D., Oyola, S., Hilley, J., Brito, L., Tosi, L., Barrell, B., Cruz, A., Mottram, J., Smith, D. and Berriman, M., 2007. Comparative genomic analysis of three *Leishmania* species that cause diverse human disease. *Nature Genetics*, 39(7), pp.839-847.

Perez-Victoria, J., Cortes-Selva, F., Parodi-Talice, A., Bavchvarov, B., Perez-Victoria, F., Munoz-Martinez, F., Maitrejean, M., Costi, M., Barron, D., Di Pietro, A., Castanys, S. and Gamarro, F. (2006). Combination of suboptimal doses of inhibitors targeting different domains of LtrMDR1 efficiently overcomes resistance of *Leishmania* spp. to miltefosine by inhibiting drug efflux. *Antimicrobial Agents and Chemotherapy*, 50(9), pp.3102-3110.

Pérez-Victoria, F., Sánchez-Cañete, M., Seifert, K., Croft, S., Sundar, S., Castanys, S. and Gamarro, F. (2006). Mechanisms of experimental resistance of *Leishmania* to miltefosine: Implications for clinical use. *Drug Resistance Updates*, 9(1-2), pp.26-39.

Perry, M., Wyllie, S., Raab, A., Feldmann, J. and Fairlamb, A., 2013. Chronic exposure to arsenic in drinking water can lead to resistance to antimonial drugs in a mouse model of visceral leishmaniasis. *Proceedings of the National Academy of Sciences*, 110(49), pp.19932-19937.

Peters, N., Egen, J., Secundino, N., Debrabant, A., Kimblin, N., Kamhawi, S., Lawyer, P., Fay, M., Germain, R. and Sacks, D. (2008). In vivo imaging reveals an essential role for neutrophils in leishmaniasis transmitted by sand flies. *Science*, 321(5891), pp.970-974.

Petritus, P.M., Manzoni-de-Almeida, D., Gimblet, C., Gonzalez Lombana, C., Scott, P. (2012) *Leishmania mexicana* induces limited recruitment and activation of monocytes and monocyte-derived dendritic cells early during infection. *PLoS Negl Trop Dis* 6, e1858.

Pimenta, P., Saraiva, E., Rowton, E., Modi, G., Garraway, L., Beverley, S., Turco, S. and Sacks, D., 1994. Evidence that the vectorial competence of phlebotomine sand flies for different species of *Leishmania* is controlled by structural polymorphisms in the surface lipophosphoglycan. *Proceedings of the National Academy of Sciences*, 91(19), pp.9155-9159.

Pimenta, P.F., Modi, G.B., Pereira, S.T., Shahabuddin, M., Sacks, D.L. (1997) A novel role for the peritrophic matrix in protecting *Leishmania* from the hydrolytic activities of the sand fly midgut. *Parasitology*, 115(4), pp.359–369.

Pinto-Martinez, A., Rodriguez-Durán, J., Serrano-Martin, X., Hernandez-Rodriguez, V. and Benaim, G. (2017). Mechanism of action of miltefosine on *Leishmania donovani* involves the impairment of acidocalcisome function and the activation of the sphingosine-dependent plasma membrane Ca²⁺ channel. *Antimicrobial Agents and Chemotherapy*, 62(1).

Polando, R., Dixit, U., Carter, C., Jones, B., Whitcomb, J., Ballhorn, W., Harintho, M., Jerde, C., Wilson, M. and McDowell, M., 2013. The roles of complement receptor 3 and Fcγ receptors during *Leishmania* phagosome maturation. *Journal of Leukocyte Biology*, 93(6), pp.921-932.

Ponte-Sucre, A., Gamarro, F., Dujardin, J., Barrett, M., López-Vélez, R., García-Hernández, R., Pountain, A., Mwenechanya, R. and Papadopoulou, B. (2017). Drug resistance and treatment failure in leishmaniasis: A 21st century challenge. *PLOS Neglected Tropical Diseases*, 11(12), p.e0006052.

Preusser, C., Jaé, N. and Bindereif, A., 2012. mRNA splicing in trypanosomes. *International Journal of Medical Microbiology*, 302(4-5), pp.221-224.

Puentes, S., Dwyer, D., Bates, P. and Joiner, K., 1989. Binding and release of C3 from *Leishmania donovani* promastigotes during incubation in normal human serum. *The Journal of Immunology*, 143(11), pp.3743-3749.

Purkait, B., Kumar, A., Nandi, N., Sardar, A., Das, S., Kumar, S., Pandey, K., Ravidas, V., Kumar, M., De, T., Singh, D. and Das, P. (2011). Mechanism of amphotericin B resistance in clinical isolates of *Leishmania donovani*. *Antimicrobial Agents and Chemotherapy*, 56(2), pp.1031-1041.

Rai, S., Bhaskar, Goel, S., Nath Dwivedi, U., Sundar, S. and Goyal, N. (2013). Role of efflux pumps and intracellular thiols in natural antimony resistant isolates of *Leishmania donovani*. *PLoS ONE*, 8(9), p.e74862.

Rakotomanga, M., Blanc, S., Gaudin, K., Chaminade, P. and Loiseau, P. (2007). Miltefosine affects lipid metabolism in *Leishmania donovani* promastigotes. *Antimicrobial Agents and Chemotherapy*, 51(4), pp.1425-1430.

Ramos, H., Valdivieso, E., Gamargo, M., Dagger, F. and Cohen, B. (1996). Amphotericin B kills unicellular leishmaniasis by forming aqueous pores permeable to small cations and anions. *Journal of Membrane Biology*, 152(1), pp.65-75.

Rasti, S., Ghorbanzadeh, B., Kheirandish, F., Mousavi, S., Pirozmand, A., Hooshyar, H. and Abani, B. (2016). Comparison of molecular, microscopic, and culture methods for diagnosis of cutaneous leishmaniasis. *Journal of Clinical Laboratory Analysis*, 30(5), pp.610-615.

Regli, I., Passelli, K., Hurrell, B. and Tacchini-Cottier, F. (2017). Survival mechanisms used by some *Leishmania* species to escape neutrophil killing. *Frontiers in Immunology*, 8, pp.1558.

Reithinger, R. and Dujardin, J. (2006). Molecular diagnosis of leishmaniasis: Current status and future applications. *Journal of Clinical Microbiology*, 45(1), pp.21-25.

Reynolds, D., Cliffe, L., Förstner, K., Hon, C., Siegel, T. and Sabatini, R., 2014. Regulation of transcription termination by glucosylated hydroxymethyluracil, base J, in *Leishmania major* and *Trypanosoma brucei*. *Nucleic Acids Research*, 42(15), pp.9717-9729.

Ribeiro-Gomes, F. and Sacks, D. (2012). The influence of early neutrophil-*Leishmania* interactions on the host immune response to infection. *Frontiers in Cellular and Infection Microbiology*, 59(2), pp.59

Ribeiro-Gomes, F., Peters, N., Debrabant, A. and Sacks, D. (2012). Efficient capture of infected neutrophils by dendritic cells in the skin inhibits the early anti-Leishmania response. *PLoS Pathogens*, 8(2), p.e1002536.

Ritter, U., Meissner, A., Scheidig, C., Körner, H., (2004). CD8 alpha- and Langerin-negative dendritic cells, but not Langerhans cells, act as principal antigen-presenting cells in leishmaniasis. *Eur J Immunol* 34, 1542–1550.

Rochael, N., Guimarães-Costa, A., Nascimento, M., DeSouza-Vieira, T., Oliveira, M., Garcia e Souza, L., Oliveira, M. and Saraiva, E. (2015). Classical ROS-dependent and early/rapid ROS-independent release of Neutrophil Extracellular Traps triggered by Leishmania parasites. *Scientific Reports*, 5(1), pp.1830

Rogers, M. and Bates, P., (2007). Leishmania manipulation of sand fly feeding behavior results in enhanced transmission. *PLoS Pathogens*, 3(6), p.e91.

Rogers, M., Chance, M. and Bates, P., (2002). The role of promastigote secretory gel in the origin and transmission of the infective stage of *Leishmania mexicana* by the sandfly *Lutzomyia longipalpis*. *Parasitology*, 124(5), pp.495-507.

Rogers, M., Hajmová, M., Joshi, M., Sadlova, J., Dwyer, D., Volf, P. and Bates, P., (2008). Leishmania chitinase facilitates colonization of sand fly vectors and enhances transmission to mice. *Cellular Microbiology*, 10(6), pp.1363-1372.

Rogers, M., Ilg, T., Nikolaev, A., Ferguson, M. and Bates, P., 2004. Transmission of cutaneous leishmaniasis by sand flies is enhanced by regurgitation of fPPG. *Nature*, 430(6998), pp.463-467.

Rolão, N., Cortes, S., Rodrigues, O. and Campino, L., (2004). Quantification of *Leishmania infantum* parasites in tissue biopsies by real-time polymerase chain reaction and polymerase chain reaction–enzyme-linked immunosorbent assay. *Journal of Parasitology*, 90(5), pp.1150-1154.

Romero, G., Costa, D., Costa, C., de Almeida, R., de Melo, E., de Carvalho, S., Rabello, A., de Carvalho, A., Sousa, A., Leite, R., Lima, S., Amaral, T., Alves, F. and Rode, J., 2017. Efficacy and safety of available treatments for visceral leishmaniasis in Brazil: A multicenter, randomized, open label trial. *PLOS Neglected Tropical Diseases*, 11(6), p.e0005706.

Rossi, M. and Fasel, N. (2017). How to master the host immune system? *Leishmania* parasites have the solutions!. *International Immunology*, 30(3), pp.103-111.

Sadeghi, S., Seyed, N., Etemadzadeh, M., Abediankenari, S., Rafati, S. and Taheri, T., 2015. In vitro infectivity assessment by drug susceptibility comparison of recombinant *Leishmania major*; expressing enhanced green fluorescent protein or EGFP-luciferase fused genes with wild-type parasite. *The Korean Journal of Parasitology*, 53(4), pp.385-394.

Sanz, L., Crespo, B., De-Cózar, C., Ding, X., Llergo, J., Burrows, J., García-Bustos, J. and Gamo, F., 2012. *P. falciparum* in vitro killing rates allow to discriminate between different antimalarial mode of action. *PLOS ONE*, 7(2): e30949.

Schallig, H., Hu, R., Kent, A., van Loenen, M., Menting, S., Picado, A., Oosterling, Z. and Cruz, I. (2019). Evaluation of point of care tests for the diagnosis of cutaneous leishmaniasis in Suriname. *BMC Infectious Diseases*, 19(1).

Schwarz, T., Remer, K., Nahrendorf, W., Masic, A., Siewe, L., Müller, W., Roers, A. and Moll, H. (2013). T cell-derived IL-10 determines leishmaniasis disease outcome and is suppressed by a dendritic cell based vaccine. *PLoS Pathogens*, 9(6), p.e1003476.

Seifert, K., Escobar, P. and Croft, S., 2010. In vitro activity of anti-leishmanial drugs against *Leishmania donovani* is host cell dependent. *Journal of Antimicrobial Chemotherapy*, 65(3), pp.508-511.

Seifert, K., Pérez-Victoria, F., Stettler, M., Sánchez-Cañete, M., Castanys, S., Gamarro, F. and Croft, S. (2007). Inactivation of the miltefosine transporter, LdMT, causes miltefosine resistance that is conferred to the amastigote stage of *Leishmania donovani* and persists in vivo. *International Journal of Antimicrobial Agents*, 30(3), pp.229-235.

Sereno, D., Holzmüller, P., Mangot, I., Cuny, G., Ouaiissi, A. and Lemesre, J. (2001). Antimonial-mediated DNA fragmentation in *Leishmania infantum* amastigotes. *Antimicrobial Agents and Chemotherapy*, 45(7), pp.2064-2069.

Shaked-Mishan, P., Ulrich, N., Ephros, M. and Zilberstein, D. (2000). Novel intracellular SbV reducing activity correlates with antimony susceptibility in *Leishmania donovani*. *Journal of Biological Chemistry*, 276(6), pp.3971-3976.

Shapiro, T., 1993. Kinetoplast DNA maxicircles: networks within networks. *Proceedings of the National Academy of Sciences*, 90(16), pp.7809-7813.

Silveira, F., Lainson, R., De Castro Gomes, C., Laurenti, M. and Corbett, C. (2009). Immunopathogenic competences of *Leishmania(V.) braziliensis* and *L.(L.)amazonensis* in American cutaneous leishmaniasis. *Parasite Immunology*, 31(8), pp.423-431.

Simpson, L. and da Silva, A., 1971. Isolation and characterization of kinetoplast DNA from *Leishmania tarentolae*. *Journal of Molecular Biology*, 56(3), pp.443-473.

Sindermann, H. and Engel, J. (2006). Development of miltefosine as an oral treatment for leishmaniasis. *Transactions of the Royal Society of Tropical Medicine and Hygiene*, 100, pp.S17-S20.

Singh, A., Raju, R., Mrad, M., Reddell, P. and Münch, G., 2020. The reciprocal EC50 value as a convenient measure of the potency of a compound in bioactivity-guided purification of natural products. *Fitoterapia*, 143, p.104598.

Singh, O. and Sundar, S. (2015). Developments in diagnosis of visceral leishmaniasis in the elimination era. *Journal of Parasitology Research*, 2015, pp.1-10.

Sinha, R., C, M., Raghwan, Das, S., Das, S., Shadab, M., Chowdhury, R., Tripathy, S. and Ali, N., 2018. Genome plasticity in cultured *Leishmania donovani*: Comparison of early and late passages. *Frontiers in Microbiology*, 9.

Siqueira-Neto, J., Moon, S., Jang, J., Yang, G., Lee, C., Moon, H., Chatelain, E., Genovesio, A., Cechetto, J. and Freitas-Junior, L., 2012. An image-based high-content screening assay for compounds targeting intracellular *Leishmania donovani* amastigotes in human macrophages. *PLoS Neglected Tropical Diseases*, 6(6), p.e1671.

Soares, R., Macedo, M., Ropert, C., Gontijo, N., Almeida, I., Gazzinelli, R., Pimenta, P. and Turco, S. (2002). *Leishmania chagasi*: lipophosphoglycan characterization and binding to the midgut of the sand fly vector *Lutzomyia longipalpis*. *Molecular and Biochemical Parasitology*, 121(2), pp.213-224.

Soto, J., Valda, L., Balderrama, M., Toledo, J., Berman, J., Rea, J. and Soto, P., 2008. Efficacy of miltefosine for Bolivian cutaneous leishmaniasis. *The American Journal of Tropical Medicine and Hygiene*, 78(2), pp.210-211.

Spadari, C., Vila, T., Rozentel, S. and Ishida, K., 2018. Miltefosine has a postantifungal effect and induces apoptosis in *Cryptococcus* yeasts. *Antimicrobial Agents and Chemotherapy*, 62(8), pp.312-318.

Stone, N., Bicanic, T., Salim, R. and Hope, W. (2016). Liposomal amphotericin B (AmBisome®): A review of the pharmacokinetics, pharmacodynamics, clinical experience and future directions. *Drugs*, 76(4), pp.485-500.

Suganuma, K., Allamanda, P., Hakimi, H., Zhou, M., Angeles, J., Kawazu, S. and Inoue, N., 2014. Establishment of ATP-Based luciferase viability assay in 96-Well Plate for *Trypanosoma congolense*. *Journal of Veterinary Medical Science*, 76(11), pp.1437-1441.

Sundar, S., Chakravarty, J., Agarwal, D., Rai, M. and Murray, H. (2010). Single-dose liposomal amphotericin B for visceral leishmaniasis in India. *New England Journal of Medicine*, 362(6), pp.504-512.

Sundar, S. and Chakravarty, J. (2010). Liposomal amphotericin B and leishmaniasis: Dose and response. *Journal of Global Infectious Diseases*, 2(2), p.159.

Sundar, S. and Chakravarty, J. (2014). An update on pharmacotherapy for leishmaniasis. *Expert Opinion on Pharmacotherapy*, 16(2), pp.237-252.

Sundar, S., Chakravarty, J., Rai, V., Agrawal, N., Singh, S., Chauhan, V. and Murray, H. (2007a). Amphotericin B treatment for Indian visceral leishmaniasis: Response to 15 daily versus alternate-day infusions. *Clinical Infectious Diseases*, 45(5), pp.556-561.

Sundar, S., Jha, T., Singh, V., Mishra, M., Buffels, R. and Thakur, C. (2002). Low-dose liposomal amphotericin B in refractory Indian visceral leishmaniasis: a multicenter study. *The American Journal of Tropical Medicine and Hygiene*, 66(2), pp.143-146.

Sundar, S., Jha, T., Thakur, C., Engel, J., Sindermann, H., Fischer, C., Junge, K., Bryceson, A. and Berman, J. (2002). Oral miltefosine for Indian visceral leishmaniasis. *New England Journal of Medicine*, 347(22), pp.1739-1746.

Sundar, S., Jha, T., Thakur, C., Sinha, P. and Bhattacharya, S. (2007b). Injectable paromomycin for visceral leishmaniasis in India. *New England Journal of Medicine*, 356(25), pp.2571-2581.

Sundar, S., Mehta, H., Suresh, A., Singh, S., Rai, M. and Murray, H. (2004). Amphotericin B treatment for Indian visceral leishmaniasis: Conventional versus lipid formulations. *Clinical Infectious Diseases*, 38(3), pp.377-383.

Sundar, S., More, D., Singh, M., Singh, V., Sharma, S., Makharia, A., Kumar, P. and Murray, H. (2000). Failure of pentavalent antimony in visceral leishmaniasis in India: Report from the center of the Indian epidemic. *Clinical Infectious Diseases*, 31(4), pp.1104-1107.

Sundar, S., Sinha, P., Rai, M., Verma, D., Nawin, K., Alam, S., Chakravarty, J., Vaillant, M., Verma, N., Pandey, K., Kumari, P., Lal, C., Arora, R., Sharma, B., Ellis, S., Strub-Wourgaft, N., Balasegaram, M., Olliaro, P., Das, P. and Modabber, F. (2011). Comparison of short-course multidrug treatment with

standard therapy for visceral leishmaniasis in India: an open-label, non-inferiority, randomised controlled trial. *The Lancet*, 377(9764), pp.477-486.

Sundar, S. and Rai, M., 2002. Laboratory diagnosis of visceral leishmaniasis. *Clinical and Vaccine Immunology*, 9(5), pp.951-958.

Sun, H., Yan, S. and Cheng, W. (2000). Interaction of antimony tartrate with the tripeptide glutathione. *European Journal of Biochemistry*, 267(17), pp.5450-5457.

Sunter, J. and Gull, K., 2017. Shape, form, function and Leishmania pathogenicity: from textbook descriptions to biological understanding. *Open Biology*, 7(9), p.170165.

Sunyoto, T., Potet, J. and Boelaert, M. (2018). Why miltefosine—a life-saving drug for leishmaniasis—is unavailable to people who need it the most. *BMJ Global Health*, 3(3), p.e000709.

Syriopoulou, V., Daikos, G., Theodoridou, M., Pavlopoulou, I., Manolaki, A., Sereti, E., Karamboula, A., Papathanasiou, D., Krikos, X. and Saroglou, G. (2003). Two doses of a lipid formulation of amphotericin B for the treatment of Mediterranean visceral leishmaniasis. *Clinical Infectious Diseases*, 36(5), pp.560-566.

Szargiki, R., Castro, E., Luz, E., Kowalthuk, W., Machado, Â. and Thomaz-Soccol, V., 2009. Comparison of serological and parasitological methods for cutaneous leishmaniasis diagnosis in the state of Paraná, Brazil. *Brazilian Journal of Infectious Diseases*, 13(1), pp.47-52.

Tadele, M., Abay, S., Makonnen, E. and Hailu, A., 2020. Leishmania donovani growth inhibitors from pathogen box compounds of medicine for malaria venture. *Drug Design, Development and Therapy*, 14, pp.1307-1317.

Talhari, A. (2018). An open label randomized clinical trial comparing the safety and effectiveness of one, two or three weekly pentamidine isethionate doses (seven milligrams per kilogram) in the treatment of cutaneous leishmaniasis in the Amazon Region. *PLOS Neglected Tropical Diseases*, 12(10), p.e0006850.

Tegazzini, D., Cantizani, J., Peña, I., Martín, J. and Coterón, J., 2017. Unravelling the rate of action of hits in the Leishmania donovani box using standard drugs amphotericin B and miltefosine. *PLOS Neglected Tropical Diseases*, 11(5), p.e0005629.

Teixeira, S., Paiva, R., Kangussu-Marcolino, M. and DaRocha, W., 2012. Trypanosomatid comparative genomics: contributions to the study of parasite biology and different parasitic diseases. *Genetics and Molecular Biology*, 35(1), pp.1-17.

Thakur, C. and Narayan, S. (2004). A comparative evaluation of amphotericin B and sodium antimony gluconate, as first-line drugs in the treatment of Indian visceral leishmaniasis. *Annals of Tropical Medicine & Parasitology*, 98(2), pp.129-138.

Topisirovic, I., Svitkin, Y., Sonenberg, N. and Shatkin, A., 2010. Cap and cap-binding proteins in the control of gene expression. *Wiley Interdisciplinary Reviews: RNA*, 2(2), pp.277-298.

Torres-Guerrero, E., Quintanilla-Cedillo, M., Ruiz-Esmenjaud, J. and Arenas, R., 2017. Leishmaniasis: a review. *F1000Research*, 6, p.750.

Turco, S. and Descoteaux, A., 1992. The lipophosphoglycan of *Leishmania* parasites. *Annual Review of Microbiology*, 46(1), pp.65-92.

Uliana, S., Trinconi, C. and Coelho, A. (2017). Chemotherapy of leishmaniasis: present challenges. *Parasitology*, 145(4), pp.464-480.

Ullah, I., Sharma, R., Biagini, G. and Horrocks, P., 2017. A validated bioluminescence-based assay for the rapid determination of the initial rate of kill for discovery antimalarials. *Journal of Antimicrobial Chemotherapy*, 72(3), pp.717-726.

Ullah, I., Sharma, R., Mete, A., Biagini, G., Wetzel, D. and Horrocks, P., 2019. The relative rate of kill of the MMV Malaria Box compounds provides links to the mode of antimalarial action and highlights scaffolds of medicinal chemistry interest. *Journal of Antimicrobial Chemotherapy*, 75(2), pp.362-370.

Uzun, S., Gürel, M., Durdu, M., Akyol, M., Fettahlioğlu Karaman, B., Aksoy, M., Aytekin, S., Borlu, M., İnan Doğan, E., Dođramacı, Ç., Kapıcıođlu, Y., Akman-Karakaş, A., Kaya, T., Mülayim, M., Özbel, Y., Özensoy Töz, S., Özgöztaşı, O., Yeşilova, Y. and Harman, M., 2018. Clinical practice guidelines for the diagnosis and treatment of cutaneous leishmaniasis in Turkey. *International Journal of Dermatology*, 57(8), pp.973-982.

Vaish, M., Chakravarty, J., Sundar, S. and Singh, O. (2012). rK39 antigen for the diagnosis of visceral leishmaniasis by using human saliva. *The American Journal of Tropical Medicine and Hygiene*, 86(4), pp.598-600.

van Zandbergen, G., Hermann, N., Laufs, H., Solbach, W. and Laskay, T. (2002). Leishmania promastigotes release a granulocyte chemotactic factor and induce interleukin-8 release but inhibit gamma interferon-inducible protein 10 production by neutrophil granulocytes. *Infection and Immunity*, 70(8), pp.4177-4184.

van Zandbergen, G., Klinger, M., Mueller, A., Dannenberg, S., Gebert, A., Solbach, W. and Laskay, T. (2004). Cutting edge: Neutrophil granulocyte serves as a vector for Leishmania entry into macrophages. *The Journal of Immunology*, 173(11), pp.6521-6525.

Vercesi, A. and Docampo, R. (1992). Ca²⁺ transport by digitonin-permeabilized *Leishmania donovani*. Effects of Ca²⁺, pentamidine and WR-6026 on mitochondrial membrane potential in situ. *Biochemical Journal*, 284(2), pp.463-467.

Vickers, T. and Fairlamb, A. (2004). Trypanothione S-transferase activity in a trypanosomatid ribosomal elongation factor 1B. *Journal of Biological Chemistry*, 279(26), pp.27246-27256.

Voak, A., Harris, A., Qaiser, Z., Croft, S. and Seifert, K., 2017. Pharmacodynamics and biodistribution of single-dose liposomal amphotericin B at different stages of experimental visceral leishmaniasis. *Antimicrobial Agents and Chemotherapy*, 61(9).

Waller, D. and Sampson, A., 2018. Chemotherapy of infections. *Medical Pharmacology and Therapeutics*, pp.581-629.

Walters, L., Chaplin, G., Tesh, R. and Modi, G., 1989. Ultrastructural biology of *Leishmania (Viannia) panamensis* (= *Leishmania Braziliensis Panamensis*) in *Lutzomyia gomezi* (Diptera: Psychodidae): A natural host-parasite association. *The American Journal of Tropical Medicine and Hygiene*, 40(1), pp.19-39.

Ward, C., Wong, P., Burchmore, R., de Koning, H. and Barrett, M. (2011). Trypanocidal furamidine analogues: Influence of pyridine nitrogens on trypanocidal activity, transport kinetics, and resistance patterns. *Antimicrobial Agents and Chemotherapy*, 55(5), pp.2352-2361.

Ware, J., O'Connell, E., Brown, T., Wetzler, L., Talaat, K., Nutman, T. and Nash, T., 2020. Efficacy and tolerability of miltefosine in the treatment of cutaneous leishmaniasis. *Clinical Infectious Diseases*, 73(7), pp.e2457-e2562.

What is leishmaniasis? (2020) *Leish @ York*. Available at: <https://yorkleish.org/what-is-leishmaniasis/> (Accessed: December 23, 2022).

WHO (1984). The leishmaniasis. Report of a WHO expert committee. World Health Organization Technical Report Series 701, 1–140.

WHO 2020. Leishmaniasis. [online] Available at: <<https://www.who.int/en/news-room/factsheets/detail/leishmaniasis>> [Accessed 18 February 2020].

WHO 2022. WHO Leishmaniasis control programme. Annual country reports. [online] Available at: <https://www.who.int/data/gho/map-gallery-search-results?&maptopics=910b5dfc-ce2e-4440-8b43-8d83f4a85485&term=leishmaniasis> [Accessed 16 Nov 2022].

Who.int. 2022. *HIV/AIDS*. [online] Available at: <<https://www.who.int/news-room/factsheets/detail/hiv-aids>> [Accessed 16 April 2022].

Wijnant, G., Croft, S., de la Flor, R., Alavijeh, M., Yardley, V., Braillard, S., Mowbray, C. and Van Bocxlaer, K., 2019. Pharmacokinetics and pharmacodynamics of the nitroimidazole DNDI-0690 in mouse models of cutaneous leishmaniasis. *Antimicrobial Agents and Chemotherapy*, 63(9).

Wiwanitkit, V. (2012). Interest in paromomycin for the treatment of visceral leishmaniasis (kala-azar). *Therapeutics and Clinical Risk Management*, 8, pp.323-328.

Wyllie, S., Cunningham, M. and Fairlamb, A. (2004). Dual action of antimonial drugs on thiol redox metabolism in the human pathogen *Leishmania donovani*. *Journal of Biological Chemistry*, 279(38), pp.39925-39932.

Yan, S., Li, F., Ding, K. and Sun, H., 2003. Reduction of pentavalent antimony by trypanothione and formation of a binary and ternary complex of antimony (III) and trypanothione. *JBIC Journal of Biological Inorganic Chemistry*, 8(6), pp.689-697.

Yardley, V., Dujardin, J., Koirala, S., Llanos-Cuentas, A., Chappuis, F., Rijal, S., Miranda, C., Croft, S. and De Doncker, S., 2005. The sensitivity of clinical isolates of *Leishmania* from Peru and Nepal to miltefosine. *The American Journal of Tropical Medicine and Hygiene*, 73(2), pp.272-275.

Zheng, W., Thorne, N. and McKew, J., 2013. Phenotypic screens as a renewed approach for drug discovery. *Drug Discovery Today*, 18(21-22), pp.1067-1073.

Zulfiqar, B., Shelper, T. and Avery, V., 2017. Leishmaniasis drug discovery: recent progress and challenges in assay development. *Drug Discovery Today*, 22(10), pp.1516-1531.